TOWARDS UNDERSTANDING THE EXPRESSION AND REGULATION OF GPER1, AND ITS SIGNIFICANCE THEREOF IN HUMAN BREAST CANCER

A thesis submitted for the degree of

Doctor of Philosophy

To

INDIAN INSTITUTE OF TECHNOLOGY GUWAHATI

By

MOHAN C M

Department of Biosciences and Bioengineering
Indian Institute of Technology Guwahati
Guwahati, Assam-781039, India
April 2018

To my beloved

Appa and Amma

DEPARTMENT OF BIOSCIENCES AND BIOENGINEERING
INDIAN INSTITUTE OF TECHNOLOGY GUWAHATI
GUWAHATI-781039

DECLARATION

I hereby declare that the contents of the research work described in this thesis titled **"Towards understanding the expression and regulation of GPER1, and its significance thereof in human breast cancer"**, is a presentation of my original research work carried out in the Department of Biosciences and Bioengineering, Indian Institute of Technology Guwahati, India, under the supervision of Dr. Anil Mukund Limaye. Studies involving clinical samples were conducted in the Department of Pathology, North Eastern Indira Gandhi Regional Institute of Health and Medical Sciences, Shillong, India, under the guidance of Dr. Vandana Raphael.

Sincere efforts have been made to duly acknowledge the contributions from others for their ideas, technical help and references or any other help which may be involved in the completion of thesis work.

4th April, 2018

Mohan C M
Roll No. 11610620
Department of Biosciences and Bioengineering
Indian Institute of Technology Guwahati

DEPARTMENT OF BIOSCIENCES AND BIOENGINEERING
INDIAN INSTITUTE OF TECHNOLOGY GUWAHATI
GUWAHATI-781039

CERTIFICATE

This is to certify that the work described in the thesis titled, **"Towards understanding the expression and regulation of GPER1, and its significance thereof in human breast cancer",** submitted by Mohan C M (Roll No. 11610620) to Indian Institute of Technology Guwahati, India, for the award of the degree of Doctor of Philosophy is an authentic record of the research work carried out under my supervision in the Department of Biosciences and Bioengineering, Indian Institute of Technology Guwahati, India.

This thesis or any part thereof has not been submitted elsewhere for award of any other degree or diploma.

4th April, 2018

Dr. Anil Mukund Limaye
Thesis Supervisor

Acknowledgements

I take this opportunity to express my gratitude towards many people in my life, without whom it would have been impossible to achieve this feat.

I would like to express my sincere gratitude to all my ***GURUs****, who have shaped me at every stage of my life. In that row, the latest one is* ***Dr. Anil Mukund Limaye,*** *a great teacher and my thesis supervisor. I could not have imagined having a better advisor and mentor. I am thankful to him for his belief in my abilities and for his patience in dealing with my scientific limitations. His guidance helped me in all the time of research and writing of this thesis. His advice on both research as well as on my career have been priceless. I hope that I will carry at least some of his best qualities and principles in rest of my life.*

I place on record my sincere thanks to the doctoral committee: ***Prof. Vikash Kumar Dubey, Dr. Bithiah Grace Jaganathan,*** *and* ***Dr. Debasis Manna,*** *for their insightful comments and timely evaluation of thesis work.*

I would like to thank..

Dr. Vandhana Raphel *for providing me an opportunity,* ***Donna*** *and* ***Betty*** *for helping me to conduct a part of my thesis work at the Department of Pathology, NEIGRIHMS.*

Dr. Rajgopal Srinivasan *for the wonderful opportunity to get the glimpse of corporate world and also to learn Next generation Sequencing analyses techniques at Innovation labs, Tata Consultancy Services, Hyderabad.*

Past and Present Head of the Department of Biosciences and Bioengineering: ***Prof. Arun Goyal, Prof. V. V. Dasu,*** *and* ***Prof. Kannan Pakshirajan.***

Dr. Manish Kumar, Dr. Sachin Kumar, Dr. Vishal Trivedi *and* ***Dr. Rajkumar Thummer*** *for providing access to their lab facilities.*

Entire staffs *of Department of Biosciences and Bioengineering, IIT Guwahati for efficient and timely help whenever required.*

IITG for providing me scholarship and necessary infrastructure for the research work.

I would like to acknowledge,

Prof. Paturu Kondiah, Neeraj *and* ***Dr.Abhijeet****, MRDG, IISc for technical inputs in microarray data analysis.*

Our collaborators, ***Dr. Pratibha Ranganathan*** *(CHG),* ***Dr. Deepak modi*** *(NIRRH) for their valuable suggestions.*

TCGA team *for their tremendous effort in generating a great database and making it publically available.*

Department of Biotechnology*, Gov. of India for financial support and* ***Department of Science and Technology****, Gov. of India for travel grant to attend the international conference.*

I am also thankful to…

My past lab members: ***Dr. Gauri, Sahil, Marine, Baskar, Abrar, Abhay, Sukhdev, Mrinal, Ramya, Sarbajeet, Pratap, Raunak, Praneetha, Chinni, Anwita, Aditi, and Sahit*** *for their suggestions and help. I find myself privileged to have worked with them.*

My present lab members: ***Ajay, Uttariya, Guarav,*** *and* ***Swati*** *for their constructive comments, discussions, constant support and also for the sleepless nights we were working together and for all the fun we have had inside and outside the lab.*

Sheeba *for her unconditional love, care and also for her extended help in editing the thesis.*

My buddies at IITG, ***Arun, Basavaraju, Deepika, Ganesh, Himanshu, Katla, Mansa, Monisha, Muthu, Payal, Ravi, Sathish, Siddharth, Subbi, Sudhir, Sunandha, Sunil, Thiyagarajan, Yashwant, and Yoganand*** *for making my campus stay memorable.*

Paridhi Singhal Gupta *for her technical help, without whom western blotting wouldn't have been so easy.*

Prajakta Ma'm, *for providing a homely environment during our lab gatherings.*

I owe special thanks to my family members,

Appa, Amma *and* ***Ajji*** *for their blessings, patience, unconditional love and care*

Umesh *and* ***Chandu*** *for their constant support. I am fortunate to have such caring brothers.*

Monica *for being with me in all my good and bad times, also for her patience and motivation.*

Mohan Chowdenahalli Manjegowda

TABLE OF CONTENTS

Chapter I

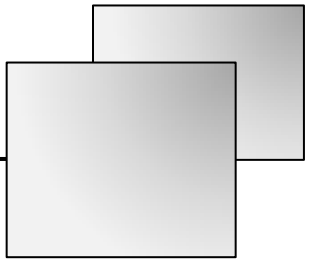

Introduction

1.1. INTRODUCTION

In the late 1990s several independent groups of investigators, with unrelated research interests, coincidentally cloned a novel cDNA[1–7]. Investigations thereafter revealed that the novel cDNA encodes a G-protein coupled receptor (GPCR) and shares highest sequence identity of 28% with angiotensin II type-1 and interleukin-8 receptors. Until the year 2000, this novel receptor was just another orphan GPCR; GPR30. In the year 2000, Filardo et al., for the first time, demonstrated that this receptor associates with G-proteins and mediates short-term non-genomic effects of 17β-estradiol (E2) in a time span of seconds to minutes[8]. Later, it was revealed that the consequences of GPER1 activation can lead to activation of Src-like tyrosine kinases, activation of the epidermal growth factor receptor (EGFR)-MAPK pathway via heparin-bound epidermal growth factor (HB-EGF) ectodomain shedding, generation of cAMP, activation of PI3K, and increase in intracellular calcium[8–10]. During the same time, Thomas et al., demonstrated the binding of estrogen to purified membranes of SkBr-3 cells, a breast cancer cell line that does not express nuclear estrogen receptors (nER)[11]. These works firmly established the identity of the bona fide ligand of GPER1; E2. A decade after its discovery, GPR30 was officially named as G-protein coupled estrogen receptor 1 (GPER), by the International Union of Basic and Clinical Pharmacology (IUPHAR)[12].

With the introduction of this new player into the estrogen signaling network, the signaling crosstalk with the other growth factor receptor-mediated pathways was extensively explored. This led to the appreciation of the role of GPER1 at various estrogen target sites including the skeletal, immune, cardiovascular and central nervous systems[13]. Independent studies have consistently demonstrated that antiestrogens, such as selective estrogen receptor modulators (SERMs) or selective estrogen receptor down-regulators (SERDs), can activate GPER1[8,10,11,14,15]. Investigations in this line, have hypothesized the possible role of GPER1 in tamoxifen resistance and tamoxifen-associated endometrial abnormalities[15–17]. Clinical studies have revealed aberrant expression of GPER1 and its association with the clinicopathological parameters, in a variety of solid tumors[18–22]. Collectively, the physiological and pathological significance of GPER1 is increasingly being investigated.

Because of its ability to relay the estrogen and antiestrogen signals to cells, presently, GPER1 is one of the major focal points of research in endocrine-related cancers.

1.2. AIM AND SCOPE OF THE PRESENT THESIS WORK

With 17 years of research after its identification as a G-protein coupled estrogen receptor, the significance of GPER1 in human physiology and pathology has begun to be appreciated. Collectively, the literature suggests that certain aspects of GPER1 are poorly understood. Amid the studies on the association between GPER1 and estrogen receptor α (ERα) in breast cancer, a handful of contradictory observations are reported[17,18,23–28]. In the light of heterogeneity across the cohorts, this is not surprising. More clinical studies with new cohorts and retrospective studies are warranted to clarify the confusion. Moreover, the clinical implications of the GPER1-ERα association deserve an in-depth investigation. This is important, given that ERα is one of the potential downstream players in GPER1 signaling[29–32].

While most of the reports have focused on immediate consequences of GPER1 signaling, very less is known as to how GPER1 expression is regulated. Clinical studies show reduced expression of GPER1 in breast cancer as compared to their normal counterparts and it is negatively associated with tumor progression[26,33]. These reports, supported by *in vitro* experimental observations[24,34,35], led to the proposition that GPER1 is a tumor suppressor in breast cancer. However, the underlying mechanisms are poorly understood.

Recent developments in the field of GPCR signaling suggest that activation of GPCRs by different ligands might give rise to diverse cellular responses by stabilizing distinct active confirmations of the receptor[36]. In case of GPER1, it is clearly established that several anti-estrogens, phytoestrogens, and xenoestrogen can also activate GPER1[8,10,11,14,37–43], but the downstream consequences of GPER1 activation by these diverse ligands need to be dissected out. This will have a great impact on our understanding of the physiological role of GPER1. However, it should be noted that, because of the complexity of estrogen biology (multiple receptors), elucidating the unique role of GPER1 signaling remains challenging.

1.3. OBJECTIVES

Considering the emerging niches within the actively growing field of GPER1 biology we have set the following objectives for the present thesis work.

1. Generation of an anti-GPER1 polyclonal antibody for analysis of GPER1 protein expression.
2. To analyze GPER1 expression in breast tumors.
3. To investigate the functional link between GPER1 and ERα in breast cancer cells.
4. To study the role of DNA methylation in the regulation of GPER1 expression.
5. To investigate the modulation in the global transcriptome of breast cancer cells treated with G1, a purported GPER1 specific agonist.

Chapter II

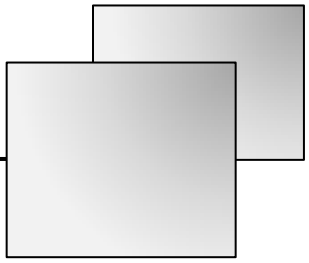

Review of literature

2.1. ESTROGEN AND ITS MECHANISM OF ACTION

Estrogens are the steroid hormones which play crucial roles in the growth and development of the human reproductive system. In the target tissues, the estrogen signals are deciphered by nuclear and/or non-nuclear estrogen receptors (ER). Among the three major molecular players responsible for relaying estrogenic signals, ERα is the first receptor to be discovered and most extensively studied. ERβ and a G-protein coupled estrogen receptor-1 (GPER1) are the contemporaneous members of estrogen receptor family. ERα and ERβ are the nuclear-ERs and GPER1 is a membrane-associated ER.

Nuclear-ERs are ligand-activated transcription factors. These receptors have similar tertiary architecture: N-terminal domain, DNA-binding domain, hinge region, ligand binding domain and C-terminal domain[44]. There are two protein-protein interaction sites called activation function (AF)-1 and AF-2 in the N-terminal domain and ligand binding-C-terminal domain, respectively. Upon activation, these sites are involved in the interactions with other transcription factors and co-regulators. Ligand binding induces conformational changes in these receptors, which subsequently leads to nuclear translocation, as dimers, and regulation of transcription of the target genes[44]. This classical axis represents the genomic actions of estrogen. Almost all organ systems in the human body are influenced by estrogen[13].

2.2. BREAST CANCER

Estrogen plays a pivotal role in the growth and development of the mammary glands[45]. However, abnormal estrogen signaling is also responsible for the development of breast cancer[46–49]. Common sites of origin are the lobules (milk glands) and the ducts which carry the milk from the lobules to the nipple[50]. Histopathological studies on breast tumors indicate that majority (~70%) of them express ERα[49]. Heterogeneity have led to the categorization of these tumors, based on the molecular signature, into five major classes (Luminal-A, Luminal-B, Basal-like, human epidermal growth factor receptor 2 (HER2)-enriched, and Normal-like)[51,52]. Etiological studies have revealed lifetime exposure to estrogen (early menarche, delayed menopause, and late pregnancy) as one of the important

risk factors for breast cancer[45]. Estrogen is included in the list of known carcinogens by the National Institute of Environmental Health Sciences (NIEHS)[53].

Breast cancer occurs in both men and women and is the leading cause of cancer-associated mortality among women worldwide[54]. Globally, for every ten new cancers diagnosed, at least one will be breast cancer[55]. As of March 2017, there are more than 3.1 million breast cancer patients in the U.S. One out of every 8 women in the United States will develop invasive breast cancer[56]. Globally, it is estimated that one in 28 women is likely to develop breast cancer during her lifetime[57]. Breast cancer is the most common cancer in Indian women and contributes to 27% of all cancers in women[57]. When compared to the scenario 25 years back, presently the percentage of incidence is increasing in younger population[58]. Especially in Guwahati, more than 68% of the breast cancer incidences occurred in the age group below 50 years. It is projected by the National Institute of Cancer Prevention and Research (NICPR) that by 2020 there will be nearly 1.8 million new cases of breast cancer. Unfortunately, the mortality rate in India is very high. One out of every two women diagnosed with breast cancer will die due to this disease. Lack of awareness, delayed diagnosis and socioeconomic status are identified as the major factors influencing this high mortality rate[59].

Surgery, radiotherapy, and chemotherapy are the standard treatment methods used in any cancer. Considering the molecular markers of the breast cancers certain specialized treatment strategies are being practiced. Unlike Herceptin, which targets the HER2, most of the specialized treatment strategies exploit the hormone dependence of the tumor. One of such kind is the endocrine therapy, where SERMs or SERDs are used to block estrogen action[60]. Alternatively, aromatase inhibitors are used to prevent the estrogen production in the body[61]. All these estrogen-related treatments are associated with side effects, since they also abrogate the estrogen signaling in other estrogen target tissues. These include uterine abnormalities, depression, reduced bone mineral density and cardiovascular related problems[13,60]. Despite its initial success, tamoxifen (SERM) treated patients show tumor relapse and endometrial abnormalities[62]. However, the mechanistic details are not completely understood.

2.3. G-Protein Coupled Estrogen Receptor 1 (GPER1)

GPER1 codes for a seven-transmembrane estrogen receptor and is located on the human chromosome 7 at the p22.3 region[4]. In humans, rats, and mice the receptor is 375 amino acids long, with a theoretical molecular weight of 42.24 kDa. It was discovered by several independent research groups in late 1990s and considered as an orphan receptor according to their perspective[1–7]. It is a member of Class A rhodopsin-like GPCR and has a sequence identity of 28% with angiotensin II type-1 receptor and interleukin-8 receptor[4]. Later in 2000, Filardo et al., demonstrated that this novel GPCR responds to estrogen stimulation by the production of intracellular second messengers[8]. Short-term response to estrogen stimuli by the production of second messengers (cAMP, PI3 and intracellular calcium) was reported much earlier than the identification of E2 selectivity of the receptor[63–65]. The molecular basis for these signaling events was explained clearly with GPER1 in the context. Thus, genomic actions of estrogen are conveyed by classical nuclear hormone receptor and non-genomic actions are predominantly mediated by GPER1. Often, these distinct signaling arms are known to crosstalk with each other and that increases the complexity of estrogen signaling in target cells[29,31,32,66–69].

To understand the biological role, GPER1 knockout mice models were generated and initial studies were keen towards understanding its role in the reproductive system. Disappointingly, all the mice were fertile[70]. Subsequent studies with the knockout mouse models highlighted the importance of GPER1 in the cardiovascular, immune, and glucose metabolism[31,71,72]. During this time, some of the reports questioned the authenticity of this receptor as an estrogen signal transducer[73–75]. Otto et al., have failed to detect the binding of radio-labeled E2. However, their experimental limitations are questioned by others[76]. Substantially large number of studies have demonstrated the role of GPER1 in pathological settings, especially in cancers of various types. In fact, GPER1 signaling was first elucidated in the breast cancer cell lines[8]. Over the course of time, these signaling events were recapitulated in other malignancies.

2.3.1. Localization of GPER1

Understanding the localization of GPCRs has been a challenging task. GPCRs' representation at the cell surface is very limited and is tightly regulated at various stages; trafficking, internalization, recycling, and degradation[77–79]. While being processed through various sorting checkpoints, these receptors spend their transit time in the intracellular compartments such as endoplasmic reticulum and trans-Golgi network[78]. This extended transit time in the cytosol is sometimes observed as the functional location of the receptor. Cellular localization of GPER1 is one of the topics of controversy in the field of GPER1 biology. Its localization has been reported to be in the plasma membrane[22,80–83], and intracellular membranes[10,17,23,41,74,84–86]. Studies in this line of investigation have convincingly demonstrated the plasma membrane localization of GPER1. It is suggested that because of multiple checkpoints during the trafficking and the constitutive endocytosis, GPER1 is frequently identified in the intracellular membranes[83,87,88].

Interestingly, independent clinical studies have reported nuclear staining of GPER1 in the breast[17,84], endometrial[89,90] and ovarian cancers[20]. Recent reports from the cell line studies have provided the experimental evidence. Estrogen stimulation in the cancer-associated fibroblasts (CAF) induced nuclear translocation of GPER1 and its recruitment to the cyclin D1 promoter, along with EGFR[91]. Further, this translocation was Importin-dependent[92]. In association with p65, nuclear/perinuclear localization of GPER1 was also reported in human primary monocytes[93]. Although traditionally GPCRs are known as cell surface receptors, their nuclear localization is not unique to GPER1[94,95]. In fact, these emerging concepts potentially open new exciting dimensions in the field of GPER1 signaling and estrogen biology. Taken together, multiple localization sites for GPER1 is evident. However, the possibility of cell-context specific localization of GPER1 cannot be ruled out.

2.3.2. Regulation of GPER1 expression

Attempts towards understanding the regulation of GPER1 expression have characterized the intron region. Progestin-mediated regulation of GPER1 expression in MCF-7 cells was demonstrated by Ahola and co-workers[96]. Here, GPER1 induction was

positively correlated with the progestin-mediated inhibition of MCF-7 cell proliferation. A series of studies, in this line of investigation, were contributed by Marcello Maggiolini's group. GPER1 was regulated by growth factors such as epidermal growth factor (EGF), transforming growth factor-α (TGFα), insulin-like growth factor-I (IGF-I), insulin, and hypoxia-inducible factor-1α (HIF-1α), in a variety of cancer cell lines and CAFs[32,97–99]. Collectively, these reports demonstrate the importance of activator protein 1 (AP-1) binding site and hypoxia responsive element (HRE) in the intron region. At the same time, the involvement of c-fos and p-ERα^{Ser118} was also revealed. These reports refer to the regulatory region as 5' flanking region, with respect to the transcript, "ENST00000617001.1". However, considering the existing mRNA reference sequences, the regulatory region lies in the intron. Consistently, in all the situations, the growth factor stimulation induced the expression of GPER1 and its target; connective tissue growth factor (CTGF). Studies above have ascribed GPER1 up-regulation to growth factor-mediated proliferation, migration and invasion. In the case of hypoxia, GPER1 is implicated in E2-mediated protection of cells from hypoxia-induced apoptosis[99]. Although growth factor stimulation induced the CTGF expression via GPER1[97–99], the corresponding experiments were conducted in an E2-free environment. It seems to be paradoxical as to how GPER1 was activated to induce its target gene expression.

In a recent study, Giessrigl et al., have demonstrated the down-regulation of GPER1 expression in fulvestrant-resistant MCF-7 cells[100]. DNA-methylation and unscheduled chromatin remodeling were suggested to be the underlying mechanisms for the suppression of GPER1 expression. Adding to this, the DNA methylation component in GPER1 expression regulation is also suggested by others[34,35]. In triple-negative breast cancer cells, the GPER1 expression is induced by heregulin-β1 (HRG-β1) stimulation, via ERBB2-ERBB3 heterodimers and MAPK/ERK pathway[101]. Apart from these reports, estrogen-mediated induction of GPER1 is also suggested[89,102]. Taken together, the regulation of GPER1 expression by diverse growth factors is evident. These connections directly link the growth factor signaling with the estrogen signaling. Moreover, it is noteworthy that these growth factors are implicated in several malignancies[103].

2.4. GPER1-MEDIATED SIGNALING

The contribution of Filardo and co-workers towards elucidating the GPER1 signaling is very significant. Filardo et al., demonstrated that estrogen induced ERK1/2 activation is mediated by the GPER1 in breast cancer cells[8]. Ectopic expression of GPER1 in MDA-MB-231 enabled the cells to respond to estrogen by activation of ERK1/2[8]. Further, GPER1 activation resulted in transactivation of EGFR/MAPK pathway via ectodomain shedding of HB-EGF. Subsequently, it was demonstrated that estrogen-mediated cAMP production was GPER1-dependent[104]. Further, it was shown that GPER1-induced cAMP suppressed the MAPK pathway, by protein kinase A (PKA)-mediated inactivation of raf-1[104] (Figure 2.1.). These initial studies elucidated the estrogen-mediated GPER1 actions and highlighted the two distinct signaling arms, cAMP and EGFR/MAPK pathway, in breast cancer cells. Revankar et al., have demonstrated that GPER1 activation leads to intracellular calcium mobilization and production of phosphatidylinositol 3,4,5-trisphosphate (PIP3)[10] (Figure 2.1.). Later, the binding of estrogen to GPER1 has been demonstrated by two independent groups[10,11,37]. The affinity of estrogen towards GPER1 was found to be 2.7 nM and 6 nM in SkBr-3[11] and COS-7[10] cells, respectively. These studies have established GPER1 as a bona fide membrane-associated estrogen receptor and mediator of non-genomic actions of estrogen.

Considering the complexity of estrogen signaling, delineating GPER1-mediated actions in systems which express classical estrogen receptors has always been challenging. Bologa et al., identified a GPER1-specific non-steroidal membrane permeable agonist “G1” (1-[4-(6-bromobenzo[1,3]dioxol-5-yl)-3a,4,5,9b-tetrahydro-3H-cyclo-penta[c] quinolin-8-yl]-ethanone) by screening a library of 10,000 molecules[105]. Followed by this, G15[106] and G36[107], the GPER1 specific antagonists were synthesized. These ligands are being used as standard tools to specifically assess the role GPER1 in estrogen signalling [14,29,39,66,108–115].

2.4.1. GPER1 ligands

To date, GPER1 is shown to be activated by a plethora of ligands. Phytoestrogens (genistein, zearalonone) and xenoestrogens (Bisphenol-A, dichlorodiphenyl-trichloro-ethane (DDT), Kepone, nonylphenol) were found to be potential GPER1 ligands[11,14,37–39,42,43]. It is

important to note here that some of these potential GPER1 ligands are endocrine disruptors[116]. Interestingly, tamoxifen and fulvestrant are demonstrated to be ligands for GPER1[8,10,11,41,104]. The list of GPER1 ligands is ever growing, the recent addition being prunetin[40] (Figure 2.1.).

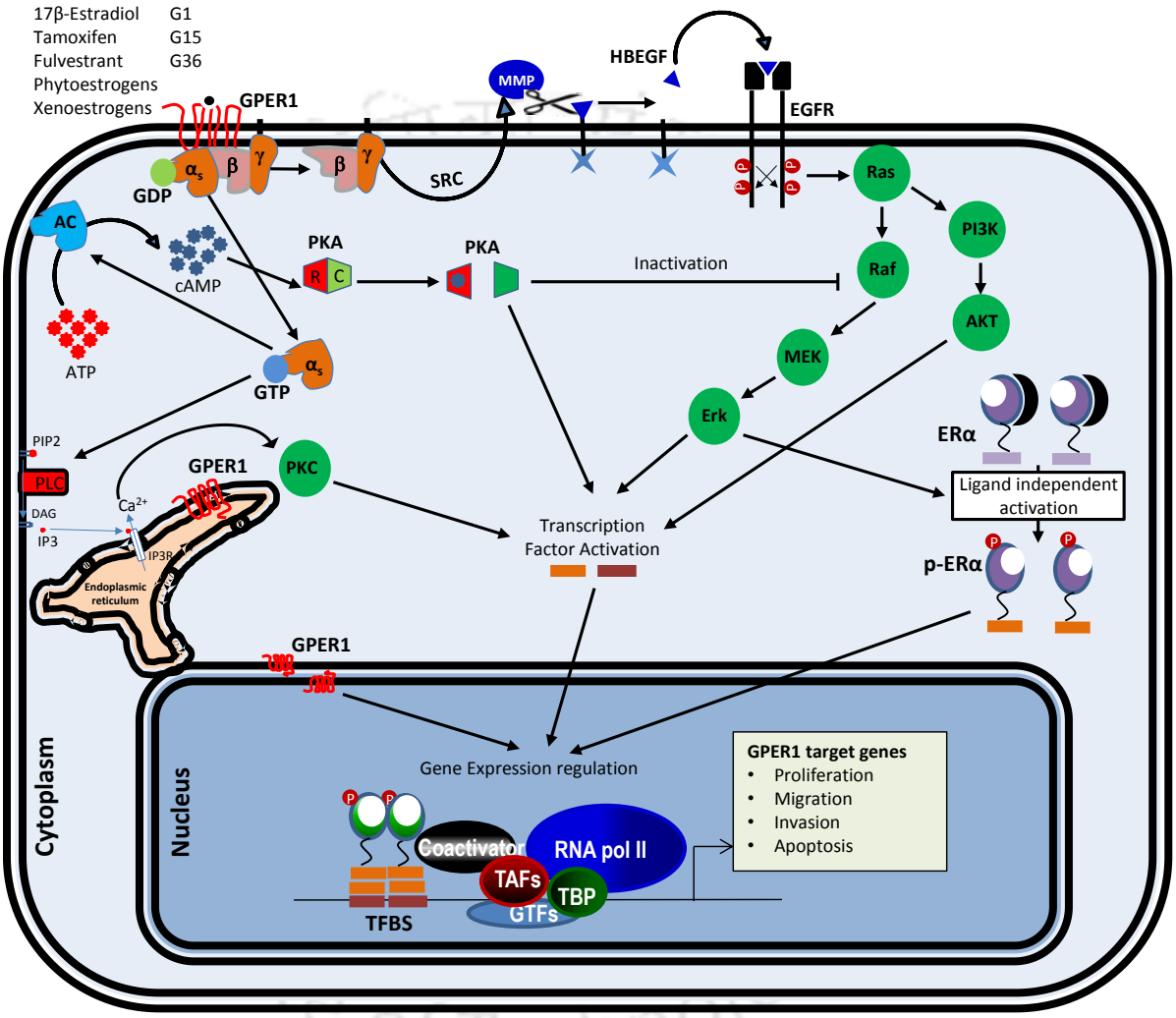

Figure 2.1. GPER1 signaling. The schematic summarizes the molecular consequences of GPER1 signaling. GPER1 ligands reported in the literature are listed along with the synthetic ligands (G1, G15 and G36). Both the arms of GPER1 signaling which activate and suppress the MAP kinase pathway are depicted. The involvement of GPER1 in ligand independent activation of ERα is also highlighted. It should be noted that GPER1 localization has been shown in plasma membrane, Endoplasmic reticulum, and in the nuclear membrane. Only for the presentation purpose the signaling has been shown from the plasma membrane-localized GPER1. However, the possibility of signaling from other localization sites is not ruled out. Presently, the significance of multiple localization sites is not clear.

2.4.2. GPER1 signaling in normal physiology

After the identification of this novel membrane estrogen receptor, several estrogen-mediated physiological actions were revisited to investigate the plausible role for GPER1. Investigations in this line have appreciated the role of GPER1 in reproductive, immune, renal, cardiovascular, skeletal and nervous systems[117]. In keratinocytes, GPER1 is involved in the estrogen-mediated protection of cells from oxidative stress-induced apoptosis[118]. GPER1 activation in macrophages induced the production of nerve growth factor (NGF), thereby promoting wound healing[119]. In collaboration with ERα, GPER1 is involved in the estrogen-mediated proliferation of mouse spermatogonial cells, GC-1[115]. The individual contributions of ERα and GPER1 in rat Sertoli cells in mediating estrogen actions were found to be distinct. While ERα-mediated signaling promoted the proliferation, GPER1-mediated signaling regulated the apoptosis, collectively maintaining the development and homeostasis of the testes[41]. In the mouse uterus, GPER1 has been implicated in the stromal epithelial interaction and was suggested to be a negative regulator of ERα-mediated estrogen signaling[67]. Recently, GPER1 signaling has been implicated in promoting bone regeneration via induction of Runt-related transcription factor-2 (RUNX2) in osteoblasts[40].

2.4.3. GPER1 signaling crosstalk with other signaling pathways

Crosstalk of GPER1 signaling with EGFR/MAPK pathway is well established. Studies have demonstrated the physical interaction of GPER1 with other molecules such as HIF-1α[120], ERα and EGFR[32]. Apart from these, GPER1 interacts with classical genomic axis by activating ERα in a ligand independent manner in the ventral hippocampus of male mice[30,38]. On the other hand, selective GPER1 activation blocked the phosphorylation of ERK1/2 and ERα in the uterus of the mice and antagonized the estrogen induced uterine growth[67]. GPER1 signaling was involved in estrogen-mediated inhibition of TGF-β signaling pathway. Although the mechanistic details are not completely understood, GPER1 crosstalk with insulin signaling is reported in diverse tumors. In endometrial and breast cancer cells, GPER1-mediated the IGF-I induced migration and proliferation[98]. GPER1 was found to be essential for insulin-mediated cell migration of leiomyosarcoma cancer cells and breast cancer-associated fibroblasts[97]. In breast cancer cells and breast cancer-associated

fibroblasts, GPER1 activation transactivated Notch signaling pathway in a γ-secretase-dependent manner[121]. Hippo signaling pathway was also found to be activated by GPER1 activation in invasive ductal carcinoma and cancer-associated fibroblasts[27]. Collectively, these reports highlight the complexity of estrogen signaling and the role of GPER1 in mediating these signaling events.

2.4.4. GPER1 and cancer

Role of GPER1 in estrogen-associated pathology is also increasingly reported. Particularly, in cancer, its expression has been found to be abnormal. GPER1 has been implicated in proliferation, migration and invasion of endometrial cancer cells[122–124]. GPER1 expression was associated with tamoxifen-induced endometrial pathology[89]. GPER1 was an indicator of poor survival[86]. Further, its expression was correlated positively with EGFR and negatively with ER and PR in endometrial carcinoma[86]. Expression of GPER1 was found to be up-regulated in lung cancer[21,125]. GPER1 activation inhibited the proliferation of ovarian cancer cells and arrested the cells in G2/M-phase of the cell cycle[126]. Activation of GPER1 by E2, genistein, and tamoxifen induced the proliferation of thyroid cancer cells[14]. In bladder carcinoma, GPER1 activation inhibited the proliferation[127]. Taken together, the significance of GPER1 in cancer is context specific.

2.4.5. GPER1 and breast cancer

The importance of GPER1 in breast cancer has been investigated because of multiple prominent interests. Majority of breast cancers are estrogen responsive. Tamoxifen and fulvestrant can activate GPER1 signaling[11]. GPER1 is a possibility to target estrogen signaling in ERα-negative tumors[28]. GPER1 signaling in breast cancer is self-regulatory[8,104]. At the same time, it counters the ERα actions[66]. Based on the context of cell, GPER1 down-stream actions overlap with that of ERα. GPER1 was implicated in progestin-mediated inhibition of MCF-7 cells[128]. In MCF-7 cells GPER1 activation inhibits the proliferation[24] whereas in SkBr-3 cells GPER1 signaling promoted the cell proliferation and migration[24,129]. In an attempt to identify early GPER1-targets, Pandey et al have reported the first microarray analysis of SkBr-3 cells treated with tamoxifen[129]. CTGF was found to be the most up-regulated gene. The induction of CTGF was associated with the enhanced migration

and proliferation potential of SkBr-3 cells[129]. Recently, for the first time the consequences of GPER1 activation in a normal breast epithelial cell line, MCF10A, were assessed. It was observed that GPER1 promoted proliferation via ERK1/2 phosphorylation[108]. With regard to the ectodomain shedding it is not consistent as to which protease is performing the task of processing the surface bound growth factors. While it is reported to be via MMP2 in[130], a recent report demonstrated that EGFR transactivation is independent of MMPs[108]. However, the cell context specific players at this stage of signaling cannot be ignored[131].

Apart from these, most importantly, fulvestrant stimulation induced the ERK1/2 phosphorylation in MCF-7 and SkBR-3 cells and also in GPER1-transfected MDA-MB-231 cells[8,104,132]. Fulvestrant disrupted the antiproliferative TGF-β pathway in MCF-7 cells via GPER1[132]. Fulvestrant stimulation mimicked the estrogen actions in rat Sertoli cells, via GPER1[41]. Interestingly, a recent study reported that GPER1 expression was epigenetically silenced in fulvestrant resistant MCF-7 cells[100]. A recent study in MCF-7 cells reported that fulvestrant-mediated GPER1 activation is associated with enhanced cell adhesion, implicating its role in promoting metastatic progression[133]. Taken together, although fulvestrant acts as a GPER1 agonist, the role of GPER1 in fulvestrant resistance is not conclusive. In the case of tamoxifen, it has been demonstrated that tamoxifen resistance is associated with enhanced estrogen sensitivity and GPER1 up-regulation[15,25]. GPER1/MAPK pathway was directly implicated in tamoxifen-resistant and long-term activation of GPER1 by G1-enhanced the agonistic property of tamoxifen[15]. Interestingly, increased plasma membrane localization of GPER1 was associated with the tamoxifen resistance[15,25]. In line with these observations, clinical studies report that GPER1 expression negatively associated with the relapse-free survival in tamoxifen treated patients[17]. Collectively, the role of GPER1 in tamoxifen resistance is evident, and these studies suggest that GPER1 status should be seriously considered at least in breast cancer treatment strategies.

Chapter III

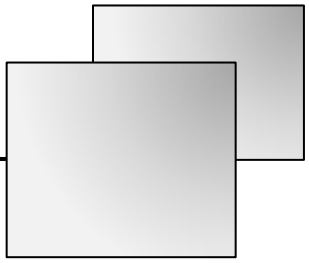

Materials and methods

3.1. PLASTICWARE, CHEMICALS AND REAGENTS

All cell culture plasticware was from Greiner Bio-One (GmbH, Germany) or Tarson (Mumbai, India). All cell culture media (with and without phenol red), fetal bovine serum (FBS) and charcoal-stripped FBS (csFBS) were purchased from Gibco (NY, USA). Methylthiazolyldiphenyl-tetrazolium bromide (MTT) reagent, Dulbecco's phosphate-buffered saline (DPBS), antibiotics and trypsin-EDTA were purchased from HiMedia (Mumbai, India). Lipofectamine® RNAiMAX transfection reagent was purchased from Thermo Scientific (PA, USA). Details of various ligands and inhibitors used in the present study are given in table 3.1. Nitrocellulose membrane (pore size 0.45 µm) was purchased from HiMedia (Mumbai, India). BstUI and TaqI were from Thermo Scientific (PA, USA). PCR master mixes and cDNA synthesis kits were from Applied Biosystems (CA, USA). PCR clean-up, gel extraction and plasmid mini-prep kits were purchased from either Macherey Nagel (Duren, Germany) or Thermo Scientific (PA, USA). All other chemicals and buffers were purchased from Merck (Mumbai, India), Sigma (MO, USA) or SRL (Mumbai, India). Antibodies for β-actin and ERα were obtained from Thermo Scientific (PA, USA) and Santa Cruz biotechnologies (CA, USA), respectively. Polyclonal anti-GPER1 antibody against the N-terminus of GPER1 was generated as described in section 3.7 of Chapter 3 and validation results are presented in Chapter 4[134].

Table 3.1. Ligands and inhibitors used in this study.

Ligand/Inhibitor	Catalogue No.	CAS No.	Company	Solvent	Abbreviation
17β-estradiol	E8875	50-28-2	Sigma	Ethanol	E2
4-hydroxytamoxifen	H7904	68047-06-3	Sigma	Ethanol	TAM
Propylpyrazoletriol	H6036	263717-53-9	Sigma	Ethanol	PPT
G1	10008933	881639-98-1	Cayman	DMSO	G1
5-azacytidine	100821	320-67-2	MP Biomedicals	DMSO	5-aza
Colchicine	CMS342	64-86-8	HiMedia	Water	Col

3.2. CELL CULTURE AND TREATMENTS

3.2.1. Cell lines and culture media

MCF-7 cells were a kind gift from Dr. Dipak Dutta, CDRI, Lucknow, India. MDA-MB-231, MDA-MB-453 and T47D cells were obtained from NCCS, Pune, India. MCF-7 cells were cultured in Dulbecco's Modified Eagle's medium (DMEM) medium and MDA-MB-231, MDA-MB-453 and T47D were cultured in Roswell Park Memorial Institute -1640 medium (RPMI-1640). All media contained antibiotics (100 U/mL penicillin and 100 µg/mL streptomycin). Both FBS and csFBS were heat inactivated at 56 °C for 30 min and stored as 50 mL aliquots at -20 °C until use.

3.2.2. Routine Culture and treatment conditions

Human breast cancer cell lines were cultured in a humidified chamber maintained at 37 °C with 5% CO_2. Cells lines were routinely cultured in phenol-red-containing media supplemented with 10% FBS (M1). The medium was replenished after every 48 h. The cultured monolayer was harvested upon ~80% confluence. The cells were either subcultured or seeded for experiments. In experiments involving steroid hormone stimulation, the M1 medium components were completely removed by culturing the cells in phenol-red-free and csFBS-containing medium (M2) for 24 h prior to the treatment. Seeding densities for cell lines in different culture dishes are given in table 3.2. Cells were grown in M1 and incubated until ~60% confluence at the beginning of the experiments. The monolayer was washed with DPBS, before starting the treatments, to remove the components of the spent medium. In experiments involving E2 and/or PPT treatments, the cells were pre-incubated in M2 for 24 h before starting the treatments to ensure complete removal of residual M1 components.

3.2.3. Cell counting by dye exclusion method

Cells were trypsinized and resuspended in 1 mL of fresh medium. 20 µL of cell suspension was mixed with 20 µL of trypan blue solution (0.4%) and incubated at room temperature for 3 min. Each side of the Neubauer chamber was loaded with 10 µL of the mixture and unstained live cells in 4 corner squares (1 mm × 1 mm) were counted under the

light microscope. The number of cells per mL of suspension was calculated using the following formula.

$$Number\ of cells\ per\ mL = \frac{(Number\ of\ cells\ counted)}{4} \times 10^4 \times dilution\ factor$$

Table 3.2. Cell seeding densities used in the present study.

Cell line	96-well plate	35 mm dish / 6-well plate	100 mm dish
MCF-7	1×10^4 cells/well	2×10^5 cells/well	1×10^6 cells/well
MDA-MB-231	5×10^3 cells/well	1×10^5 cells/well	5×10^5 cells/well
MDA-MB-453	1×10^4 cells/well	2×10^5 cells/well	1×10^6 cells/well
T47D	1×10^4 cells/well	2×10^5 cells/well	1×10^6 cells/well

3.3. MTT ASSAY

After the experiment, the spent medium was removed. The monolayer was washed with DPBS and treated with 100 µL MTT reagent (0.5 mg/mL) for 3 h. Excess MTT reagent was removed and formazan crystals were dissolved in DMSO. Absorbance was measured at 570 nm and 690 nm. The difference in the absorbance ($A_{570} - A_{690}$) was considered as a measure of cell viability.

3.4. CELL CYCLE ANALYSIS BY FLOWCYTOMETRY

3.4.1. Sample preparation

Cells were trypsinized and washed in phosphate-buffered saline (PBS). Thereafter, the cells were permeabilized and fixed by resuspending in ice-cold methanol for 1 h at 4 °C. After fixing, methanol was removed by PBS washes. Cells were then treated with RNase A for 30 min at 37 °C and stained with propidium iodide (PI, 20 µg/mL solution in PBS). PI-stained cells were stored at 4 °C until flow cytometry.

3.4.2. Data acquisition and analysis

PI-stained cells were analyzed by FACSCalibur (Becton, Dickinson and Company, USA) in FL2 channel (585/42 bandpass filter). A dot plot of FL2-area *vs.* FL2-width was used to discriminate doublets. The distribution of cells at different stages of the cell cycle was estimated using FCS Express 6 software. Histogram of FL2-area for the gated population was plotted for the visual representation of cells in various stages of cell cycle.

3.5. siRNA TRANSFECTION

Cells were seeded in 6-well plates and allowed to grow for 48 h. Lipofectamine® RNAiMax transfection reagent was used for siRNA transfection according to the manufacturer's instructions. Equal volumes of the transfection reagent and the siRNA were mixed to obtain a final siRNA concentration of 0.1 µM. The RNA to reagent ratio of 1:3 (v/v), was maintained in all the experiments and every well of a 6-well plate received 25 pmol of siRNA. 250 µL of the complex was added to each well, containing 2.5 mL media and swirled gently to mix the contents. Cells were incubated with the complex for 24 h, before proceeding to subsequent steps.

3.6. GENE EXPRESSION ANALYSIS

3.6.1. Primers

All the primers were manually designed. The primers for gene expression analysis were designed with the preferred conditions of 20 bases long and 60% GC content. Primers were strategically designed to amplify each transcript variant of GPER1 specifically. A separate set of primers (GPER1 3'UTR) was designed in the 3'UTR region to represent the total GPER1 by simultaneously amplifying all the three variants. The sequences and their PCR conditions are given in supplementary table 3.1. In all the experiments, involving the assessment of GPER1 mRNA levels, the expression of all the three transcript variants was quantified. The total GPER1 transcripts were quantified only in those experiments where the genomic-DNA (gDNA) carry over in the total RNA preparations was not detected.

3.6.2. Total RNA isolation and cDNA synthesis

Total RNA was isolated using TRIzol (Invitrogen Corporation, Grand Island, NY, USA), or a similar RNA extraction reagent prepared in-house. It was treated with DNaseI (New England Biolabs, Ipswich, MA, USA) to remove DNA contamination, and cleaned-up using RNeasy® mini kit (Qiagen, Valencia, CA, USA). RNA integrity was checked by agarose gel electrophoresis and quantified using BioSpectrometer® (Eppendorf, Hamburg, Germany). Typically, 2 µg of total RNA was reverse transcribed using High-Capacity cDNA Reverse Transcription kit as per the manufacturer's instructions.

3.6.3. Routine RT-PCR and quantitative real-time RT-PCR

cDNA equivalent to 20 ng of total RNA was used as the template for PCR reactions with gene-specific primers (Supplementary table 3.1). RPL35A served as an internal control. In the case of routine RT-PCR, the PCR products were resolved on 2% agarose gels and the images of ethidium bromide stained bands were captured using Gel Doc™ EZ Imager (Bio-Rad Laboratories, Hercules, CA, USA). Images were processed with ImageJ[135]. Inverted and background subtracted images are presented throughout this thesis.

For quantitative real-time RT-PCR (qRT- PCR) Applied Biosystems® 7500 real-time PCR platform was used. Reactions were set up in 1X AmpliTaq Gold PCR master mix supplemented with 0.6X SYBR Green (Invitrogen, Carlsbad, CA, USA). ROX dye served as a passive reference. Each sample was analyzed in triplicates for all gene-specific primer pairs (Supplementary table 3.1). RPL35A served as an internal control. Expression levels of genes in test samples relative to control were analyzed by $\Delta\Delta C_t$ method[136].

3.7. GENERATION OF POLYCLONAL ANTIBODY

3.7.1. Immunization and immune serum collection

Polyclonal antibody generation and peptide affinity purification were performed by Abgenex Pvt. Ltd., Bhubaneswar, INDIA. N-terminus Peptide of GPER1 (MDVTSQARG-VGLEMYPGTAQPAA)[10] was chemically synthesized with an extra cysteine residue at the

C-terminus of the peptide and cross-linked to keyhole limpet hemocyanin (KLH) using maleimide-sulfhydryl chemistry. KLH was activated by treating with sulfosuccinimidyl 4-(N-maleimidomethyl) cyclohexane-1-carboxylate (Sulfo-SMCC). Maleimide-activated KLH was then purified by gel filtration chromatography and mixed with peptide for crosslinking. The efficiency of conjugation was assessed by comparing the free sulfhydryl groups in peptide before and after conjugation using Ellman's reagent. Two New Zealand White Rabbits (A and B) were immunized with KLH conjugated peptide in complete Freund's adjuvant (CFA) or incomplete Freund's adjuvant (IFA), after the collection of pre-immune serum. First immune serum was collected after primary immunization (200 µg antigen/rabbit in CFA) followed by five boosters (100 µg antigen/ rabbit in IFA). Subsequently, the second and third batches of immune sera were collected after 6^{th} and 7^{th} boosters, respectively.

3.7.2. Affinity purification

The column was filled with 6 mL of sulfo-link coupling resin slurry and was equilibrated with four resin bed volume (RBV) of coupling buffer. Peptide column was prepared by mixing 5 mL of peptide solution (6 mg of GPER1 N-terminus peptide, dissolved in 5 mL of coupling buffer) with equilibrated resin at room temperature for 15 min followed by overnight incubation at 4 °C. On day two, the peptide column was equilibrated to room temperature and then washed with three RBV of coupling buffer. The unbound surface of the resin was blocked using one RBV of 50 mM L-cysteine (prepared in coupling buffer) by mixing at room temperature for 15 min and then at 4 °C overnight. On day three, the column was washed with six RBV of 1 M NaCl and then with two RBV of degassed PBS. 10-12 mL of hyper-immune serum was filtered through Whatman paper and diluted with PBS (1:1). The diluted hyper-immune serum was mixed with the peptide-linked resin and incubated on a shaker for 4 h at room temperature. Non-bound components were removed by washing the column with six times the column volume of PBS. Bound protein was eluted using elution buffer (50 mM Glycine-HCl, pH 2.7) as 1 mL fractions and each fraction was neutralized with 100 µL of neutralization buffer (1 M Tris-HCl, pH 8.0, 1.5 M NaCl, 1 mM EDTA, 0.5% sodium azide). Eluted fractions with high absorbance at 280 nm were pooled and dialyzed against 1 L PBS. The purified protein was stored at 4 °C after adding sodium azide (final concentration 0.05%).

3.7.3. Indirect ELISA

On day 1, the peptide antigen (200 ng/well) was coated on a 96-well plate (Nunc-Immuno plate, Cat. No. 439454, F96 Cert. MaxiSorp) for 2 h at room temperature followed by overnight at 4 °C. On day 2, the plates were kept on a shaker at room temperature for 2 h. The wells were then washed with PBS containing 0.05% Tween 20 (PBST), followed by blocking with 5% skimmed milk in PBST for 1 h. Wells were again washed three times with PBST. 100 µL of pre-immune serum (PIS), hyper-immune serum or peptide-affinity-purified antibody, diluted 1:5000 in PBST containing 1% skimmed milk, was added to each well and incubated for 2 h at room temperature. The wells were washed as above. 100 µL of HRP-conjugated secondary antibody (1:5000 diluted in PBST containing 1% skimmed milk) was added to each well and incubated for 1 h. After three washes with PBST, 100 µL of 1X TMB/H_2O_2 solution was added and kept in the dark for 3-5 min. Thereafter, the 96-well plate was read at 450 nm.

3.8. WESTERN BLOTTING

3.8.1. Total protein isolation and quantification

Total protein was isolated either from the organic phase of TRIzol® lysates or by lysing the cells in ice-cold radioimmuno precipitation assay (RIPA) buffer containing protease inhibitor cocktail (TAKARA, CA, USA). In case of TRIzol® lysates, total protein was isopropanol-precipitated from the organic phase and washed with 95% ethanol containing 0.3 M guanidinium chloride. The pellets were solubilized in 1% SDS solution by sonication for 15 sec at 25% amplitude. The insoluble fraction was separated by centrifugation at 15,000 × g for 15 min at 4 °C. The supernatants were transferred to fresh tubes and stored at -20 °C until use. Total protein was estimated by Lowry's method[137]. Bovine serum albumin (BSA) standards were used to generate a standard curve and unknown concentrations were determined by interpolation. The assay was performed in the total reaction volume of 1.2 mL. For each sample, the reaction was set up in triplicates. At the end of the reaction, 200 µM of the solution was transferred into 96-well plate and

absorbance was measured at 750 nm. Reactions containing BSA standards contained an equivalent volume of lysis buffer to negate the effect of buffer components.

3.8.2. SDS-PAGE, transfer and detection

Equal quantities of total protein were resolved by 10% SDS-PAGE and transferred to nitrocellulose membrane using semi-dry transfer method. Blotting was done at 18 V for 90 min. After the transfer, blots were stained with Ponceau S and imaged in ChemiDoc XRS+ system (Bio-Rad Laboratories, Hercules, CA, USA). Ponceau S stain was removed by washing in PBS for 5 min followed by a 5 min wash with Tris-buffered saline containing 0.05% Tween 20 (TBST). The blots were blocked in 1% gelatin in TBST for 1 h at room temperature and then probed with primary antibody diluted in 0.1% gelatin in TBST for 1 h at room temperature. Blots were washed for 30 min with TBST (3 × 10 min) to remove unbound antibody. Blots were then incubated with the HRP-tagged secondary antibody (1:5000 dilution in 0.1% gelatin in TBST) for 1 h followed by three TBST washes of 10 min each. Bands were visualized with enhanced chemiluminescence reagent (Bio-Rad Laboratories, Hercules, CA, USA). Images were captured with Chemidoc XRS+ system and analyzed using Image Lab software.

3.9. IMMUNOHISTOCHEMISTRY (IHC)

Immunohistochemical procedures were performed in the Department of Pathology, NEIGRIHMS (North Eastern Indira Gandhi Regional Institute of Health and Medical Sciences), Shillong, India, under the supervision of Dr. Vandana Raphael and her colleagues.

3.9.1. IHC staining

Sections (4 µm thick) were cut from the paraffin-embedded blocks and mounted on silane-coated microscopic slides. They were then incubated overnight in hot air oven set at 60 °C in order to remove any water trapped between the slide and the section. Slides were deparaffinized and rehydrated by incubating in xylene for 5 min followed by decreasing concentrations of ethanol (90%, 80% and 70%) and water. Slides were then processed for antigen retrieval in citrate buffer (10 mM, pH 6) by heating in the microwave oven for 10

min at 450 W followed by 15 min at 600 W. The slides were allowed to cool and then rinsed once with PBS. Immunohistochemical staining was done using Super Sensitive™ IHC detection system from BioGenex Laboratories (CA, USA) as per the manufacturer's instructions. Briefly, endogenous peroxidase activity was quenched by peroxide block for 10 min followed by three PBS washes of 5 min each. Sections were then probed with primary antibody for 1h at a dilution of 1:50. Sections were then incubated with super enhancer (20 min), polymer-HRP (30 min) and DAB substrate (10 min). After each step, the excess reagent was removed by three PBS washes of 5 min each. DAB staining was stopped by rinsing the slides in running tap-water. Sections were counter-stained with Harris hematoxylin and dehydrated by incubating in increasing concentrations of ethanol followed by xylene. Slides were air-dried and mounted using DPX mountant and observed under a light microscope.

In the case of peptide blocking experiment, the complete setup had 4 slides of serial sections. These slides were incubated with the anti-GPER1 antibody (+ve control), anti-GPER1 antibody pre-incubated with the peptide (blocked antibody) or peptide resuspension buffer for 1 h (resuspension buffer control), or no primary antibody (-ve control). The peptide blocking was performed on two independent samples. The peptide blocking validation results are presented in Chapter 4[134].

3.9.2. Evaluation of immunostaining pattern

Each slide was examined under a light microscope without the knowledge of the patient's other data. According to the intensity of staining of neoplastic cells and the percentage of positive cells, the results of immunostaining in tissues were scored. All the IHCs were examined and scored by two independent observers.

Modified semi-quantitative scoring of IHC for GPER1 was done only for the cytoplasmic staining. The staining intensity was classified as negative (-), very weak (1+), weak (2+) and strongly positive (3+). H score was calculated by multiplying the intensity score with percentage of positive cells giving a score ranging from 0 to 300. In every batch of slides, normal tissue within the biopsy was taken as internal control and slide with no primary antibody was taken as negative control. In the present study, though an occasional tumor

showed membrane and nuclear positivity, GPER1 staining was predominantly cytoplasmic. The H score of the normal breast tissue was less than 100 in 29/35 cases and ranged from 80-90 mostly, and stained mainly the cytoplasm. H score, which takes into consideration of both the staining intensity and the percentage of cells, of more than 40 was taken as positive in the present study.

For ER, PR, and HER2 staining, the paraffin embedded sections of the tumor were stained by monoclonal antibodies raised against ER (Dako, Denmark, Clone EP1), PR (Dako, Denmark, Clone PgR 636) and HER2 (Dako, Denmark, Clone c-erb-2 polyclonal oncoprotein), respectively. Immunoreactivity for ER and PR was classified into the following three categories based on the percentage of tumor cells showing nuclear reactivity. The staining intensity was classified as negative (-), very weak (1+), weak (2+) and strongly positive (3+). H score was calculated by multiplying the intensity score with percentage of positive cells giving a score ranging from 0 to 300. Cytoplasmic staining was considered non-specific and not scored. Normal tissue within the biopsy was taken as internal control and a known positive was run with every batch of slides and slide with no primary antibody was taken as negative control.

Positivity for HER2 was calculated based on the membrane positivity and followed CAP/ASCO guidelines[138]. Based on which the samples were classified as 0 (negative) when no staining is observed or membranous staining is observed in less than 10% of the tumor cells, 1+ (negative) when a faint/barely perceptible staining is detected in more than 10% of the tumor cells, 2+ (equivocal) when a weak to moderate complete membrane staining is observed in more than 10% of the tumor cells OR strong complete membranous staining in less than 30% of tumor cells and 3+ (positive) when a strong complete membrane staining was observed in more than 30% of tumor cells. In all equivocal cases, HER2-FISH was performed for further characterization. Cytoplasmic staining is considered nonspecific and negative.

3.10. MICROARRAY EXPERIMENTS

3.10.1. RNA isolation, labeling, hybridization and image acquisition

Experimental procedures for microarray starting from total RNA isolation to the extraction of raw signal intensities were carried out by Genotypic Technology (P) Ltd., Bangalore, India. Total RNA was extracted from TRIzol® lysates and purified using RNeasy® Mini Kit. RNA concentrations were determined based on absorbance at 260 nm wavelength of light. The quality of RNA was assessed on Agilent 2100 Bioanalyzer (Agilent Technologies, Paulo Alto, CA, USA). RNA samples were considered to be of good quality if they satisfied the following criteria a) A_{260}/A_{280} ratio > 1.8, and b) RNA integrity number > 7. All our total RNA samples satisfied these criteria. The RNA quality control data are provided in supplementary table 3.3. For each sample, 500 ng of total RNA was labeled (Cy3) using Agilent's Low Input RNA linear amplification kit (Cat No. 5188–5339). The labeled complementary RNAs were purified using RNeasy® Mini Kit, checked for quality (Supplementary table 3.4) and hybridized to Agilent' s human gene expression study 8 × 60 K microarray slides (AMADID:27114), using the Agilent's in-situ hybridization kit (Cat No. 5184–3568). Following hybridization and washes, the images were scanned in a microarray scanner (Model G2565BA, Agilent). The raw intensity data were extracted using Agilent's Feature Extraction Software. The images were manually checked for uneven hybridizations, streaks, blobs and other artifacts. Images were found to be clean with low background noise.

3.10.2. Data analysis

The microarray data, obtained as raw signal intensities, was analyzed in R platform using LIMMA package from Bioconductor[139]. Background correction was performed using "normexp" method, with an offset of 16[140]. The "quantile" method was used for normalization of the data between arrays. Further, the "avereps" function was used to average replicate spots. We applied "lmfit" (linear model) and "eBayes" (Empirical Bayes method) for determination of differentially regulated genes. The R code used for processing of the data is as follows:

```
Library (limma)

Targets = readTargets ("targets.txt")
```

```
x = read.maimages (targets, source = "agilent", green.only = TRUE)

y = backgroundCorrect (x, method = "normexp", offset = 16)

y = normalizeBetweenArrays (y, method = "quantile")

y.ave = avereps (y, ID = y$genes$ProbeName)

f = factor (targets$Condition, levels = unique(targets$Condition))

design = model.matrix (~0+f)

colnames (design)=levels(f)

fit = lmFit(y.ave, design)

contrast.matrix = make Contrasts ("T1-C", "T2-C", levels= design)

fit2 = contrasts.fit(fit, contrast.matrix)

fit2 = eBayes(fit2)

output = toptable (fit2, adjust = "BH", coef= "T1-C ", gene list =
y.ave$gene , number = Inf)

write.table (output, file = "T1-C.txt", sep="\t", quote = FALSE)

output = toptable (fit2, adjust = "BH", coef= "T2-C ", gene list =
y.ave$gene , number = Inf)

write.table (output, file = "T2-C.txt", sep="\t", quote = FALSE)
```

3.11. DNA METHYLATION ANALYSES

3.11.1. Modified COBRA assay

The combined bisulfite restriction analysis (COBRA) assay described earlier[141] was modified to avoid the use of radiolabeled tracers and differs in terms of visualization of the restriction fragments post-amplification of bisulfite converted gDNA. gDNA was isolated from 10^6 cells using PureLink® genomic DNA kit (Invitrogen, Carlsbad, CA, USA). 1 µg gDNA was used for bisulfite conversion using EpiJET™ Bisulfite Conversion Kit (Thermo Scientific, Pittsburgh, PA, USA). Primers were designed such that the amplicons did not contain any CpG dinucleotides in the priming region. For every region to be amplified two sets of primers were designed to separately amplify gDNA and bisulfite converted gDNA with the assumption that bisulfite conversion efficiency will be 100%. Using the AmpliTaq Gold® 360 master mix, PCR for 40 cycles was carried out to amplify the region of interest

using 20 ng of bisulfite converted gDNA as the template. The cycling conditions were 95 °C for 20 s, annealing temperature (Supplementary table 3.2) for 20 s and 72 °C for 30 s. Products amplified in 20 µL reactions in duplicates were pooled and gel purified using gel purification kit. Equal quantities of gel purified PCR products were digested in 20 µL reaction volumes with 2 units of BstUI or TaqI for 12 h. Negative control reactions without the enzyme were included for every digestion reaction. Equal quantities of amplified fragments generated using unconverted gDNA were used as positive controls for enzyme activity and to ensure that the incubation time for restriction digestion was sufficient for complete digestion. Digested products were resolved in 6% TBE-PAGE. The DNA fragments were stained with ethidium bromide and images were captured with Chemidoc-XRS+ gel documentation system. The images were processed in ImageJ[135] and inverted images are presented.

3.11.2. Bisulfite sequencing

The upstream CpG island region (upCpGi) amplicons generated using bisulfite-converted gDNA, as described in the previous section, were ligated to linearized pGEM®-T Easy vector (Promega, Madison, WI, USA) or pMD-19 vector (TAKARA, Dalian, China) as per manufacturer's instructions. Competent cells of *E. coli* DH5α were transformed with the ligation mix and recombinant colonies were selected in the presence of the appropriate antibiotic. Plasmids were isolated from recombinant colonies, and their inserts were sequenced. The sequence of the expected amplicon was retrieved from NCBI and cytosine bases were manually converted to thymine assuming that all the CpG sites are methylated. This *in silico* converted template was used to assess the methylation status by pairwise alignment using ClustalW[142]. The methylation status of all the CpG sites in each of the inserts was represented as a lollipop model.

3.12. TCGA DATA ANALYSIS

TCGA (The Cancer Genome Atlas) is a cancer genomics project by the National Cancer Institute (NCI), in collaboration with National Human Genome Research Institute (NHGRI). This project consists of 7 genome-wide data types for 11,000 patients across 33

cancer types. While on the verge of the project completion the team has made most of the genomic data publically available. We have used the breast cancer (BRCA) transcriptome (RNA-Seq) and methylation (Infinium® Human Methylation-450K Bead Chip) data from TCGA-BRCA dataset[143]. The data were retrieved from TCGA using the UCSC Cancer Genomics Browser[144]. For RNA-Seq data, mRNA expression values (log_2 transformed) of all the genes were retrieved. For methylation data, beta values of all the probes corresponding to GPER1 locus were retrieved.

3.12.1. Analysis of associations between GPER1 mRNA expression and histo-pathological parameters

Out of 1215 RNA-Seq records, 1102 were for tumor samples and 113 were for normal breast tissue. The tumor samples were classified based on either the expression status of ERα, PR and HER2, or the molecular subtypes (PAM50). The information about the expression status of ERα, PR and HER2, determined by IHC, was available in the dataset. The GPER1 mRNA expression values of the tumor samples, in each of the above-mentioned groups, were retrieved from the expression table. The expression data was represented as box plots and the differences in the mean GPER1 mRNA expression was tested either by a Welch two-sample *t*-test (for 2 groups) or ANOVA followed by a Tukey's HSD (for multiple groups). For association studies, the tumor samples were classified into GPER1-high and -low using the median expression value as a cut-off. The association of GPER1 expression with ERα, PR, HER2, tumor stage, and molecular subtypes was assessed by chi-square test in Microsoft Excel.

3.12.2. Survival analysis

Expression and survival data from several breast cancer cohorts were accessed through the Kaplan-Meier (KM) Plotter online tool (www.kmplot.com)[145]. Tumor samples were divided into two groups (GPER1-high and GPER1-low) using the median expression value as the threshold. As suggested by the KM Plotter guidelines, the JetSet best probe "210640_s_at" for GPER1 was used for the analyses. The association between GPER1 expression and survival (overall and relapse-free) was graphically represented as Kaplan-Meier plots using the default settings.

3.12.3. Expression-methylation correlation (EMC) analysis using TCGA-BRCA data

Out of 1215 samples in the TCGA-BRCA dataset[143], 870 samples (84 normal and 786 tumors) have paired expression and methylation data. Out of these, we chose only the 786 tumor samples (781 primary and 5 metastatic) for our analyses. Data were integrated with respect to sample IDs in MS Excel. For a probe-wise analysis of the relationship between GPER1 expression and methylation, two approaches were used. In EMC analysis, the GPER1 expression data and probe-wise methylation data across the tumor samples were analyzed by Spearman rank correlation test using the R statistical package. The correlation was judged on the basis of the Spearman's rho (ρ) and its *p*-value. Additionally, tumors were first classified into hypo-methylated or hyper-methylated groups based on a beta value threshold of 0.3 for a given probe. This threshold has been employed earlier[146]. This was followed by a probe wise analysis of the difference in the mean GPER1 expression in hypo- and hyper-methylated groups using a Welch two-sample *t*-test.

3.13. ChIP-Seq ANALYSIS

Breast cancer-related studies in the Sequence Read Archival (SRA) database were searched for ERα related ChIP-Seq studies in MCF-7 cells. The subset of files from the project ERP000380 was selected and the details of the files are tabulated in table 3.3. The complete analysis was performed in Galaxy web-based platform[147]. The quality of all the input read files were assessed by FASTQC[148] with the default settings. The quality scores were converted to Sanger quality type by FASTQ Groomer[149]. Reads were mapped to reference human genome (hg19) using "Map with Bowtie for Illumina" tool[150]. Reads mapping to multiple locations were discarded and unmapped reads in the output SAM file were filtered using "Filter SAM or BAM, output SAM or BAM" tool[151]. The genomic regions enriched by reads were identified by MACS (Model-based analysis of ChIP-Seq) tool[152]. The peaks were visualized in UCSC genome browser[153] after converting Wig files to bigWig files using "Wig/BedGraph-to-bigWig" tool.

Table 3.3. Read files used in ChIP-Seq analysis.

SRA_ID	Sample name	Antibody	Read length
ERR022025	Vehicle_BR1	ER-alpha	42bp
ERR022026	E2_BR1	ER-alpha	42bp
ERR022027	TAM_BR1	ER-alpha	42bp
ERR022018	Vehicle_BR1	ER-alpha	45bp
ERR022021	E2_Si-control_BR1	ER-alpha	42bp
ERR022023	E2_Si-FOXA1_BR1	ER-alpha	42bp
ERR022054	input_BR1	IgG	36bp
ERR022055	input_BR2	IgG	36bp

3.14. STATISTICAL ANALYSES

All the quantitative data have been represented as mean ± SD. The number of replicates for each experiment has been indicated in respective figure legends. The digital images were quantified using ImageJ or Image Lab software. The association of GPER1 expression status with clinicopathological parameters was tested for statistical significance using non-parametric chi-square test, Fisher's exact test, or Mann-Whitney U-test. The difference in means between two groups was tested using student's *t*-test. Multiple comparisons were performed using one-way ANOVA followed by Tukey's HSD test. The correlation of GPER1 mRNA expression with other breast cancer molecular markers was tested by Pearson's correlation test. In experiments related to estrogen-mediated regulation of GPER1 expression the difference between means of two groups was tested by Welch two-sample *t*-test and in case of multiple groups, one-way ANOVA followed by Tukey's HSD test was used. Bisulfite sequencing results were analyzed by non-parametric chi-square test. The correlation between CpG site methylation and GPER1 expression across clinical breast tissue samples was analyzed by Spearman's rank correlation test. MTT assay results were analyzed by one-way ANOVA followed by Tukey's HSD test. In all the statistical analyses $p < 0.05$ was considered as statistically significant. The level of significance designated statistically significant are as follows: * $p < 0.05$, ** $p < 0.01$, *** $p < 0.001$.

Chapter IV

Generation of an anti-GPER1 polyclonal antibody for analysis of GPER1 protein expression

The results presented and discussed in this chapter are published in Manjegowda et al., (2016), Data in Brief[133]

4.1. INTRODUCTION

To understand the role of GPER1 in physiology and pathology, it is important to be able to specifically detect and localize it in cells and tissues. Antibodies specific to GPER1 are commercially available, which have been used in earlier published investigations[21,85,88,90,102,154–156]. However, there are inconsistencies in the data generated from *in vitro*, *in vivo* and clinical studies. For instance, the calculated molecular weight of GPER1 is 42.24 kDa, but the apparent molecular weight of GPER1 from the published western blotting results range from 35 kDa to 100 kDa[21,85,88,90,102,154–156]. Immuno-histochemical studies have detected GPER1 protein in the cytosol[10,17,74,84–86], plasma membrane[22,39,80–82,87], and the nucleus[17,20,84,90]. These conflicting observations about the localization of GPER1 are prevalent in cell line models as well[10,82,91].

Considering the scope of the research work presented in the thesis, a polyclonal peptide-affinity-purified antibody was generated. The detailed methodology used for generation of this antibody is described in section 3.7 of Chapter 3. Here, the data for characterization and validation of the antibody using western blotting and immunohistochemistry are presented.

4.2. RESULTS

4.2.1. Polyclonal anti-GPER1 antibody generation and affinity purification

A total of six batches of hyper-immune serum were obtained, three batches per rabbit. The protocol is described in the section 3.7.1 of Chapter 3. The first and the third batches of hyper-immune serum were tested for their performance by indirect ELISA. The pre-immune sera (PIS) served as negative controls. The hyper-immune sera collected from rabbit-B were more reactive as compared to those from rabbit-A (black bars, Figure 4.1). The hyper-immune serum, harvested from the third bleed of rabbit-B (RB3), was found to be the most reactive.

RB3 was tested for its performance by western blotting. A western blot of total protein from breast cancer cell lines showed a prominent band of ~52 kDa (black arrow),

corresponding to GPER1, along with other non-specific signals (Figure 4.2.A). This band was not obtained in blots treated only with the HRP-tagged secondary antibody (Figure 4.2.B). In order to authenticate the specific signal corresponding to GPER1 protein, we performed western blotting with the total protein of four breast cancer cell lines, namely MCF-7, MDA-MB-231, T47D, and BT474. Comparison of HRP signals, obtained in blots probed with RB3 (Figure 4.3.A) and PIS (Figure 4.3.B), clearly showed that the prominent band of ~52 kDa (black arrow) represented the specific signal.

To reduce the non-specific bands, RB3 was subjected to peptide affinity purification (described in section 3.7.2 of Chapter 3). After the affinity purification, 1.8 mL of purified antibody was obtained with a concentration of 0.75 mg/mL protein. Immunoreactivity of the affinity-purified antibody was again confirmed by indirect ELISA (Figure 4.4). ELISA results showed that the reactivity against the peptide was retained after affinity purification. Thereafter, the performance of the purified antibody was assessed by western blotting analysis of the total protein of breast cancer cell lines. The quality of the blots, in terms of the specific signal detection, was greatly enhanced when probed with the affinity-purified antibody as compared to those probed with RB3. A single prominent band of ~52 kDa (indicated by a black arrow), with the negligible non-specific background, was observed (Figure 4.5.A). The relative mRNA levels of GPER1 in the same panel of breast cancer cell lines were assessed by qRT-PCR. The relative GPER1 protein levels in the breast cancer cell lines were similar to the GPER1 mRNA levels estimated by qRT-PCR (Figure 4.5.B).

4.2.2. Immunohistochemical assessment of the peptide-affinity-purified antibody

4 µm thick serial sections of paraffin-embedded breast cancer tissues were mounted on microscope slides. The sections were processed for immunohistochemistry as described in section 3.9 of Chapter 3. The peptide-affinity-purified antibody, when used alone or with the peptide dilution buffer, produced cytoplasmic staining (brown) of the tumor cells against hematoxylin stained nuclei (blue) (Figure 4.6 D and C, respectively). On the other hand, secondary antibody alone or the peptide-affinity-purified antibody, which was pre-incubated with a 6-fold excess of the peptide, did not produce any staining (Figure 4.6 A and B, respectively).

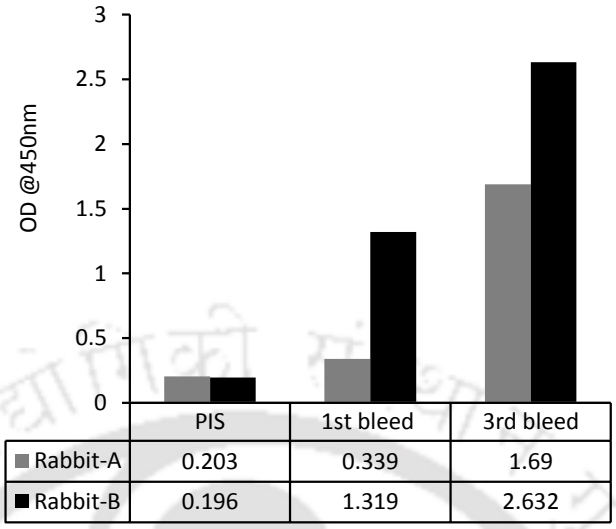

	PIS	1st bleed	3rd bleed
Rabbit-A	0.203	0.339	1.69
Rabbit-B	0.196	1.319	2.632

Figure 4.1. Indirect ELISA for testing the reactivity of hyper-immune serum. Hyper-immune sera, harvested from first and third bleeds of two rabbits (A and B) were compared with their respective pre-immune sera (PIS) by indirect ELISA. The detailed protocol is described in the section 3.7.3 of Chapter 3.

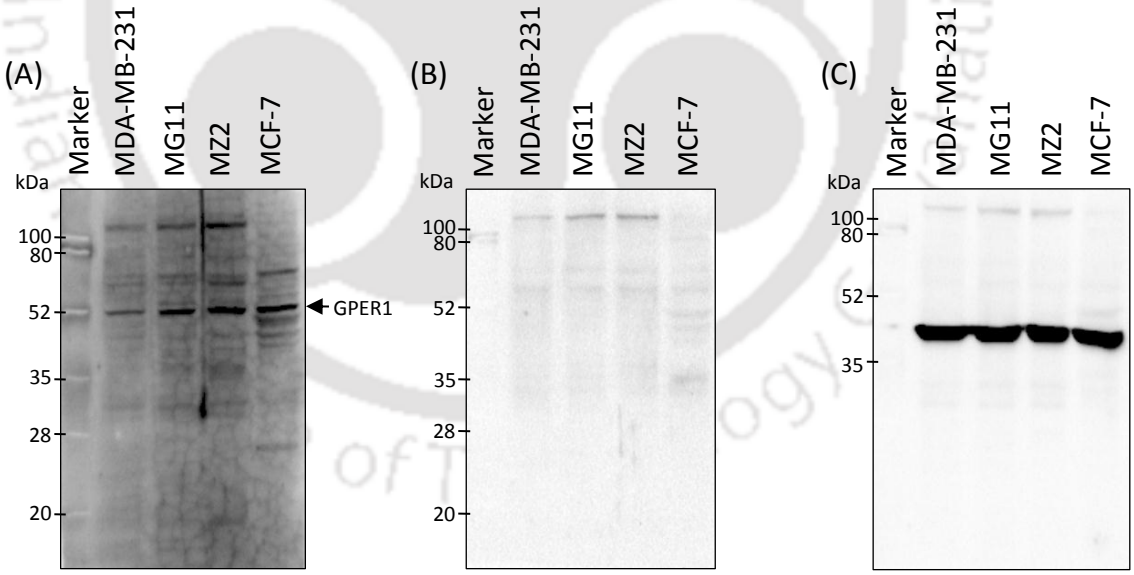

Figure 4.2. Quality assessment of RB3. Total proteins from the indicated breast cancer cell lines were fractionated by 10% SDS-PAGE under denaturing conditions and were transferred to nitrocellulose membranes. Membranes were probed with 1:1000 dilution of RB3 (A), no primary antibody (B), or 1:5000 dilution of a commercial anti-β-actin antibody (C) followed by the HRP-conjugated secondary antibody. The membranes were processed for chemiluminescence detection using ECL reagent. Images were captured in Chemidoc XRS+ system.

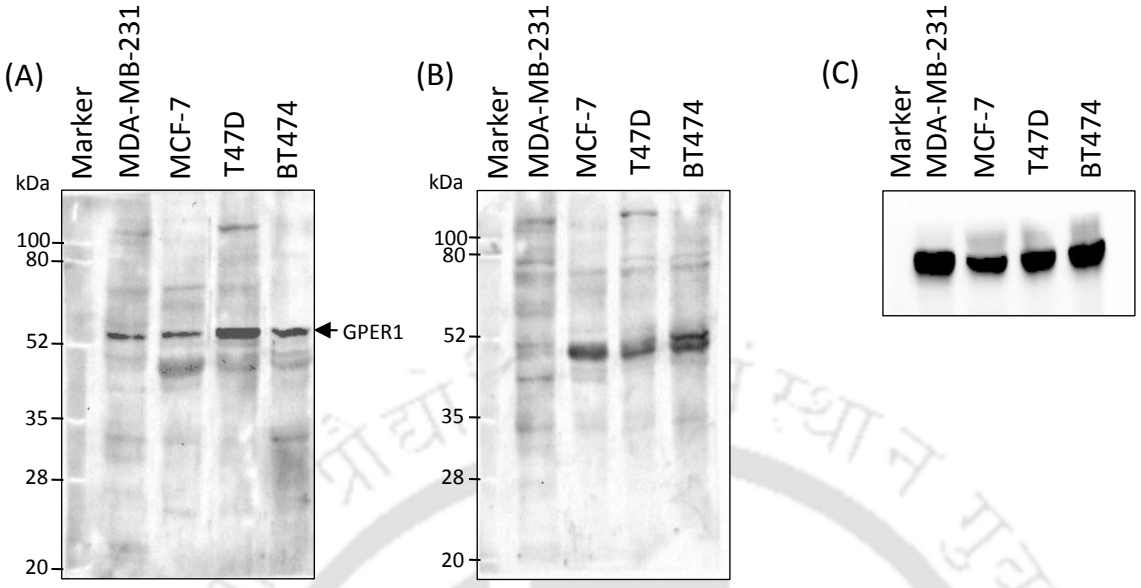

Figure 4.3. Assessment of RB3 specificity. Total proteins from the indicated breast cancer cell lines were fractionated by 10% SDS-PAGE under denaturing conditions and were transferred to nitrocellulose membranes. Membranes were probed with 1:10,000 dilution of RB3 (A), 1:10,000 dilution of PIS of rabbit-B (B), or 1:5000 dilution of a commercial anti-β-actin antibody (C) followed by HRP-conjugated secondary antibody. The membranes were processed for chemiluminescence detection using ECL reagent. Images were captured in Chemidoc XRS+ system.

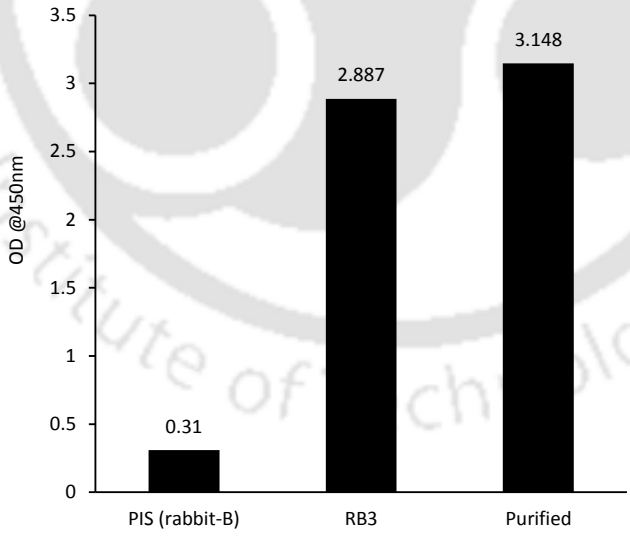

Figure 4.4. Indirect ELISA for testing the reactivity of the peptide-affinity-purified antibody. After the peptide-affinity purification, the immunoreactivity of the purified antibody was tested by indirect ELISA (described in section 3.7.3 of Chapter 3). For comparison, the reactivity of RB3 and the corresponding PIS was also used.

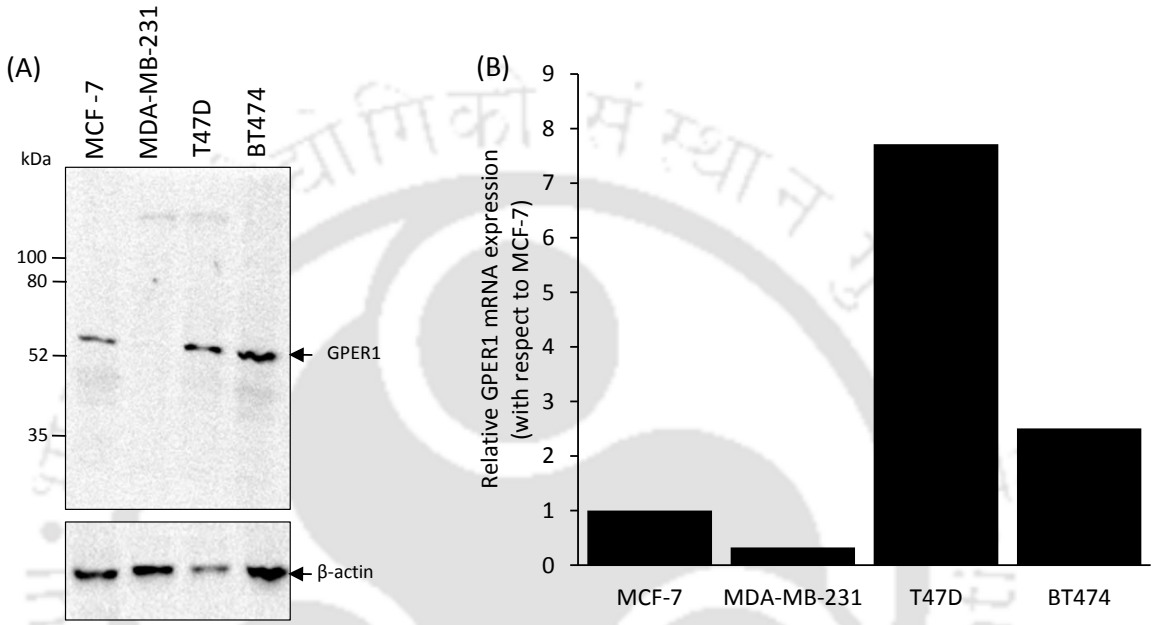

Figure 4.5. Detection of GPER1 by peptide-affinity-purified antibody. GPER1 expression in breast cancer cell lines was detected at protein and mRNA levels by western blotting (A) and qRT-PCR (B), respectively. Total proteins from the indicated breast cancer cell lines were fractionated by 10% SDS-PAGE under denaturing conditions and were transferred onto nitrocellulose membranes. Membranes were probed with the primary antibodies against GPER1 or β-actin followed by HRP-conjugated secondary antibody. The peptide-affinity-purified antibody was used at a dilution of 1:15,000 and the anti-β-actin antibody was used at a dilution of 1:5000. The membranes were processed for chemiluminescence detection using ECL reagent. Images were captured in Chemidoc XRS+ system. Total RNA was isolated from breast cancer cell lines cultured in M1 medium. The RNA preparations were treated with DNaseI and purified by isopropanol precipitation. 2 µg of total RNA was taken for cDNA synthesis and cDNA equivalent to 20 ng of total RNA was taken as the template for the PCR reactions. GPER1 3'UTR primer set was used to assess the representation of total GPER1 mRNA (Supplementary table 3.1). The results are represented as relative expression of GPER1 mRNA with respect to that in MCF-7 cells. RPL35A was considered as normalizing control. The bar graph shows the result of one biological replicate. The relative expression was computed from the mean of C_t values of three technical replicates.

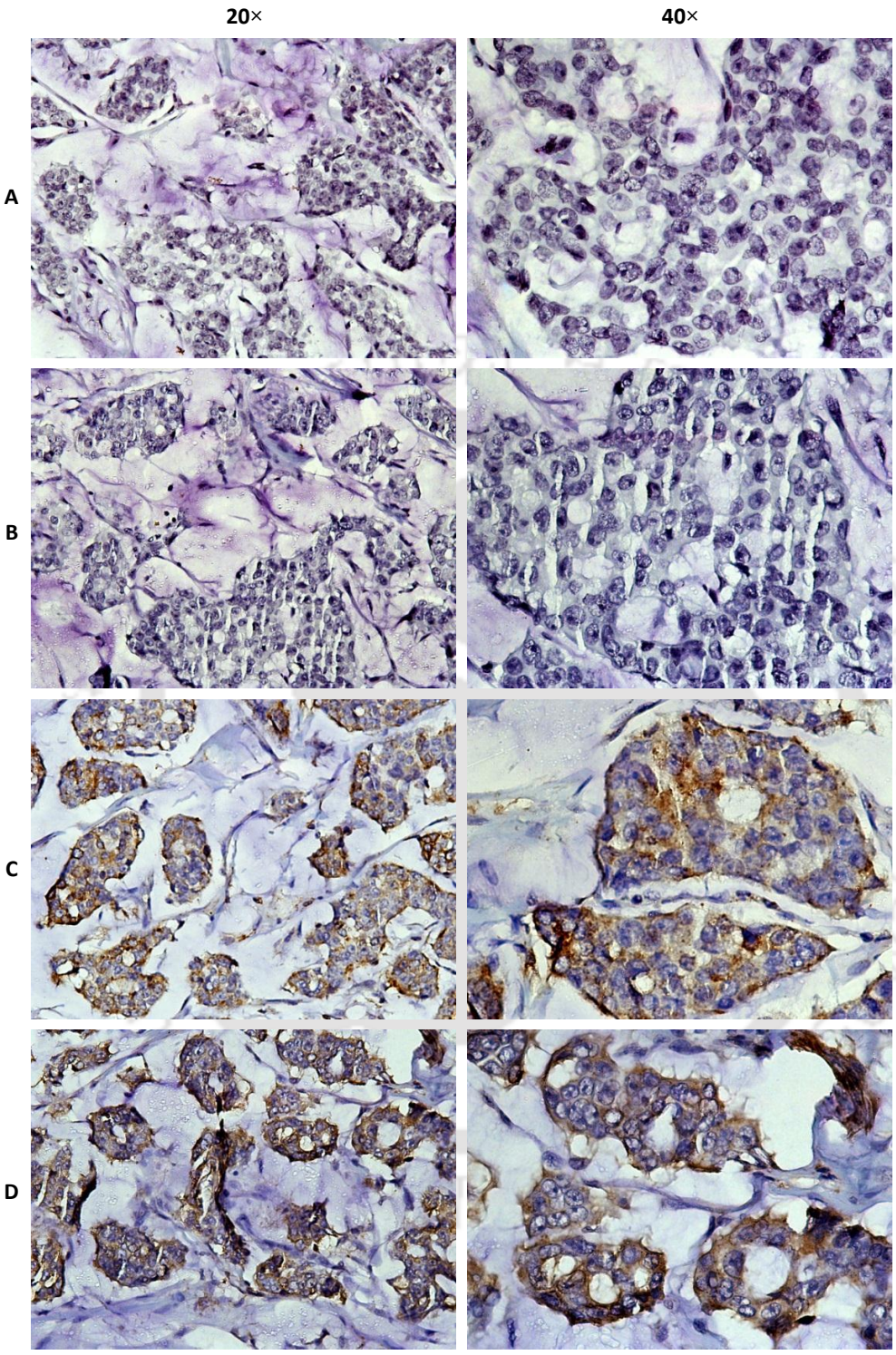

Figure 4.6. Specific detection of GPER1 in breast cancer tissue sections. Immunohistochemical staining was performed as described in section 3.9 of Chapter 3. The tissue sections were probed with no antibody (A), peptide-affinity-purified antibody pre-incubated with the 6-fold excess of peptide (B), peptide-affinity-purified antibody pre-incubated with equivalent volume of peptide resuspension buffer (C) or peptide-affinity-purified antibody (D), for 1 h at a dilution of 1:50. In case of (B) and (C), the peptide-affinity-purified antibody was incubated with peptide (B) and peptide resuspension buffer (C) for 1h before using on sections.

4.3. DISCUSSION

Generating a polyclonal antibody in-house is advantageous in many respects. It ensures sufficient quantity of the antibody at an affordable price and potentially bypasses the problems associated with batch-to-batch variability. At the same time, the requirement of sufficient antibody for proper optimization of the detection protocols and thorough assessment of the specificity is also fulfilled. Here, we have generated a polyclonal peptide-affinity-purified antibody, against the N-terminus of human GPER1. Henceforth in this thesis, the peptide-affinity-purified antibody is referred as the anti-GPER1 antibody. The sequence of the peptide antigen was adapted from the work of Revankar and co-workers[10].

Our western blotting analysis demonstrated a prominent ~52 kDa band for GPER1. Reports from others[21,88,102,155] also show the detection of GPER1 with similar apparent molecular weight in breast cancer cell lines and endometrium tissue samples. However, our results are different from a subset of reports[81,82,85,90,154] and also from the theoretically predicted molecular weight, ~42.24 kDa. Post-translation modifications like glycosylation could be the possible reason for the observed differences[21,88]. Moreover, the extent of denaturation and detergent loading on the denatured proteins could potentially create a difference in the rate of migration. This unusual migration is frequently observed in proteins with the helix-loop-helix structures, such as membrane proteins[157]. Apart from this, the quality (representation of proteins) of protein extraction and their detection on the blot are influenced by the composition of the lysis buffer[158]. Collectively, these technical limitations suggest that the extent to which epitopes are exposed finally on the blot determines the chance of detection. Towards this, the lysis buffer composition plays a significant role.

Western blotting of total proteins, isolated from breast cancer cell lines, detected GPER1 protein levels similar to the mRNA profiles of respective cell lines. The staining pattern for GPER1 in the breast cancer tissue sections was similar to those in the existing reports[19,22,28]. Distinct cytoplasmic staining was observed in the breast cancer tissue sections when probed with the anti-GPER1 antibody. This staining was not observed in the adjacent sections of the same tissue blocks when probed with the antibody which was pre-incubated

with the peptide. Collectively, these results demonstrate the specificity of the anti-GPER1 antibody.

In summary, the anti-GPER1 antibody generated in the present work successfully detects the human GPER1 protein in breast cancer cells using the standard methods of western blotting and immunohistochemistry. This served as a valuable tool for the analysis of GPER1 expression in breast tumors and its quantification in human breast cancer cell lines, described in the subsequent chapters of this thesis.

Chapter V

GPER1 expression in human breast tissues: an immunohistochemical and in silico study

5.1. INTRODUCTION

The seven transmembrane G-protein coupled receptors are the major class of proteins that transduce the external stimuli across the cell membrane. Nearly 40% of the drugs, which are being prescribed, target these incredible signal transducers[159]. Being the most targeted protein family in modern drug discovery their role in tumor growth and progression was underestimated until very recently. The importance of GPCRs in tumor biology is now being appreciated in various malignancies[160].

GPER1 signaling mediates the short-term non-genomic actions of estrogen. The role of estrogen in breast cancer development and progression is well established and GPER1, being identified as a signal transducer of estrogen, has attracted the interest of several research groups. Experimental evidence, from cell line models, highlight the significance of GPER1 in various physiological and pathological conditions including breast cancer. By virtue of its ability to crosstalk with several other growth-factor-driven signal transduction pathways, GPER1 can be one of the key players in tumor progression and metastasis[8,27,161]. GPER1 signaling is also reported in CAFs[91,120]. Recent studies have implicated GPER1 signaling in tumor-stroma interactions[120,121]. In CAFs, activation of GPER1 promotes the proliferation and induces E2 production[162]. Despite these advancements, inputs from the clinical studies are very limited. The present knowledge about the clinical significance of GPER1 in breast cancer is still in its nascent stage. Although not consistent across the studies, GPER1 expression was found to be associated with tumor size, lymph node invasion and classical molecular markers of breast cancer viz; ERα, PR and HER2[17,18,23–28,33,84,163,164]. A limited number of studies indicating contradicting associations of GPER1 expression with clinicopathological parameters, renders it difficult to ascertain the theranostic potential of GPER1 in breast cancer.

This chapter focuses on advancing our knowledge about the clinical significance of GPER1 in breast cancer. In this vein, the GPER1 protein expression in breast tumors, obtained from an independent cohort of breast cancer patients in the North-East Indian population was studied. The expression data, in the form of H-scores, across breast tumors were analyzed for identifying plausible associations with other clinicopathological

parameters. Additional inputs, with regard to understanding the clinical significance of GPER1 in breast cancer, were drawn by analyzing breast cancer data from TCGA and performing survival analysis using a web-based tool, KM-plotter.

5.2. RESULTS

5.2.1. GPER1 expression in tumor samples of breast cancer patients from the North-East Indian population.

This study was planned as a retrospective analysis of archived breast carcinoma cases from 2007 to 2016. All the patients who have been diagnosed and treated as breast carcinoma at NEIGRIHMS during the study period were included. Those cases with inadequate material for further testing and who had adjuvant chemotherapy were excluded from the study. Information regarding age, clinical presentation and data regarding the tumor including the tumor size, stage, grade, type, lymph node status, and, status of margins were collected from the archived records in the *pro forma*. This study was approved by the NEIGRIHMS ethics committee (NIEGR/IEC/2013/12) and the certificate is provided in the copyrights and permissions section of the appendix. The cohort consisted of a total of 65 cases. The mean age of the cohort was 47 years (range: 26-86 years). The samples were coded and the extent of GPER1 staining was scored (H score) by two independent pathologists. On a scale of 0-300, an H score of 40 was used as a cut-off to segregate the GPER1-positive ($H > 40$) from the GPER1-negative tumors ($H \leq 40$). Considering the cut-offs used by reported studies in the literature [17,23,25,90,164], an equivalent cut-off of 40 was decided by the pathologists.

IHC revealed predominant cytoplasmic staining of GPER1 in both normal and tumor tissues. GPER1 expression was observed in ductal and lobular luminal cells, myoepithelial cells, and also stromal fibroblasts. Cytoplasmic staining was consistent across all the positive cases, with an occasional tumor showing nuclear and membrane positivity. However, for the evaluation of GPER1 staining, only cytoplasmic positivity was considered. Representative images, showing varied intensities of GPER1 staining, are presented in figure 5.1. About 68% of the tumors (44/65) were positive for GPER1 and 32% (21/65)

were negative. The association between the expression of GPER1 and the clinicopathological parameters of breast cancer was tested (Table 5.1). GPER1 expression was not associated with the TNM stage, Bloom Richardson Grade, age, tumor type, margin type, tumor size, lymph node status, and molecular types. GPER1 staining was significantly associated with lymphovascular invasion ($p = 0.031$) and GPER1-positive tumors were more frequent in lymphovascular invasion-negative tumors. Among the immunohistological markers tested, GPER1 expression was significantly associated with ERα ($p = 0.048$) and PR ($p = 0.028$). The GPER1-positive cases were more frequent in ERα-positive or PR-positive tumors (Table 5.2). However, no significant association was observed with respect to HER2 expression.

5.2.2. Results from the analyses of TCGA-BRCA dataset

GPER1 mRNA expression, expressed as $\log_2(RPKM+1)$, in tumors was significantly lesser than that in normal samples (Figure 5.2). While the average expression of GPER1 mRNA in the normal breast tissue was 7.42 ± 1.04, in tumors, it was 5.74 ± 1.63. Overall, the variation in GPER1 expression within tumors ($\sigma^2 = 2.63$) was relatively more than that in normal samples ($\sigma^2 = 1.09$). The distributions of GPER1 mRNA expression in breast tumors, classified based on the status (IHC) of ERα, PR, or HER2, are represented as box plots in figure 5.2. Expression of GPER1 mRNA in ERα-positive tumors (5.95 ± 1.61) was significantly higher ($p < 0.00001$) as compared to ERα-negative tumors (4.99 ± 1.29). Further, GPER1 expression was considerably higher ($p < 0.00001$) in PR-positive tumors (5.95 ± 1.63) as compared to PR-negative tumors (5.26 ± 1.43). In case of HER2-positive tumors (5.30 ± 1.59), the GPER1 expression was significantly lesser ($p = 0.0021$) as compared to HER2-negative tumors (5.81 ± 1.58). The distributions of GPER1 mRNA expression in molecular subtypes are presented as box plots in figure 5.3. GPER1 was differentially expressed in molecular subtypes of breast tumors. The mean GPER1 expression was highest in Luminal-A type (6.18 ± 1.46) and was least in HER2-enriched tumors (4.68 ± 1.38). No significant difference in the mean GPER1 expression across the tumor stage was observed (data not shown).

Table 5.1. Analysis of the association of GPER1 expression with clinicopathological parameters.

	GPER1-positive (44/65)	GPER1-negative (21/65)	*p*
TNM stage			
Early (Stage 1 & 2)	21	9	F: 0.79
Advanced (stage 3 & 4)	23	12	C: 0.92
Bloom Richardson Grade			
1	11	4	F: 0.838
2	18	8	
3	15	9	
Lymphovascular invasion			
Positive	21	4	F: 0.031
Negative	23	17	
Age			
Mean ± SD	47 ± 11.95	48.9 ± 11.17	T: 0.55
Median	46.5	48	M: 0.77
Range	26 to 86 yrs	35 to 86 yrs	
Tumor type			
IDC	39	20	F: 0.65
Others	5	1	
Margin type			
Invasive	39	19	F: 1.00
Pushing	5	2	
Tumor size			
Mean ± SD	4.020 ± 1.896	4.476 ± 1.735	T: 0.355
Median	3.75	4	M: 0.246
Range	1.5 to 11 cm	1.5 to 6 cm	
Lymph node status			
Involved	23	12	F: 0.79
Uninvolved	21	9	
Molecular type			
Luminal A	20	7	F: 0.115
Luminal B	13	3	
Triple negative	2	4	
HER2/neu type	9	7	

The *p* values (*p*) are from C: chi-squared test, T: student's *t*-test, F: Fisher's exact test, M: Mann-Whitney U test. In all the tests $p < 0.05$ was considered as significant.

Analysis of TCGA-BRCA data for association of GPER1 mRNA expression with histopathological parameters revealed that its expression was significantly associated with ERα, PR, HER2 status and molecular subtypes of breast cancer. However, no significant association was found with respect to tumor stage (Table 5.3). GPER1-high tumors were frequently associated with ERα-positive or PR-positive or HER2-negative status. Except for

Luminal A, GPER1-high tumors were relatively less frequent in rest of the four subtypes. Luminal-A subtype had the highest representation of GPER1-high cases (66.38%) followed by Normal-like (50.00%), Luminal-B (44.58%), Basal-like (26.02%) and HER2-enriched (17.24). However, there was no significant association found between GPER1 expression and tumor stage (Table 5.3)

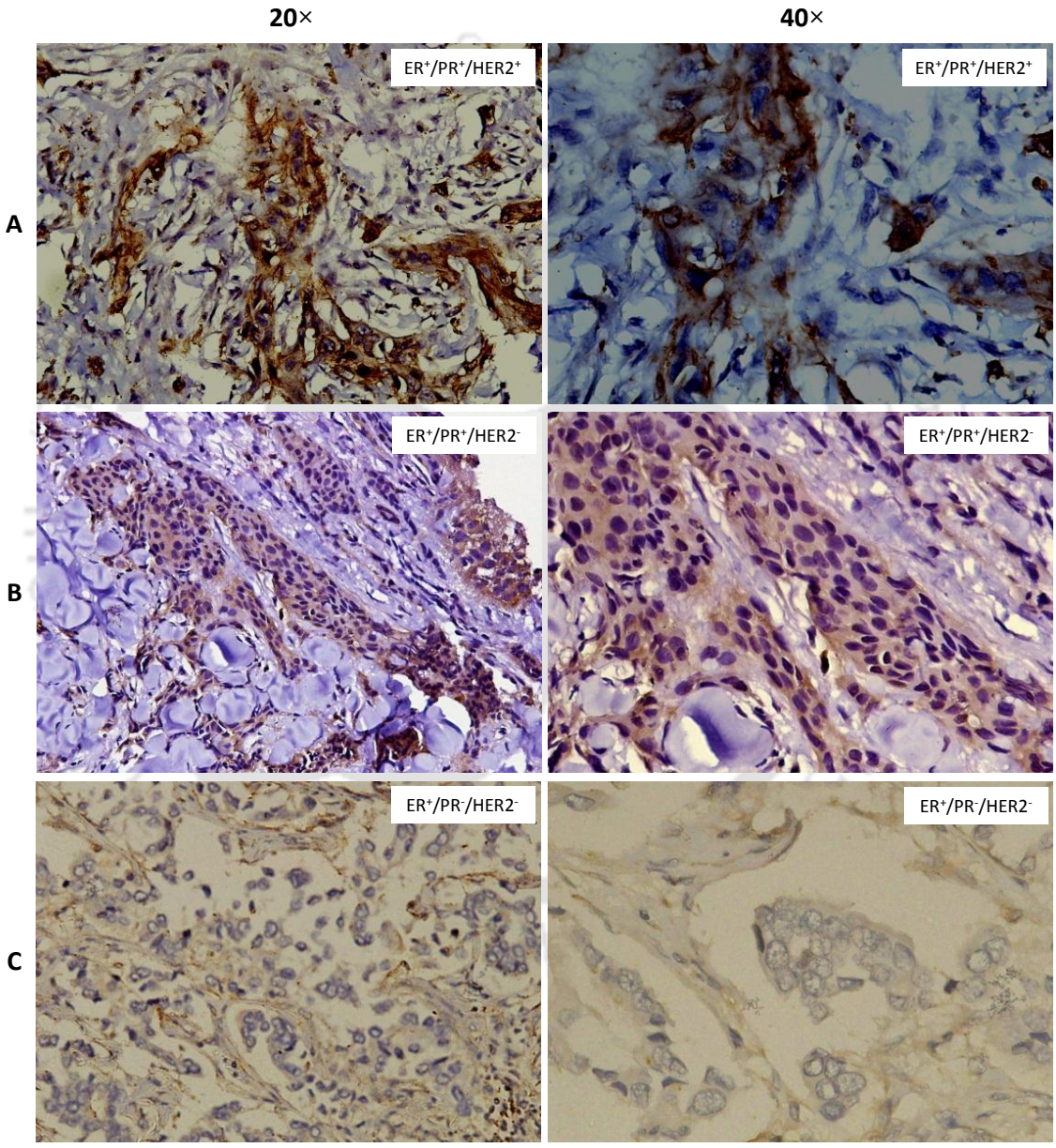

Figure 5.1. Expression of GPER1 in breast tumors. IHC was performed on formalin-fixed, paraffin-embedded breast tumor sections using, anti-GPER1 antibody, as described in section 3.9 of Chapter 3. A total of 65 cases were analyzed. Representative images for staining of high (A), medium (B), and low (C) GPER1 expression are shown. The corresponding H-score for high, medium, and low groups was 290, 130, and 20, respectively.

Table 5.2. Association of the GPER1 expression with the immunohistological markers.

	GPER1-positive (44/65)	GPER1-negative (21/65)	*p*
ERα			
Positive	33	10	0.048
Negative	11	11	
PR			
Positive	32	9	0.028
Negative	12	12	
HER2			
Positive (3^+ FISH +ve)	22	10	1.00
Negative ($1^+/2^+$ FISH -ve)	22	11	

The *p* values (*p*) are from Fisher's exact test and $p < 0.05$ was considered as significant.

Table 5.3. Association of the GPER1 expression with the histopathological parameters (TCGA-BRCA dataset).

	GPER1-high	GPER1-low	*p*
Age			
Mean ± SD	57.6 ± 14.0	58.3 ± 12.7	T: 0.4875
Median	58	58	
Range	26-90	31-90	
ERα			
ERα-positive	319 (57.48)	236 (42.52)	< 0.0001
ERα-negative	39 (24.22)	122 (75.78)	
PR			
PR-positive	283 (58.23)	203 (41.77)	< 0.0001
PR-negative	75 (32.61)	155 (67.39)	
Her2			
HER2-positive	41 (34.75)	77 (65.25)	0.0002
HER2-negative	317 (53.01)	281 (46.99)	
Molecular type			
Normal-like	9 (50.00)	9 (50.00)	
Luminal A	233 (66.38)	118 (33.62)	<0.0001
Luminal B	74 (44.58)	92 (54.42)	
Basal-like	32 (26.02)	91 (73.98)	
HER2-enriched	10 (17.24)	48 (82.76)	
Tumor Stage			
Stage I	68 (56.67)	52 (43.33)	0.2075
Stage II	196 (47.80)	214 (52.20)	
Stage III	85 (52.47)	77 (47.53)	
Stage IV	4 (28.57)	10 (71.43)	
Stage X	5 (50.00)	5 (50.00)	

Number within the braces indicates % of GPER1-high or -low in various categories. The *p*-values (*p*) are from chi-squared test, T: student's *t*-test. In all the tests $p < 0.05$ was considered as significant.

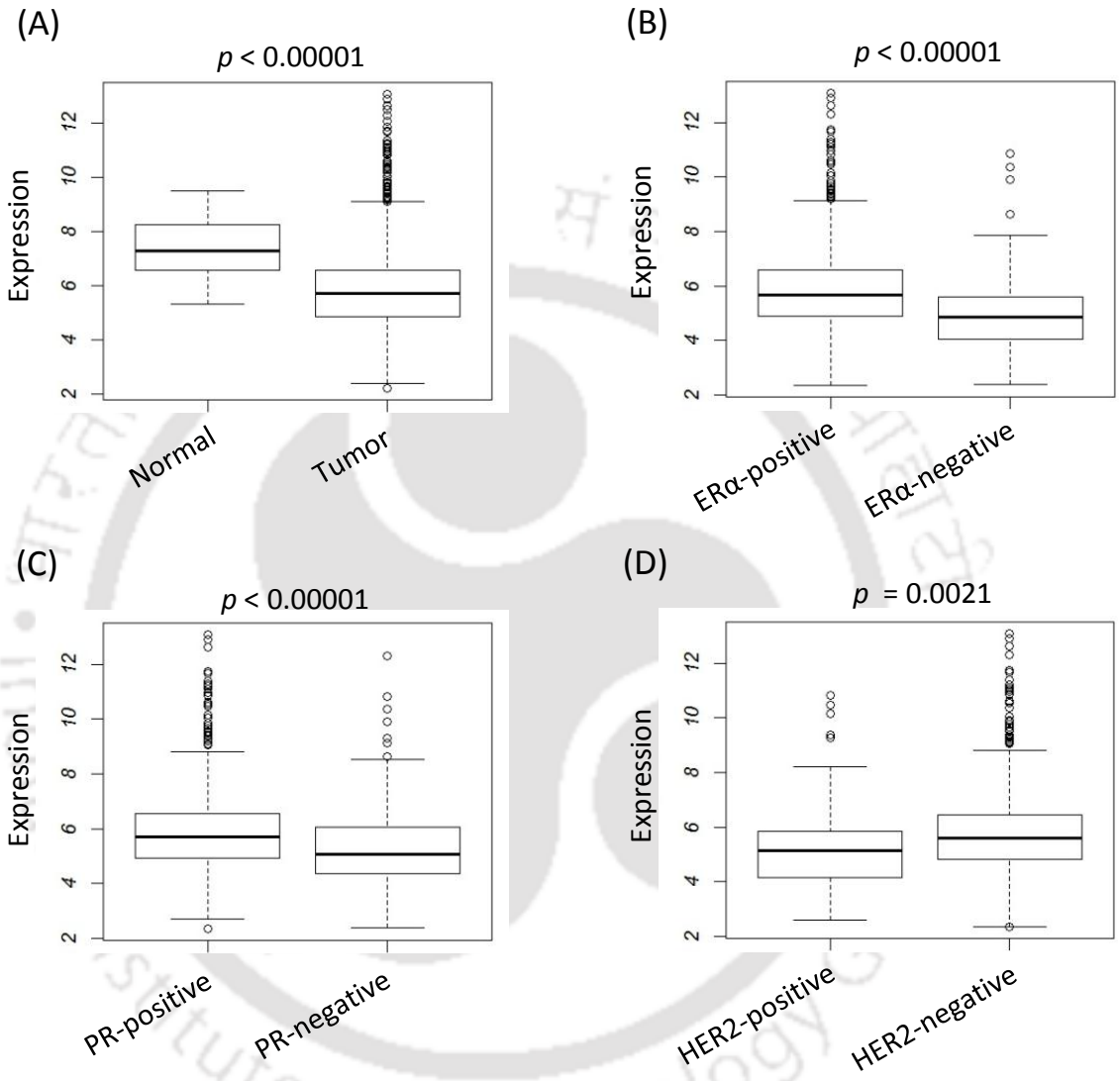

Figure 5.2. Expression of the GPER1 mRNA in normal and tumor tissues of the breast. The distribution of GPER1 mRNA expression values in normal and tumor (A), ERα-positive and -negative (B), PR-positive and -negative (C), and HER2-positive and -negative (D) tumors are showed as box plots. The analysis of the difference in the mean expression values between the groups was done by a Welch two-sample *t*-test. Numbers above the box plots indicate the *p*-values.

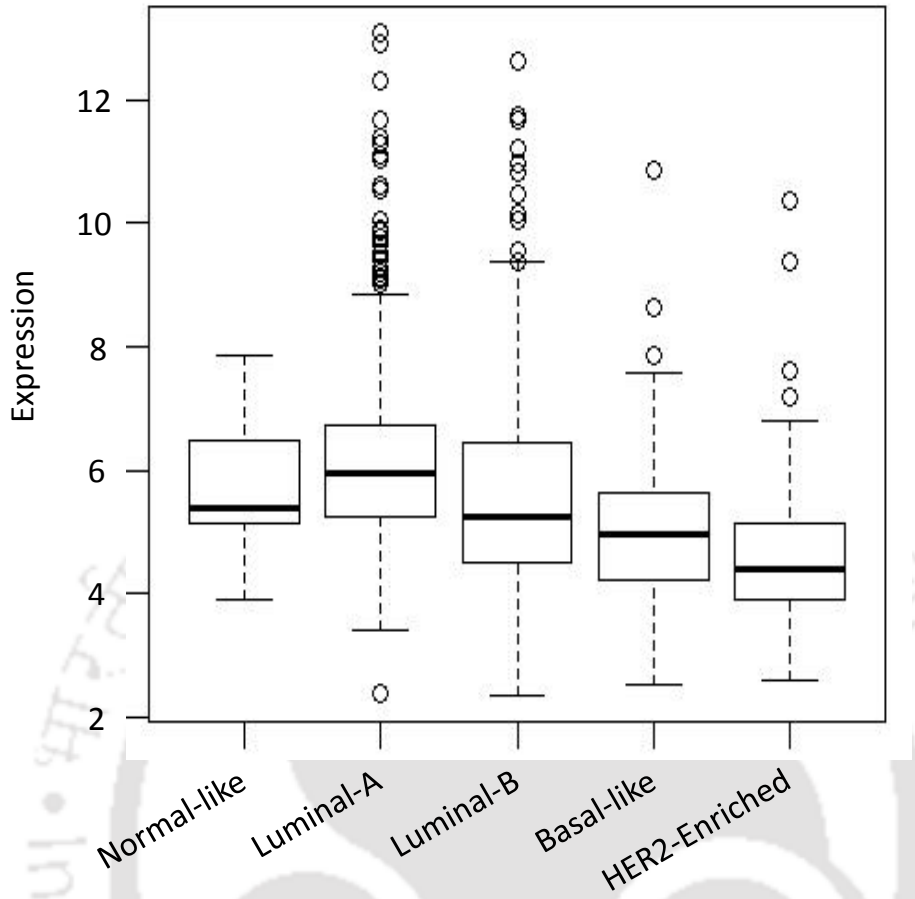

Figure 5.3. Expression of GPER1 mRNA in molecular subtypes of breast cancer. The distribution of GPER1 mRNA expression values in 5 distinct molecular subtypes of breast cancer is plotted as boxplots. The difference in the mean GPER1 expression values, across the molecular subtypes, was analyzed by ANOVA followed by a Tukey's HSD. GPER1 mRNA expression was significantly different between the following paired combinations. Luminal-A vs Luminal-B (p.adj = 0.0244), Luminal-A vs Basal-like (p.adj = 0.0000), Luminal-A vs HER2-enriched (p.adj = 0.0000), Luminal-B vs Basal-like (p.adj = 0.0006), and Luminal-B vs HER2-enriched (p.adj = 0.0001) subtypes.

5.2.3. Correlation of the GPER1 mRNA expression with that of the breast cancer molecular markers

The correlation of the mRNA expression of GPER1, with that of ERα, PR, HER2, and ERβ, was assessed in normal and tumor samples. All the records with the RNA-Seq data were considered for this analysis. Accordingly, there were 113 and 1102 normal and tumor samples, respectively. In tumors, the GPER1 mRNA expression was found to be positively correlated, significantly, with that of ERα ($r = 0.29$, $p < 0.00001$) and PR ($r = 0.22$, $p <$

0.00001). No significant correlation was found between ERβ and GPER1 mRNA expression in breast cancer samples (r = -0.02, p = 0.465). However, with respect to HER2 (r = -0.11, p = 0.0002), a significant negative correlation was observed. Further, the correlation between the pairs above-mentioned was also assessed in normal samples. Surprisingly, in the normal breast tissue the mRNA expression level of GPER1 was strongly negatively correlated with that of ERα (r = -0.40, $p < 0.00001$) and PR (r = -0.56, $p < 0.00001$). The negative correlation between GPER1 and HER2, observed in case of tumors, was even stronger in normal breast tissues (r = -0.64, $p < 0.00001$). Intriguingly, unlike tumors, a strong positive correlation between GPER1 and ERβ mRNA expression was observed in normal samples (r = 0.69, $p < 0.00001$). These correlations are tabulated in table 5.4. Apart from this, ERβ was negatively correlated with ERα in normal (r = -0.44, $p < 0.00001$) and in tumor (r = -0.31, $p < 0.00001$) samples.

Table 5.4. Correlation of GPER1 expression with ERα, ERβ, HER2, and PR.

	Normal	Tumor
ERα	-0.40027	0.26754
PR	-0.5639	0.218198
HER2	-0.64262	-0.11071
ERβ	0.693973	-0.022

The correlation of GPER1 mRNA expression with that of ERα, PR, HER2, and ERβ was analyzed by Pearson's correlation test. The Pearson's correlation coefficients are given in the table. The correlations were analyzed in normal (113) and tumor (1102) samples, separately. All the correlations were statistically significant ($p < 0.05$), except that between GPER1 and ERβ in the tumor was not (p = 0.46).

5.2.4. GPER1 expression and prognosis of breast cancer patients

In order to understand the prognostic utility of GPER1 expression, we performed the Kaplan-Meier survival analysis using KM-plotter, a web-based tool for survival analysis. Here, the cohort was divided into GPER1-high and GPER1-low, based on the median GPER1 mRNA expression of only tumor samples. Survival analysis revealed that GPER1 expression was significantly associated with the better overall survival (OS) and relapse-free survival (RFS) of breast cancer patients, with hazard ratio of 0.8 (95% CI = 0.65-1, p = 0.045) and 0.75 (95% CI = 0.64-0.8, $p < 0.00001$), respectively (Figure 5.4).

-

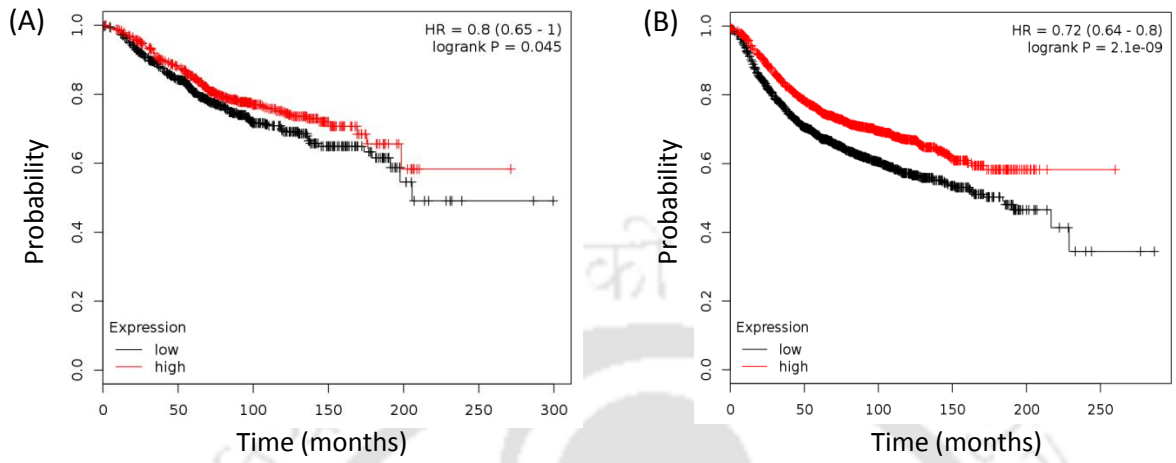

Figure 5.4. Significance of GPER1 expression in the clinical outcome of breast cancer patients. Kaplan-Meier plots were generated using web-based tool Kaplan-Meier plotter (www.kmplot.com). In the present survival analysis, a collection of breast cancer mRNA expression datasets inbuilt in the website was used along with the JetSet best probe set for GPER1, "210640_s_at". Breast tumors were divided into GPER1-high and GPER1-low using the median expression value as the threshold and the patient survival data was analyzed for overall survival (A) and relapse-free survival (B).

5.3. DISCUSSION

Although the mechanistic details of GPER1 signaling are unravelled by cell line models, the inputs from the clinical studies are valuable in ascertaining its importance in pathology. The clinical significance of GPER1 in breast cancer is still not clearly understood. Reports addressing this issue are very sparse in the literature. In clinical samples of breast cancer, the GPER1 expression is assessed at protein[15,23,25,27,28,33,84,163–165] and mRNA levels[18,24,26]. Overall, the GPER1 expression is associated with classical histological markers (ERα, PR, and HER2), EGFR, tumor size, and lymph node invasion. However, these associations are not consistent across the studies. While a set of independent studies revealed a significant positive association of GPER1 expression with ERα[18,23,24], some reports suggest negative[27,28,164] or no association[17,26,33,165]. The GPER1 expression is also reported to be associated with HER2 and EGFR[17,18,25].

A majority of reports revealed the reduced GPER1 expression in tumors, as compared to normal breast tissue[18,23,26,33]. However, few studies observed its overexpression

in tumors[27,28]. The significance of GPER1 expression in terms of patient survival is also not consistent. Although, reports suggest that GPER1 alone is not an indicator of the patient survival, in the presence of ERα and/or PR its expression is associated with prolonged survival[18,28]. However, Ignatov et al., reported that GPER1 expression is positively associated with OS and disease-free survival (DFS) in breast cancer[33]. Taken together, the ambiguity calls for more clinical studies.

Amidst the ambiguity in the literature, consistent observations across the studies are noteworthy. Overall, about 60% of the tumors express GPER1. Its expression is consistently associated with lymph node status where tumors with lymph node metastasis express lesser GPER1 as compared to lymph node non-metastasized tumors[17,26,165]. Interestingly, GPER1 is expressed in certain less common and more aggressive breast cancer types[28,163]. Tumors relapsed after tamoxifen treatment, express higher GPER1 as compared to the primary tumors[17,25]. GPER1 is an indicator of poor relapse-free survival in tamoxifen treated tumors[17]. The clinical significance of GPER1 in primary tumor might be different from that in drug-resistant or metastatic tumors.

In the present work, with an IHC-validated peptide-affinity-purified antibody against the N-terminus of GPER1 at our disposal (described in Chapter 4[134]), we embarked on a study of GPER1 expression in breast tumors obtained from an independent cohort of breast cancer patients in the North-East Indian population. To the best of our knowledge, this is the first study addressing the GPER1 clinical significance in breast cancer, from an Indian population. Our results from IHC and TCGA-BRCA analyses suggest that GPER1 expression is associated with the ERα in breast cancer. Reduced expression of GPER1 in tumors and positive association with OS and RFS strongly support the notion that GPER1 is a tumor suppressor. At the same time, our results are contradicting with those reported by others[25,27,28,164]. The difference in the scoring methodologies, subjectivity associated with scoring, and heterogeneity across the cohorts could be potential reasons for the present inconsistencies. It is noteworthy that across the cohorts, including our results, the expression of GPER1 decreases with increased lymph node invasion[17,26,165]. This negative association supports the fact that GPER1 expression decreases during tumor progression[26,33].

The results from TCGA-BRCA correlation analyses have revealed some novel insights. The correlation between GPER1 and the nuclear ERs is altered in tumors as compared to normal breast tissue. GPER1 inhibits the proliferation of ERα-positive MCF-7 cells[24,128] and promotes the proliferation of ERα-negative SkBr-3 cells[129]. Often, the crosstalk between these two receptors, in mediating estrogen actions, is reported[29,31,32]. Collectively, these reports highlight the influence of ERα on GPER1 signaling. In light of this evidence, the altered correlation indicates the abnormal signaling crosstalk in tumors. In order to appreciate the consequences of this altered correlation, the GPER1 signaling and coordination between the receptors need to be understood in normal breast tissue. However, the molecular basis for the observed correlations is yet another interesting question to address.

Our observations, from this study, led us to ask two fundamental questions regarding the regulation of GPER1 expression in breast cancer. Firstly, what could be the possible biological reason for the positive correlation between ERα and GPER1 in breast cancer? In general, epigenetic silencing of tumor suppressors is a well-known mechanism during tumor progression. Considering the case of GPER1 in breast cancer, it appears that it could be a potential tumor suppressor. These observations motivated us to put forth the second interesting question, is there a role of epigenetics in the regulation of basal GPER1 expression levels? These questions are addressed in the sixth and seventh[166] chapters of this thesis.

Chapter VI

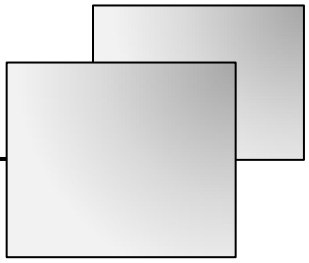

Functional link between GPER1 and ERα in breast cancer

6.1. INTRODUCTION

Estrogens are a group of steroid hormones which influence diverse biological process, ranging from migration to proliferation and apoptosis, at various organ systems in the human body[44,167]. The diversity and the tissue specificity of estrogen signaling are conferred by the combination of estrogen receptors and downstream signaling molecules at the target sites[117]. The biological significance of estrogen signaling in growth and development of secondary sex organs, such as the breast and uterus, is well established[168]. Pathological conditions at the estrogen target sites are frequently associated with abnormal estrogen signaling[46]. One such case, which is of major concern globally, is breast cancer. Although chemotherapy, surgery, and radiotherapy are the common strategies used for the treatment, targeted therapies such as hormone therapy and Herceptin have been more promising in breast cancer management[59]. However, drug resistance and tumor relapse still remain challenging. Continuous efforts in unraveling the underlying mechanistic details have led to the identification of key molecular players[25,169,170]. One such crucial player, which has been increasingly ascribed to tamoxifen resistance and tumor relapse, is a novel G-protein coupled estrogen receptor GPER1[15,17,25]. Since a majority of the reported breast cancers express ERα (~70%)[49], the only known estrogen signal transducer till 1996, research addressing the importance of estrogen signaling in breast malignancies was ERα centric. Results from chapter 5 and evidence from in vitro, ex vivo and clinical studies have underscored the role of GPER1 in breast cancer.

Nearly two decades of research by several groups has significantly established the GPER1 signaling in various tissue and cell line contexts. While the area of GPER1 signaling is rapidly advancing, the regulation of GPER1 expression has not been given due attention. The GPER1 expression is reported to be regulated by progestin[96], growth factors like EGF[171], TGF-α[32], IGF-I[98], heregulin-β1[101], and insulin[97]. Hypoxia is also demonstrated to regulate the GPER1 expression in tumors of the breast[99]. Although circumstantial evidence suggest the possible role of estrogen in regulating GPER1 expression[15,24,102], the underlying molecular details are not completely understood.

In this chapter, molecular evidence for the estrogen-mediated regulation of the GPER1 expression, are reported. Estrogen regulates GPER1 expression in MCF-7 breast cancer cells. Involvement of ERα in estrogen-mediated regulation is established by using ERα specific ligands and siRNA. In silico analyses of the GPER1 upstream sequence provided additional insights into the mechanism of estrogen regulation of GPER1 and the role of ERα therein.

6.2. RESULTS

6.2.1. GPER1 transcript variants

Three mRNA variants of GPER1 with the following accession numbers - NM_001505.2 (variant-2), NM_001039966.1 (variant-3), and NM_001098201.1 (variant-4) were found in the NCBI nucleotide database. These variants are hereafter referred to as GPER1v2, GPER1v3, and GPER1v4, respectively. The transcript variant-1 (NM_001031682.1) which has an unusual intron with a non-consensus splice junction resulting in a frame shift is permanently suppressed in the database (communication from NCBI help desk). The three variants were analyzed using BLAT[172] and the results are shown schematically in figure 6.1. They differ in their lengths, exon-intron organization and 5'UTRs, but have the same coding region (encoding a 375 amino acid protein) and a 3′UTR.

6.2.2. 17β-estradiol induces the mRNA levels of GPER1 in MCF-7 breast cancer cells

Effect of estrogen stimulation on the expression of GPER1 mRNA in MCF-7 cells was studied by treating the cells with E2. GPER1 transcript variants were induced in the presence of estrogen at concentrations ranging from 0.1 nM to 100 nM (Figure 6.2.A). GPER1v2 was found to be significantly induced at all the concentrations tested except, 1 nM E2. A similar trend of induction was observed with respect to GPER1v3 and GPER1v4 but failed to be statistically significant. Further, the estrogen-mediated induction was observed to be time-dependent. In the presence of 10 nM E2, a significant induction of GPER1v2 was observed by 24 h and the induction peeked at 72 h. There after a decline was observed (numbers above bars in Figure 6.2.B). A similar trend was observed with respect to the

expression of GPER1v3 and GPER1v4 (numbers above bars in Figure 6.2.C and D). However, because of the variation across the biological replicates, the induction was not statistically significant at some of the time-points. Interestingly, when the relative levels of GPER1 mRNA variants were assessed, with respect to the 6 h vehicle treated group, a time-dependent modulation of mRNA variants was also evident in the vehicle treated groups (Figure 6.2.B-D). Unlike in E2 treated cells, the mRNA levels were found to be depleted with time in E2 deprived vehicle treated groups.

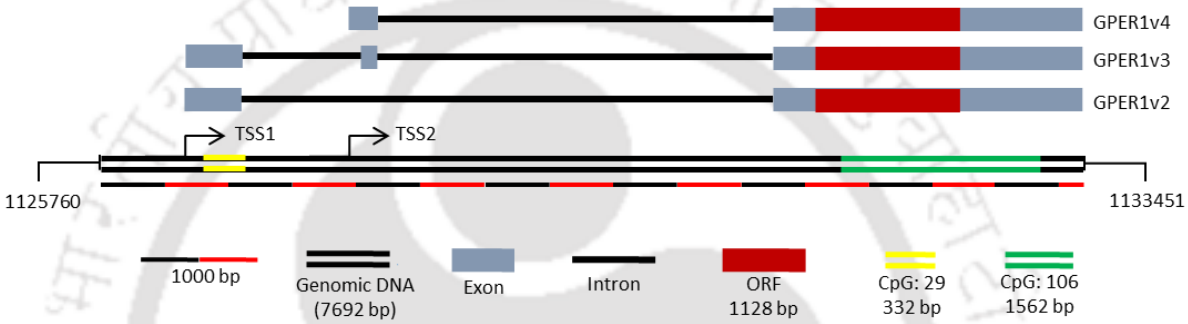

Figure 6.1. Graphical representations of the GPER1 mRNA variants. mRNA sequences for GPER1 transcript variants were retrieved from NCBI nucleotide database. Their alignment against the human chromosome 7 is represented graphically. Two transcription start sites, TSS1 and TSS2, are indicated by the arrows. The NCBI accession numbers for the variants are NM_001505.2, NM_001039966.1, and NM_001098201.1 for GPER1v2, GPER1v3, and GPER1v4, respectively.

6.2.3. The involvement of ERα in the estrogen-mediated induction of GPER1 expression in MCF-7 cells

In order to investigate the involvement of ERα in the observed estrogen-mediated induction, the cells were stimulated with selective ERα ligands. Here, PPT (an ERα-specific agonist) and tamoxifen (SERM) were used. PPT stimulation induced the mRNA levels of GPER1 variants. A stimulation of 100 nM PPT for 48 h significantly induced all the three transcript variants of GPER1 in MCF-7 cells (Figure 6.3.A). Further, a stimulation of 10 µM TAM for 72 h significantly suppressed the expression of GPER1 variants (Figure 6.3.B).

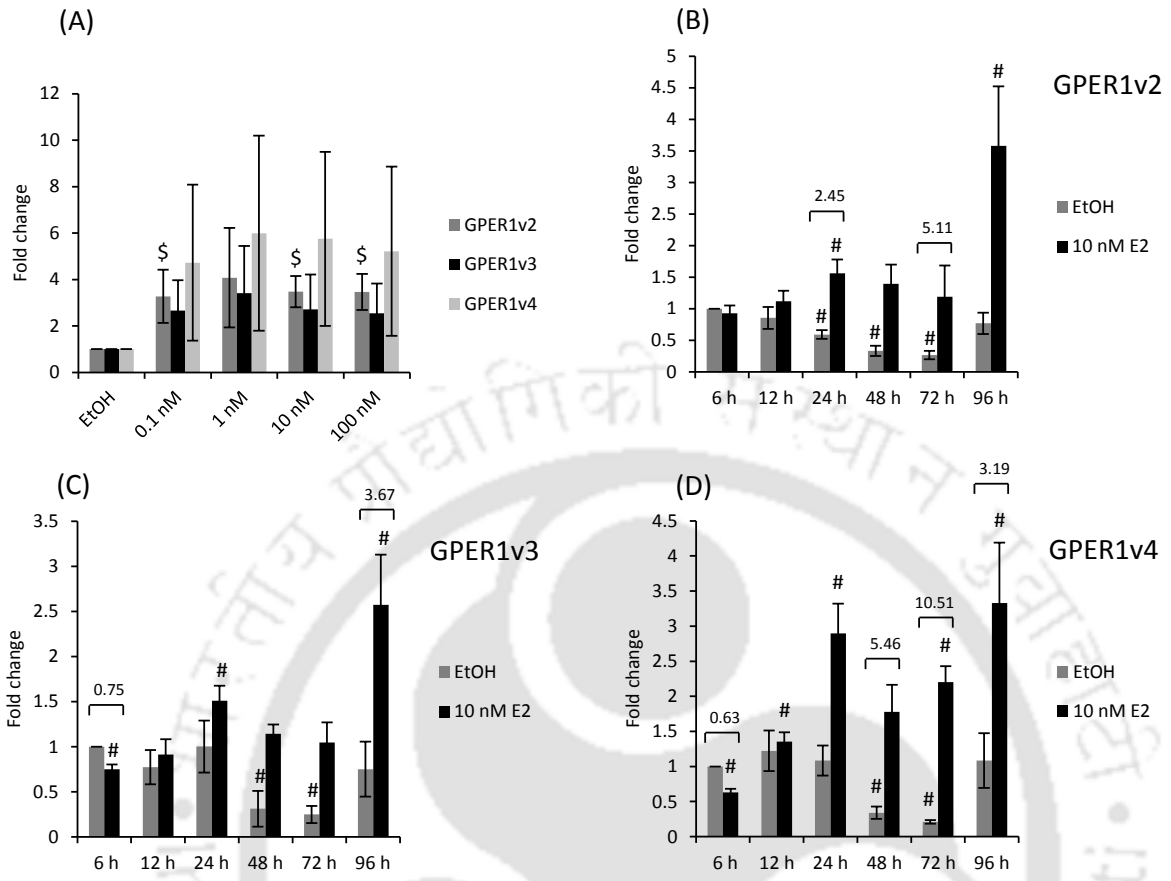

Figure 6.2. Effect of estrogen stimulation on the mRNA expression levels of GPER1 transcript variants in MCF-7 cells. MCF-7 cells were seeded in 35 mm dishes and grown for 48 h in M1. The medium was replaced by M2 and incubated for 24 h. Cells were treated with indicated concentrations of E2 for 72 h (A) or with 10 nM E2 for indicated periods of time (B-D) in M2. After the treatment, cells were lysed in TRIzol and total RNA was isolated. cDNA was synthesized using 2 µg of total RNA. cDNA equivalent to 20 ng of total RNA was taken as the template in qRT-PCR reactions. RPL35A was used as an internal control. The relative expression levels of GPER1 mRNA variants were analyzed by $\Delta\Delta C_t$ method and expressed as fold change in E2 treated groups with respect to the corresponding EtOH groups (A), or with respect to 6 h EtOH group (B-D). Bars represent mean fold-change ± SD. Numbers above the bars indicate the mean fold change in E2 groups with respect to corresponding control groups. The fold change values are given for only those time points at which the difference was significant ($p < 0.05$). In graph A, n = 4 and $ indicates $p < 0.05$ versus the corresponding bar in EtOH group. In graphs B-D, n = 3 and # indicates $p < 0.05$ versus 6 h EtOH.

The role of ERα was further confirmed by using siRNA. Here, the expression of ERα in MCF-7 cells was suppressed by gene-specific siRNA. As observed earlier, GPER1 mRNA levels in the scrambled siRNA transfected groups were significantly upregulated by estrogen treatment (10 nM E2) as compared to the corresponding vehicle-treated groups (Figure 6.4.A). Interestingly, the estrogen-mediated induction of GPER1 mRNA variants was abrogated in the absence of ERα (Figure 6.4.A). Assessment of protein levels showed

marginally significant induction of GPER1 protein expression by E2 in scrambled siRNA transfected groups (Figure 6.4.C). Further, the GPER1 protein expression in ERα siRNA transfected groups was found to be drastically reduced and E2-mediated induction was not observed (Figure 6.4.C). We next assessed the GPER1 protein levels in PPT treated MCF-7 cells, after ERα knockdown. Surprisingly, GPER1 expression was significantly induced by PPT stimulation in scrambled siRNA treated groups and the induction was abrogated in ERα siRNA transfected groups (Figure 6.5). Further, the reduction in the GPER1 protein levels in vehicle-treated ERα knockdown groups, as compared to vehicle-treated scrambled siRNA groups, was consistently observed in all our experiments.

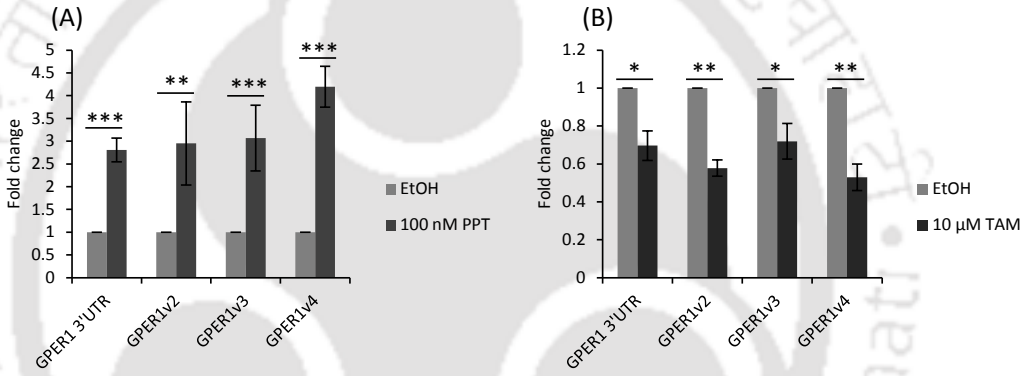

Figure 6.3. Effect of PPT and TAM on the regulation of GPER1 in MCF-7 cells. MCF-7 cells were seeded in 35 mm dishes and grown for 48 h in M1. The medium was replaced by M2 and incubated for 24 h. Cells were treated with 100 nM PPT for 48 h (A), or 10 μM TAM for 72 h (B). After the treatment, cells were lysed in TRIzol and total RNA was isolated. cDNA was synthesized using 2 μg of total RNA. cDNA equivalent to 20 ng of total RNA was taken as the template in qRT-PCR reactions. RPL35A was used as an internal control. The relative expression levels of GPER1 mRNA variants were analyzed by $\Delta\Delta C_t$ method and expressed as fold change with respect to the corresponding vehicle treated groups. Bars represent mean fold-change ± SD. (n = 6 for A, n = 3 for B, * $p < 0.05$, ** $p < 0.01$, *** $p < 0.001$)

6.2.4. *In silico* analyses of ERα binding sites at GPER1 locus

In silico analysis of GPER1 locus in the human genome using Matinspector software (a promoter analysis tool from Genomatix software suite) revealed three potential estrogen response elements (EREs). Amongst the sites predicted, only ERE2 was found to be in the positive strand of the genomic DNA. The positions of ERE2 and ERE3 were overlapping

and ERE1 was 94 bases upstream of the later. Details of the prediction results and the genomic coordinates on human chromosome 7 are given in table 6.1.

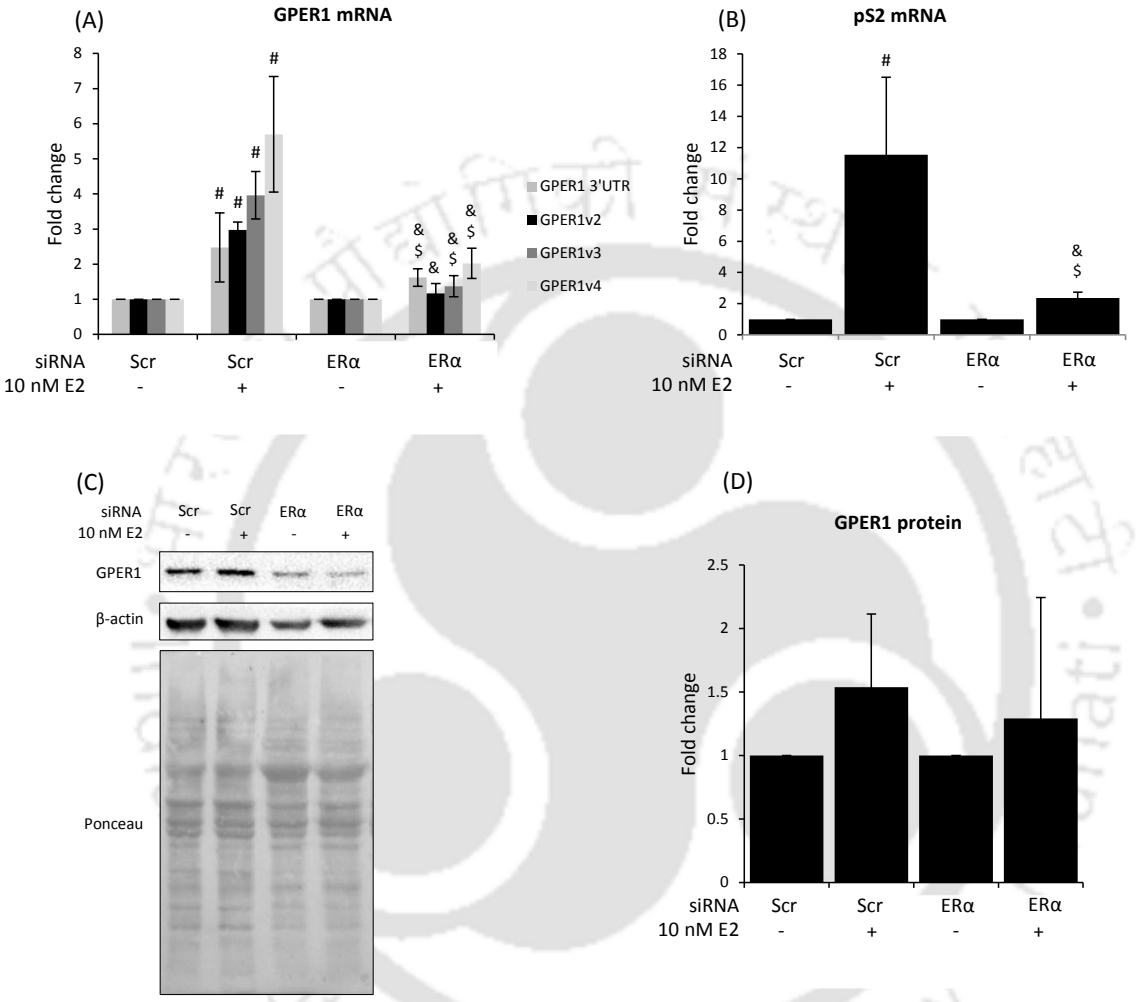

Figure 6.4. Regulation of GPER1 expression in MCF-7 cells: ERα knockdown followed by E2 treatment. MCF-7 cells were seeded into 35 mm dishes and grown for 48 h in M1. Cells were incubated with scrambled siRNA (Scr) or ERα-specific siRNA (ERα) for 24 h in M1. The medium was replaced by M2 and incubated for 24 h. Cells were treated with 10 nM E2 for 48 h. Total protein and RNA were isolated from TRIzol fractions. cDNA was synthesized using 2 µg of total RNA. cDNA equivalent to 20 ng of total RNA was used as the template in qRT-PCR reactions. The relative expression levels of mRNA of GPER1 variants (A) and pS2 (B) were analyzed by $\Delta\Delta C_t$ method. RPL35A was used as internal control and pS2 was used as positive control for E2 treatment. 30 µg of total protein was used in western blotting to assess the GPER1 and β-actin protein levels (C). The bands were quantified and normalized against the total lane intensity of ponceau S (D). Bars represent mean fold-change ± SD. (n = 6, # indicates $p < 0.05$ versus Scr + EtOH, $ indicates $p < 0.05$ versus ERα + EtOH, and & indicates $p < 0.05$ versus Scr +10 nM E2). Representative western blots showing the expression levels of ERα in these samples are presented as Supplementary figure 6.1.A.

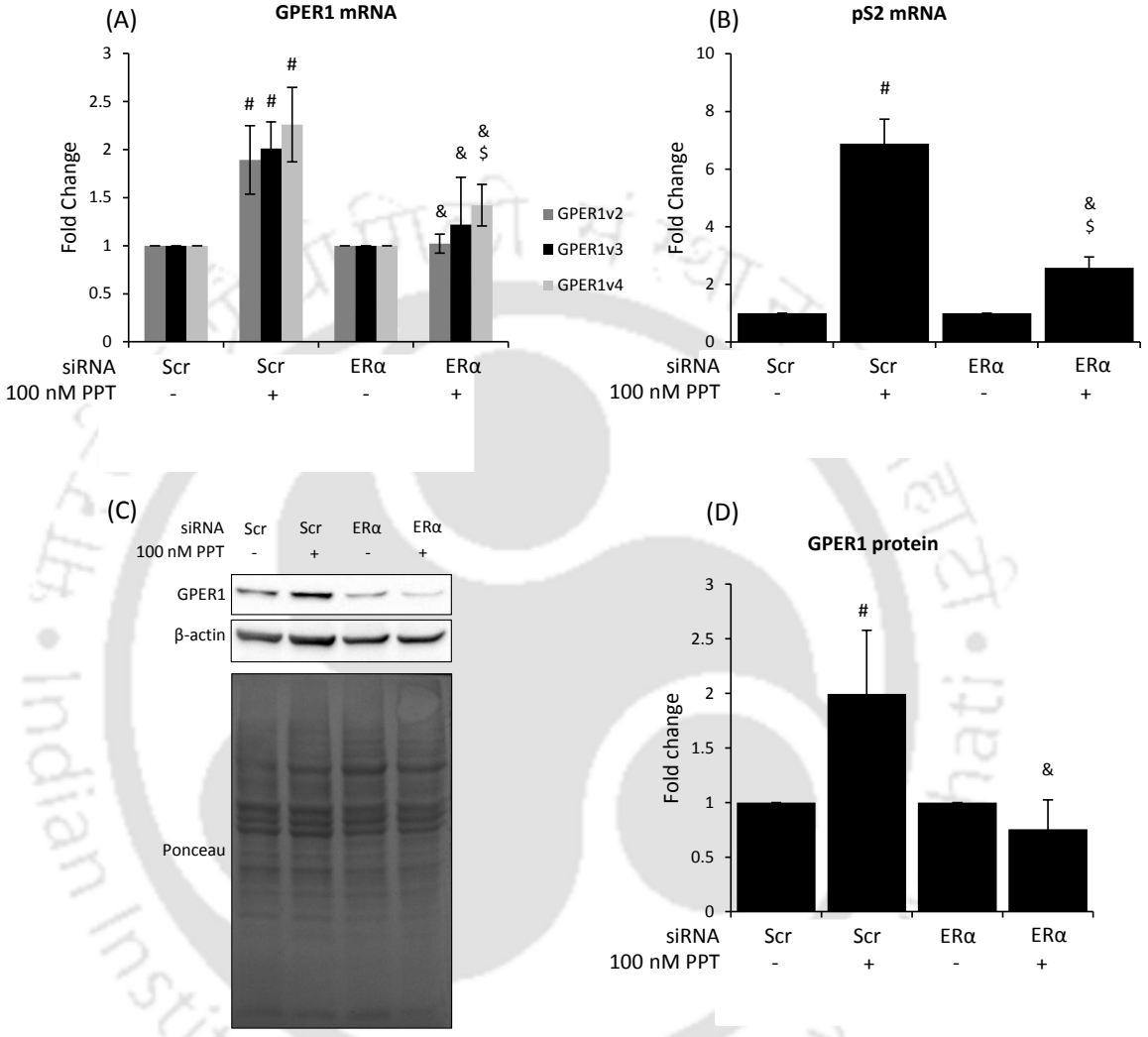

Figure 6.5. Regulation of GPER1 expression in MCF-7 cells: ERα knockdown followed by PPT treatment. MCF-7 cells were seeded into 35 mm dishes and grown for 48 h in M1. Cells were incubated with scrambled siRNA (Scr) or ERα-specific siRNA (ERα) for 24 h in M1. The medium was replaced by M2 and incubated for 24 h. Cells were treated with 100 nM PPT for 48 h. Total protein and RNA were isolated from TRIzol fractions. cDNA was synthesized using 2 µg of total RNA. cDNA equivalent to 20 ng of total RNA was used as the template in qRT-PCR reactions. The relative expression levels of mRNA of GPER1 variants (A) and pS2 (B) were analyzed by $\Delta\Delta C_t$ method. RPL35A was used as internal control and pS2 was used as positive control for E2 treatment. 30 µg of total protein was used in western blotting to assess the GPER1 and β-actin protein levels (C). The bands were quantified and normalized against the total lane intensity of ponceau S (D). Bars represent mean fold-change ± SD. (n = 6, # indicates $p < 0.05$ versus Scr + EtOH, $ indicates $p < 0.05$ versus ERα + EtOH, and & indicates $p < 0.05$ versus Scr + 10 nM PPT). Representative western blots showing the expression levels of ERα in these samples are presented as Supplementary figure 6.1.B.

Table 6.1. Estrogen Response Elements at GPER1 upstream region in the human genome.

Name	Strand	Start	End	Core	Matrix	Sequence
ERE1	-	1121818	1121840	1	0.879	aacaatgGTCAgactgagaggaa
ERE2	+	1121910	1121932	1	0.935	cggtaagGTCAgagtgctcccgc
ERE3	-	1121912	1121934	1	0.823	gggcgggagcactctGACCttac

+ and – indicate forward and reverse orientation of the predicted ERE sites, respectively. The numbers in the third and fourth column indicate the genomic coordinates of the predicted elements on chromosome 7. The fidelity of the prediction is measured in terms of core similarity and matrix similarity. The scores for both the parameters range from 0 to 1, correspondingly, represent no-match to perfect-match. A matrix similarity score of 0.8 and above is considered as good match. The upper case letters in the sequence column indicate the bases in the query sequence matched to the core sequence of the matrix (usually 4 bases). All the three predicted sites are with perfect match for the core sequence (core = 1).

Publically available ChIP-Seq data, from the Sequence Read Archive (SRA) database, was analyzed to identify ERα binding sites. Data from the project ERP000380 was selected for the analysis. A subset of FASTQ files (Table 3.3) for the ChIP-Seq data corresponding to MCF-7 cells treated with vehicle, E2, or tamoxifen was identified. The data was analyzed using various software tools from Galaxy, a web based platform, as mentioned in the section 3.13 of Chapter 3. The results were visualized in the UCSC genome browser[153] and a snapshot is represented as figure 6.6. The analysis revealed that ERα was found to be enriched at the GPER1 upstream region upon E2 treatment in MCF-7 cells. Interestingly, this ERα occupancy was not observed with the TAM stimulation.

Analysis of GPER1 locus of the human genome in the UCSC genome browser revealed ERα enrichment in the GPER1 upstream region. The "ENC TF Binding" super track in the UCSC genome browser was searched for ERα ChIP-Seq data and enriched regions in the GPER1 locus was visualized in the UCSC genome browser (Figure 6.6). ERα ChIP-Seq data was available from "Transcription Factor ChIP-Seq Uniform Peaks from ENCODE/Analysis" track set, for only ECC-1 and T47D cell lines. ECC-1 is an endometrial cancer cell line and T47D is a breast cancer cell line. Here, ERα was found to be engaged at GPER1 upstream region upon E2, Bisphenol-A (BPA), or Genistine stimulation. The binding was observed only in ECC-1 cells and not in T47D cells.

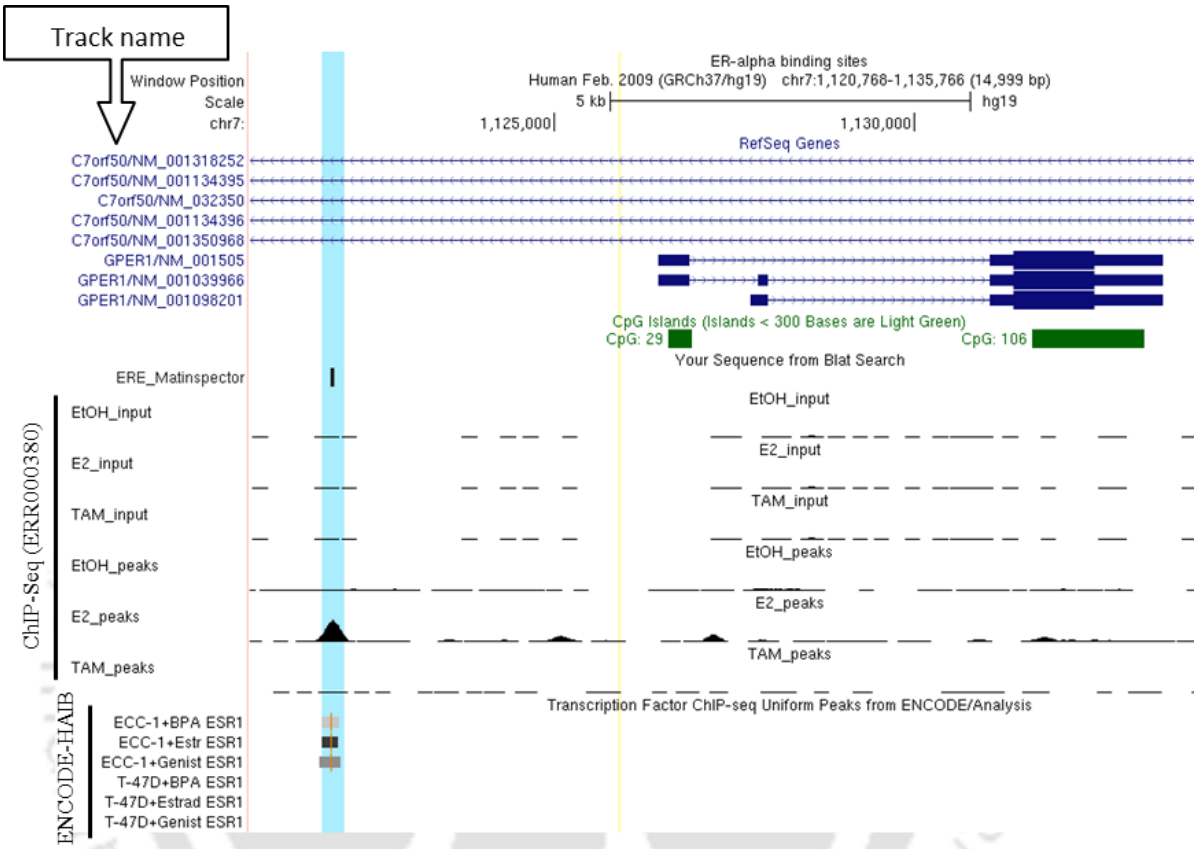

Figure 6.6. ERα binding sites at the GPER1 locus in the human genome. A snapshot of GPER1 locus in the human genome, as viewed from the UCSC genome browser along with various tracks for ERα binding sites. The highlighted portion (vertical light-blue strip) shows the ERα binding site at the GPER1 upstream region. The track **"**ERE_Matinspector" indicates the putative ERE (Estrogen Response Element) predicted by Matinspector software tool from the Genomatix software suite. Tracks within "ChIP-Seq (ERP000380)" track set show the results of ChIP-Seq analysis in six tracks. The track names indicate the treatment conditions and the suffix "input" and "peaks" indicates the IgG and anti-ERα antibody immunoprecipitated samples, respectively. The vertical viewing range of all the tracks was set to 100 and visualized in full mode. The Fastq files of the dataset ERP000380 were imported from the Sequence Read Archive (SRA) database into GALAXY platform and analyzed as mentioned in the section 3.13 of chapter 3. The tracks of "Transcription Factor ChIP-Seq Uniform Peaks from ENCODE/Analysis", from the "ENC TF Binding" super track in the UCSC genome browser was searched for ERα ChIP-Seq data and visualized in the UCSC genome browser in dense mode. These tracks are represented within "ENCODE-HAIB" track set.

6.3. DISCUSSION

In the present study, we have gathered evidence from both *in vitro* and *in silico* analyses to demonstrate the involvement of ERα in the regulation of GPER1 expression in breast cancer cells. For our *in vitro* experiments, we have selected MCF-7, a well-studied breast cancer cell line as our model system. MCF-7 cells represent the Luminal-A subtype, which accounts for the majority of ERα-positive breast cancer. Assessment of the significance of GPER1 expression in breast cancer increasingly suggested an association between the expressions of GPER1 and ERα[18,23,24]. Results from our clinical study also supported this supposition (Chapter 5). Adding to this, Kolkova et al., while studying the GPER1 expression in endometrium and early pregnancy decidua, hypothesized that in the epithelium of fertile endometria the GPER1 expression is driven by estrogen[102]. Ignatov et al., while understanding the role of GPER1 in tamoxifen resistance, have demonstrated that its expression was up-regulated by E2 in MCF-7 cells and in tamoxifen-resistant clonal variant, TAM-R[15]. In order to understand the role of GPER1 expression in ERα positive breast cancer cells, Ariazi et al., used a clonal variant of MCF-7 cells (MCF-7:WS8) which were selected for estrogen sensitivity. Interestingly, Estrogen-mediated down-regulation of GPER1 expression via ERα was observed in these cell lines in a time-dependent manner[24]. Collectively, these observations suggest the possibility of GPER1 expression regulation by ERα. Towards this, here we have made a systematic approach to investigate into the molecular insights.

Estrogen stimulation induced the mRNA levels of GPER1 transcript variants in MCF-7 cells. Further, the induction was found to be time-dependent. However, this is contradictory to the observations of Arizai et al., and we speculate that the use of different cell line MCF-7:WS8 (a clonal variant of MCF-7) could be the reason[24]. Interestingly, the temporal modulation was also observed in the vehicle treated groups. This trend possibly indicates the effect of deprivation of steroids in the vehicle treated group. At the same time, the importance of individual time point controls is also highlighted. Using an ERα-specific ligand (PPT) and siRNA we have demonstrated the involvement of ERα in the observed estrogen-mediated induction of GPER1 expression. Of note, the induction of GPER1 expression (particularly the protein) was prominent in experiments with PPT compared to

E2 (Figure 6.4.C and 6.5.C). However, it is possible that activation of GPER1 by E2, which is not expected in case of PPT, might be affecting the receptor turnover. Tamoxifen, a selective estrogen receptor modulator, known to produce anti-estrogenic effects in the breast tissue, down-regulated the GPER1 expression in MCF-7 cells (Figure 6.3.B).

Our *in silico* analyses revealed a substantial evidence for the mechanism of ERα-mediated regulation of GPER1 expression. Promoter analysis identified putative EREs in the GPER1 upstream region (Figure 6.6). Analysis of publically available ChIP-Seq data revealed an ERα enriched region, coinciding with one of the putative EREs (ERE2) predicted by the Matinspector (Table 6.1 and Figure 6.6). Interestingly, the enrichment was observed upon E2 stimulation and not by TAM, clearly supporting our *in vitro* results (Figure 6.6). Further, a search for the ERα binding sites at GPER1 locus, using the tracks for transcription factor binding sites in the UCSC genome browser, revealed an ERα binding region at the same locus that was observed by the previous two analyses. Here again, the enrichment was observed upon E2, BPA, or Genistein stimulation. The ERα binding was observed in ECC-1 and not in T47D cells. This clearly suggests that the ERα-mediated regulation might be cell type specific. Nevertheless, the enrichment clearly highlights the affinity of the locus for ERα.

ERE2 is a half-ERE and one of the regulatory elements predicted, by the matinspector, in the close its proximity is SP1 (data not shown). The involvement of SP1 in ERα-mediated transcriptional activity, particularly in the context of half-ERE, has been observed in the case of several estrogen target genes[173–175]. Moreover, this pathway could be cell context dependent[176]. This possibly explains why the region is engaged by ERα in only ECC-1 and not in T47D, despite both the cell lines are ERα positive. Collectively our results provide clear evidence for the involvement of ERα in the regulation of GPER1 expression in MCF-7 breast cancer cells. This potentially explains the molecular basis for the observed association between the receptors, in breast cancer.

Chapter VII

CpG island shore methylation determines the basal GPER1 expression levels in breast cancer cells

The results presented and discussed in this chapter are published in Manjegowda et al., (2017), Gene[164]

7.1. INTRODUCTION

The significance of GPER1 signaling in breast cancer stems from its ability to activate EGFR via HB-EGF ectodomain shedding[9]. It provides a mechanistic basis not only for EGF like effects of estrogen, but also for the ER-independent growth of breast tumors. Furthermore, tamoxifen acts as a GPER1 agonist[11,14,15,25], which directly implicates this receptor in the emergence of tamoxifen resistance. In view of these data, the clinical relevance of GPER1 expression in breast tumors cannot be ignored. Investigators, who have studied and correlated GPER1 expression in breast tissues with other histopathological parameters, have reported conflicting results. However, the reduced expression of GPER1 in breast tumors compared to normal tissues, as reported by some and also in chapter 5 indicates its role as a tumor suppressor[26,33].

Epigenetic silencing of tumor suppressors is a well-known phenomenon[177]. Given the diagnostic and prognostic potential of GPER1, the present work is based on the hypothesis that reduced expression of GPER1 in breast tumors may be due to epigenetic silencing. Using MCF-7 and MDA-MB-231 cells as model systems, and employing modified COBRA assay and bisulfite sequencing techniques, we show that reduced expression of GPER1 inversely correlates with hyper-methylation of a cluster of eight downstream CpGs within an upCpGi, which maps to the first exon of two GPER1 variants (GPER1v2 and v3). Furthermore, through the expression-methylation correlation (EMC) analysis of TCGA breast cancer data, we found support for the role of DNA methylation in GPER1 repression and the involvement of regions flanking the upCpGi.

7.2. RESULTS

7.2.1. GPER1 expression in MCF-7 and MDA-MB-231 cells

Previous studies on the expression of GPER1 in human cell lines and tissues using RT-PCR have used primers that amplify the common regions across the variants. Thus, the available data reflects the expression level of total GPER1 mRNA. Since variant-specific GPER1 mRNA expression data are not available, we studied their expression in two breast

cancer cell lines, namely MCF-7 (ERα-positive and non-invasive) and MDA-MB-231 (ERα-negative and highly invasive). Total RNA from these cells were subjected to routine RT-PCR and qRT-PCR analyses using primer pairs, which are either common to or specific to each variant (listed in Supplementary table 3.1). Routine RT-PCR analysis revealed that MDA-MB-231 cells expressed low or undetectable levels of total GPER1 and its variants compared to MCF-7 cells (Figure 7.1.A). A qRT-PCR experiment confirmed lower levels of total GPER1 and variant mRNAs in MDA-MB-231 cells (Figure 7.1.B). Consistent with the mRNA expression, GPER1 protein expression was detected in MCF-7 but not in MDA-MB-231 cells (Figure 7.1.C).

7.2.2. CpG islands in the GPER1 locus

Upon examination of other features present in the GPER1 genomic locus using the UCSC genome browser[153], we found two distinct CpG islands. The first (upstream) CpG island (CpG: 29 within upCpGi, yellow lines in Figure 7.2) of length 332 bp overlaps with the first exon of GPER1v2 and v3 and extends into 30 nucleotides of the adjacent downstream intron. The second (downstream) CpG island (CpG: 106 within dnCpGi (a-e), green lines in Figure 7.2) of length 1562 bp overlaps with the open reading frame and the 3'UTR.

7.2.3. Differential methylation of the upCpGi

Using a modified COBRA assay, we analyzed the methylation status of upCpGi and dnCpGi regions in MCF-7 and MDA-MB-231 cells. This assay is based on the fact that a methylated BstUI site (CGCG) is retained after bisulfite treatment of gDNA. This site is represented unaltered in PCR amplified products, which is susceptible to BstUI digestion. On the other hand, an unmethylated CGCG site in gDNA would get converted to TGTG after bisulfite treatment and PCR amplified products will resist digestion with this enzyme. Similarly, the same PCR amplified products can also be analyzed by digestion with TaqI (TCGA). Additionally, bisulfite conversion of methylated CCGA in gDNA will create a TaqI site. Assuming 100% methylation of CpG sites in a given amplicon, supplementary table 3.2 shows the expected number of fragments upon digestion with BstUI or TaqI.

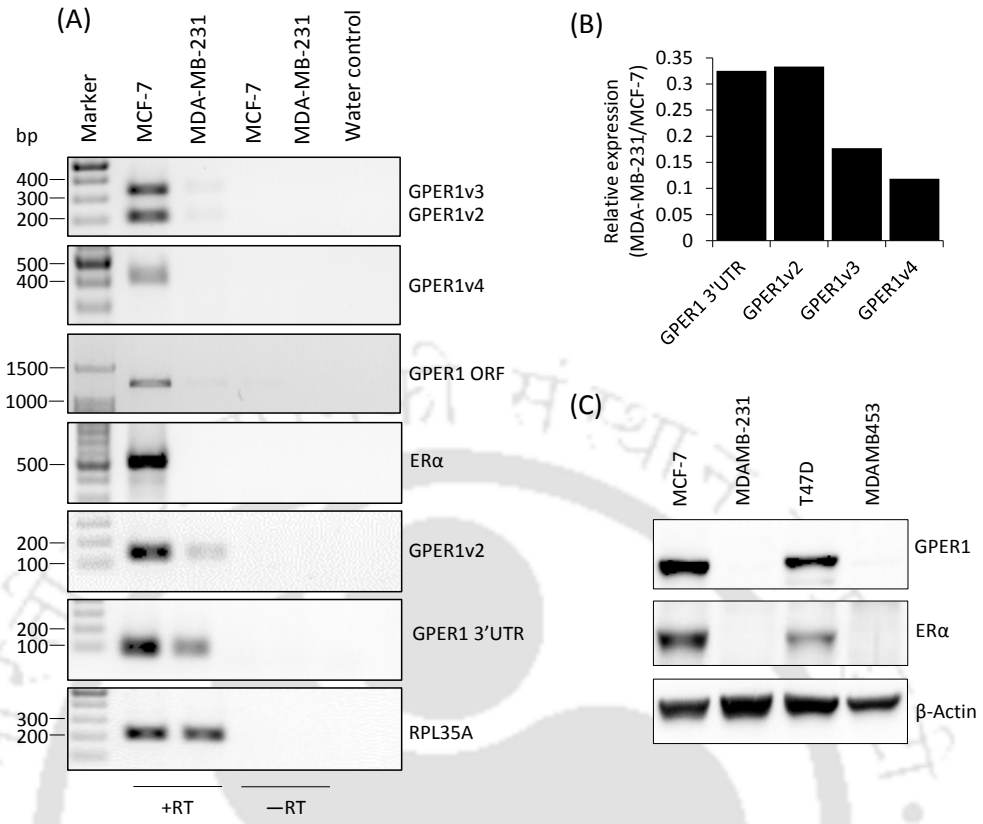

Figure 7.1. Differential expression of GPER1 in MCF-7 and MDA-MB-231 cells. Total RNA samples from MCF-7 and MDA-MB-231 cells were isolated subjected to routine RT-PCR (A) or real-time qRT-PCR analysis (B) using primers specific to GPER1 mRNA variants (Supplementary table 3.1). RPL35A served as an internal control. (C) Western blots showing differential expression of GPER1 protein in the indicated cell lines. ERα mRNA and protein served as a distinguishing marker for the two cell lines in RT-PCR and western blotting experiments, respectively.

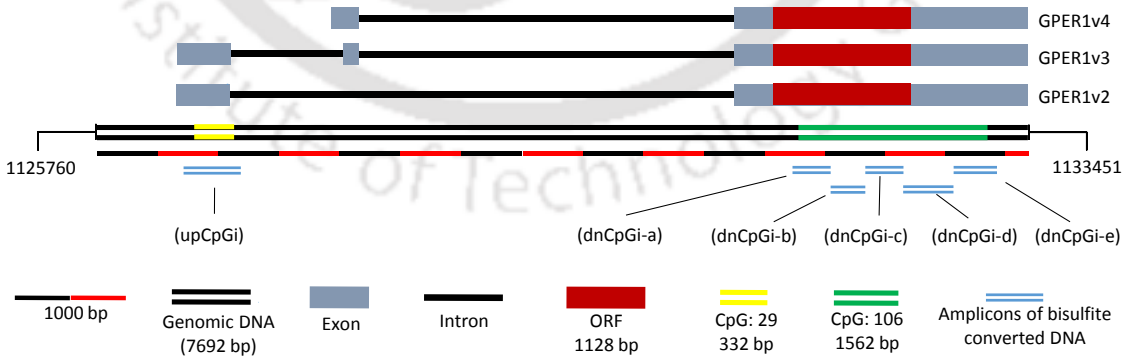

Figure 7.2. Graphical representation of the GPER1 mRNA variants and CpG islands in the GPER1 locus. The NCBI accession numbers for the variants are NM_001505.2, NM_001039966.1 and NM_001098201.1 for GPER1v2, GPER1v3 and GPER1v4, respectively. The upCpGi and dnCpGi(a-e) harbor the upstream and downstream CpG islands, namely CpG:29 and CpG:106, respectively. In addition to 29 CpGs of CpG:29 as per the UCSC genome browser, the upCpGi contains three additional CpGs; one in the 5' end and two in the 3' end of this region.

Ensuring that equal quantities of PCR products are digested with the enzymes, a difference in the intensities of the ethidium bromide stained fragments, relative to the undigested DNA, would indicate differential methylation at one or more BstUI or TaqI sites. Analysis of the upCpGi in the two cell lines shows visibly greater intensities of 387 and 78 bp fragments (* and # respectively, Figure 7.3.A, left panel) generated by BstUI, and 367 and 98 bp fragments (* and # respectively, Figure 7.3.A, right panel) generated by TaqI in MDA-MB-231, compared to MCF-7 cells. This is due to the fact that the amplicons generated from the bisulfite treated gDNA of MDA-MB-231 cells are more susceptible to digestion. This in turn indicates a relative hyper-methylation of two CpG sites within the upCpGi in MDA-MB-231. We also analyzed bisulfite-treated genomic DNA from two other cell lines, namely T47D and MDA-MB-453. The greater intensities of digested fragments of MDA-MB-453 (indicated by * and #, Figure 7.3.A) indicate hyper-methylation of upCpGi in MDA-MB-453 compared to T47D. This correlates well with the observation that unlike T47D, MDA-MB-453 cells hardly express the GPER1 protein (Figure 7.1.C). Using the same method, the dnCpGi was analyzed as five overlapping fragments (dnCpGi a-e, Figure 7.2). However, the results indicated similar extent of CpG methylation in this region in both the pairs of cell lines (Supplementary figure 7.1).

On the basis of our modified COBRA assay results, we chose to analyze the differential methylation of upCpGi in MCF-7 and MDA-MB-231 cells by bisulfite sequencing. gDNA was bisulfite modified and PCR amplified using the primers flanking the upCpGi (Supplementary table 3.2). The PCR amplified products were cloned in TA vector and inserts were sequenced. Analysis of 23 inserts from each of the two cell lines revealed that out of 32 CpGs encompassed by the upCpGi, eight CpGs in the 3' end were hyper-methylated in MDA-MB-231 cells (Figure 7.3.B). The region encompassing these eight CpGs is hereafter referred to as the differentially methylated region (DMR). A non-parametric chi-square test showed the observed difference in the methylation in the DMR to be statistically significant ($p < 0.0001$). The extent of methylation in the remaining portion of upCpGi was similar in both the cell lines. This is consistent with the results of the modified COBRA assays, which showed enhanced digestion at the 3' restriction site of the upCpGi amplicon from MDA-MB-231 cells.

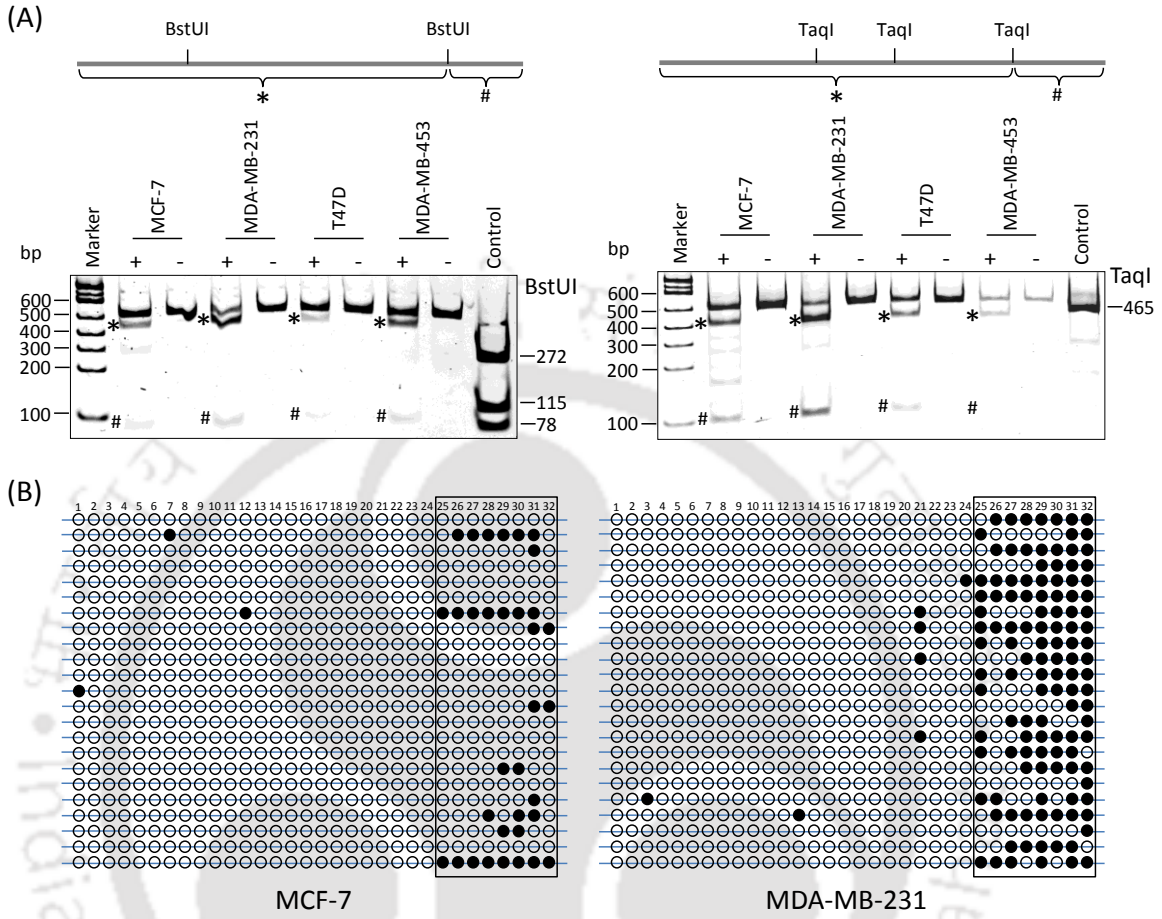

Figure 7.3. Differential methylation of the upCpGi in MCF-7 and MDA-MB-231 cells. A. The upCpGi region was PCR amplified with upCpGi-fT and upCpGi-rT primers (Supplementary table 3.2) using the bisulfite converted gDNA from the indicated cell lines as template. The products were digested with BstUI (left panel) or TaqI (right panel) or mock digested in the absence of these enzymes (indicated by + or – above the lanes). The digestion products were analyzed on 6% TB-PAGE. The control indicated in each panel was the upCpGi region amplified with upCpGi-fW and upCpGi-rW primers (Supplementary table 3.2) using un-converted gDNA as template, and digested with the indicated restriction enzyme. Note, that the fragments of bisulfite converted DNA always migrate slightly slower than un-converted counterparts. The observed bands on the gel (marked as * or #) are mapped against the appropriate fragments in the schematic above each panel that shows the positions of the respective enzyme sites in the upCPGi amplicon. B. Lollipop display showing the bisulfite sequencing results. The upCpGi region was amplified with upCpGi-fT and upCpGi-rT primers using bisulfite converted gDNA of the indicated cell lines as template. The amplicons were cloned in TA cloning vector and the inserts of 23 recombinant plasmids were sequenced. Each circle represents a CpG site (numbered 1-32 above). Open circles and filled circles represent, unmethylated and methylated sites, respectively. The black rectangle demarcates the differentially methylated region (DMR) of the upCpGi.

7.2.4. 5-aza induces GPER1 mRNA expression in MDA-MB-231 cells

We tested whether the expression of GPER1 mRNA in MDA-MB-231 cells could be enhanced by global demethylation of CpGs using 5-aza, a DNMT inhibitor. MDA-MB-231 cells were treated with 10 µM 5-aza for 5 days and the expression levels of the GPER1 mRNA variants were compared to those of vehicle treated cells. As shown in figure 7.4, 5-aza treatment caused a significant increase in total GPER1 mRNA and its variants in MDA-MB-231 cells.

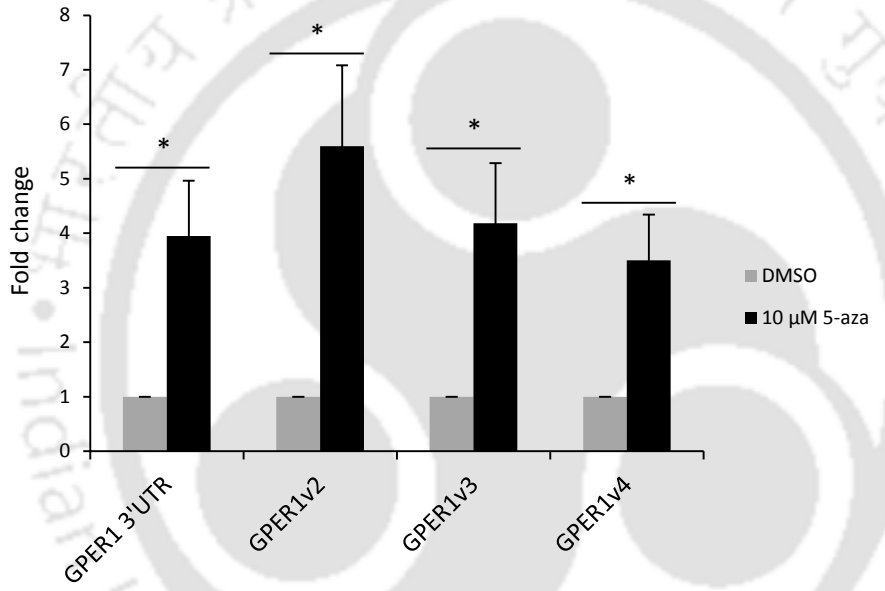

Figure 7.4. 5-aza induces the expression of GPER1 mRNA variants in MDA-MB-231 cells. MDA-MB-231 cells were treated with DMSO (grey bars) or 5-aza (black bars) in phenol-red-free RPMI-1640 medium supplemented with 10% cs-FBS. The experiment comprised of three biological replicates; each replicate comprised of one dish each for DMSO and 5-aza treatments. After 5 days, total RNA was extracted and levels of the GPER1 mRNA variants were analyzed by qRT-PCR (Supplementary table 3.1 for primer details). For each biological replicate the qRT-PCR analysis was done twice, each with three technical replicates. RPL35A served as an internal control. The expression levels of the variant mRNAs in 5-aza treated cells were analyzed by $\Delta\Delta C_t$ method and expressed as fold increase relative to those observed in DMSO treated controls, which were assigned a value of 1. Data from the two qRT-PCR runs for each biological replicate was averaged. The figure is a graphical representation of the data from three biological replicates. For each of the variant mRNAs, separate Welch two-sample *t*-tests were performed using R statistical package to test if the mean fold increase in the expression level of each variant in 5-aza treated cells is significantly different from the mean fold increase in DMSO treated cells (set to 1). The bars represent mean fold increase (± s.d.) in the expression level of the variants indicated along the x-axis (n=3, * $p < 0.05$)

7.2.5. GPER1 expression inversely correlates with methylation

Using the UCSC Cancer Genomics Browser, we accessed the GPER1 expression (RNA-Seq) and methylation (Infinium® Human Methylation-450K Bead Chip) data corresponding to the GPER1 locus for 786 breast tumor samples of the TCGA-BRCA dataset. CpG sites at the GPER1 locus are represented by 118 probes in the 450K Bead Chip, out of which 3 and 7 probes overlap with upCpGi and dnCpGi, respectively (indicated below the mRNA in Figure 7.5.A). EMC analysis with respect to 9 out of these 10 probes did not reveal any significant correlation of methylation with GPER1 expression (data not shown). However, methylation at the site represented by cg11697111, a probe that matches with the 5' terminus of the DMR, showed a significant inverse correlation, (ρ = -0.129, p = 0.000302). Unfortunately, this is the only probe in the array that maps to the DMR. Hence, we looked for other probes in this locus whose methylation data significantly correlated with expression. The 118 probes that represent the GPER1 locus were selected by a two-tiered selection process. First, probes that had an interquartile range (IQR) of beta scores greater than 0.15 were selected. It was assumed that probes, which represent the CpG sites actually involved regulation of GPER1 expression, will have a high variation in beta values. This resulted in selection of 20 probes. In the second tier, 12 probes that showed ρ value less than -0.20 were selected. Each of these 12 probes (indicated above the mRNA in Figure 7.5.A) produced significant results ($p < 0.000001$) in EMC analysis (Supplementary table 7.1). Upon probe-wise segregation of tumors into hypo-methylated or hyper-methylated groups, the mean GPER1 expression in hypo-methylated tumors was significantly greater than that of the hyper-methylated tumors (Supplementary figure 7.2). We also considered a composite methylation score in the upCpGi region as the average beta score of these 12 probes. The composite methylation score was significantly inversely correlated with expression (ρ = -0.36, $p < 0.000001$, Figure 7.5.B). When the tumors were divided based on a threshold composite methylation score of 0.3, the mean expression in hypo-methylated tumors was significantly greater than that in the hyper-methylated tumors (Figure 7.5.C). We noticed that changing the threshold ρ value to -0.30 in the two-tiered selection process would leave only 4 probes for analysis (indicated in red in Figure 7.5.A). A composite methylation score for these 4 probes showed a stronger inverse correlation with expression (ρ = -0.44, $p <$ 0.000001, Figure 7.5.D). Furthermore, when these 4 probes were considered, the hypo-

methylated tumor showed significantly higher mean GPER1 mRNA expression compared to the hyper-methylated tumors (Figure 7.5.E).

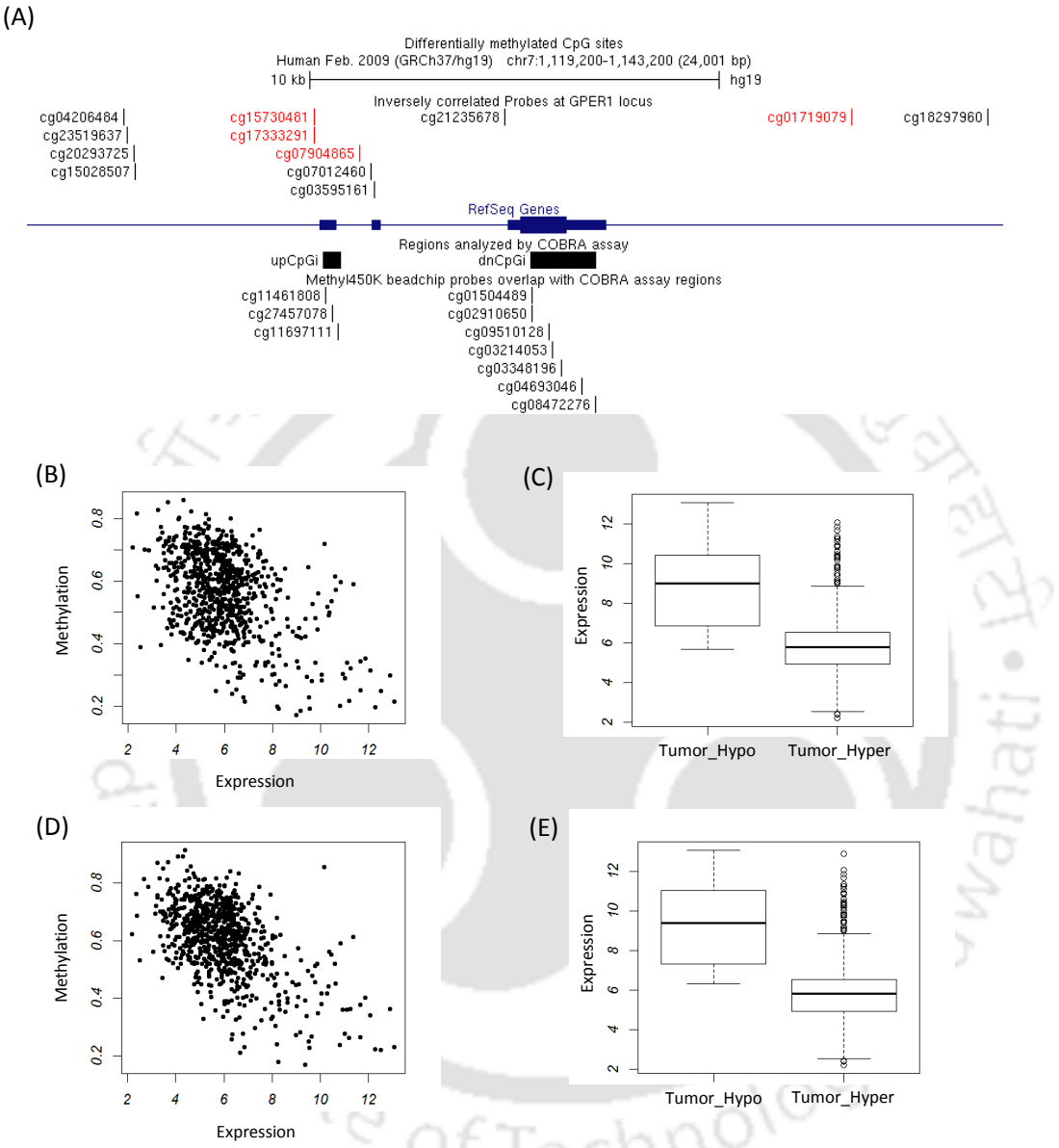

Figure 7.5. Expression-methylation correlation analysis. A. A snapshot from the UCSC Genome Browser showing the location of selected 450K Bead Chip probes. The mRNA is shown in blue. The locations of upCpGi and dnCpGi are shown as black rectangles. The probe IDs appear in the format cgxxxxxxxx (x is any digit). The vertical line after the probe IDs indicate the location with respect to the CpG island regions. The probes that represent the upCpGi or dnCpGi are indicated below the blue line representing the chromosome. The 12 probes that were selected by the two-tiered selection process are shown above the chromosome. The probes indicated in red have an IQR > 0.15 and $\rho < -0.3$. B and D. Scatterplots of composite methylation score of 12 probes (B) or 4 probes (D) versus GPER1 expression. C and E. Box plots showing the distribution of GPER1 expression in hypo-methylated and hyper-methylated tumors. Tumors were grouped into hypo-methylated or hyper-methylated categories based on the threshold value of 0.3 for the average beta score of 12 (C) or 4 probes (E). In all the panels the *p* values are < 0.0001

7.3. DISCUSSION

This work was an attempt to obtain mechanistic insights into the differential expression of GPER1 in breast cancer cells. Silencing of tumor suppressors, mediated by promoter methylation, is a well-known phenomenon[177]. Hence, we evaluated the extent of methylation in the two CpG islands that were found in the GPER1 locus; one encompassed by upCpGi and the other by dnCpGi (Figure 7.2). While the upCpGi maps to the first exon and is proximal to the transcription start sites of GPER1v2 and GPER1v3, the dnCpGi overlaps with the coding sequence and the 3'UTR. The modified COBRA assays clearly showed differential methylation in the former but not in the latter. According to our bisulfite sequencing result, the core of the upCpGi is hypo-methylated in both the cell lines. However, a cluster of eight 3' terminal CpGs in the upCpGi constitutes the DMR in the two cell lines. The involvement of the CpG island "shores" and not the core regions has emerged recently[178]. The DMR apparent from our bisulfite sequencing results seems to be a reiteration of the importance of the shore regions. Hyper-methylation of the DMR in MDA-MB-231 cells and induction of GPER1 mRNA post 5-aza treatment suggests that DNA methylation in the upCpGi shore could be one of the mechanisms of GPER1 silencing.

Our results and conclusions from the *in vitro* study parallel with those reported by Weißenborn and co-workers. Using methylation-specific PCR they demonstrated that demethylation of a CpG island in the GPER1 promoter region by 5-aza enhances the expression of GPER1 in MCF-7 and SK-Br-3 cells[34]. They also showed 5-aza-mediated induction of GPER1 expression in two triple-negative breast cancer cells, namely MDA-MB-231 and MDA-MB-468[35]. 5-aza-mediated induction of GPER1 in MDA-MB-231 cells shown in our study is consistent with those of Weißenborn and co-workers. Despite the similarities in the model systems and the conclusions, our study differs on several grounds. In our work, the choice of MCF-7 and MDA-MB-231 cells was based on the difference in their invasiveness and ERα expression to corroborate with the clinical observations. While Weißenborn and co-workers' data uphold the role of promoter CpG island methylation in GPER1 expression, our work demonstrates that the difference in the level of GPER1 expression in a pair of cell lines under study inversely correlates with the extent of DNA methylation. We have used a modified COBRA assay to identify the differentially

methylated CpG islands and then employed bisulfite sequencing method to confirm the results. Moreover, bisulfite sequencing allowed the analysis of methylation status at each CpG in the upCpGi, and the identification of the DMR.

The *in vitro* data suggest a potential mechanism of GPER1 repression in breast cancer cells. In order to validate the *in vitro* findings, our future investigations will study the DNA methylation in the GPER1 locus in clinical samples of breast tissue. However, in the present work, we could at least analyze the paired expression and methylation data of 786 breast tumor samples of TCGA-BRCA dataset to examine the correlation between expression and CpG methylation in the GPER1 locus. Few pointers to the validity of the *in vitro* results have emerged from the analyses. None of the probes that mapped to the dnCpGi showed any significant result in the EMC analyses. Out of the three probes that mapped to the upCpGi, two (cg11461808 and cg27457078) did not show any significant results in EMC analyses. This was expected, since these probes mapped to that region in upCpGi that was poorly methylated in MCF-7 and MDA-MB-231 cells. Methylation score of the probe mapping to the 5' end of the DMR (cg11697111) showed statistically significant inverse correlation with GPER1 expression (ρ =-0.129).

Except for cg11697111 none of the probes in the 450K Bead Chip represented the DMR. Hence, it was not possible to perform the EMC analyses for almost all CpG sites that are present in the DMR. This shows the limitations of the 450 Bead Chip. Therefore, the subsequent analysis was aimed at finding probes that represent other CpG sites where methylation has and inverse correlation with GPER1 expression. The methylation data for 786 breast tumor samples that have beta values for 118 probes mapping to the GPER1 locus is humongous and a rigorous analysis of this dataset is beyond the scope of this work. Hence, we reduced the number of probes analyzed in this study by a two-tiered selection process, which is described in the Results section. Probes which were selected based on ρ value < -0.2 (12 probes) or -0.3 (4 probes), individually showed statistically significant results in EMC analyses. Also, tumors which were hypo-methylated at CpG sites represented by each of these probes had significantly higher GPER1 expression than those which were hyper-methylated. Furthermore, when composite methylation score was used to represent methylation status at sites represented by 12 or 4 probes, a much stronger inverse

correlation with expression was observed. It is important to note that these groups of 12 or 4 probes mapped neither the upCpGi nor dnCpGi core regions, but instead mapped the near flanking regions of the upCpGi. This observation, yet again, highlights the importance of upCpGi shores or flanking regions in DNA methylation dependent silencing of GPER1.

Taken together, results from *in vitro* cell culture experiments and analysis of TCGA data strongly indicate the role of DNA methylation in the suppression of GPER1 expression in breast cancer cells and the importance of the CpG sites that likely represent the upCpGi shore regions. Considering the prognostic and therapeutic potential of GPER1, the results from our study provide compelling reasons to investigate the clinical utility of GPER1 re-activation in breast cancer cells by pharmacological interventions.

Chapter VIII

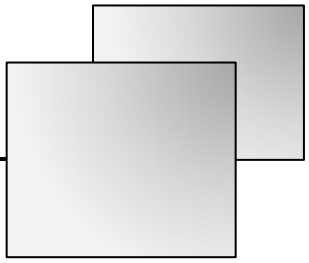

Effect of GPER1 activation on the global transcriptome in breast cancer cells

8.1. INTRODUCTION

The role of estrogen in breast cancer development and progression is indispensable[47]. Estrogen actions in breast malignancies have been majorly ascribed to ERα[48,49]. With the addition of a new membrane-associated estrogen receptor (GPER1) to the estrogen receptor family, the complexity of estrogen signaling is increased. Although the immediate consequences of GPER1 signaling are second messenger production and activation of enzyme cascades, the influence of these signaling events on transcription cannot be ignored. To date, GPER1 is known to regulate the expression of genes involved in cell proliferation[14,29,109,111,129], migration[16,97,98,101,129], invasion[101,179–181] and apoptosis[24,66,110,112] in various cellular contexts. These diverse GPER1 signals are conveyed as a result of crosstalk with other signaling pathways. One such signaling crosstalk is of immediate interest is genomic-signaling of estrogen, which is mediated by nuclear ERs. Several studies have reported that GPER1 signaling interferes with ERα signaling in different cellular context including breast cancer[66,67,69]. The consequences of this crosstalk at the global transcriptome level are not clear. While ERα-mediated transcriptional changes are extensively studied, the contribution of GPER1 in this regard is not adequately considered. Towards understanding the GPER1-mediated global transcriptional changes, Pandey et al., have profiled the early effects of estrogen in SkBr-3 cells[129]. Another report studying the early GPER1 effects has highlighted the importance of ERs in GPER1 signaling. Here, only membrane-initiated GPER1-actions were studied[182]. However, the long-term consequences of GPER1 activation, at global transcriptome level, are not entirely known. Considering the fact that estrogen actions are mediated by, at least, three major receptors, it is challenging to ascertain GPER1-specific effects. In this regard, screening of a selective GPER1 ligand, G1, has made a great contribution[105]. G1 is extensively used to unravel the GPER1-specific effects[14,29,66,108–115].

It is well established that, GPER1 activation leads to the activation of kinase cascades which then activate the transcription factors to regulate gene expression and the associated biological processes. Therefore, transcriptomic profile of long-term GPER1 activation will reveal the secondary pathways which are influenced by GPER1 signaling. Considering the antiproliferative effect of GPER1 activation in MCF-7 cells, we have

attempted to capture the associated transcriptomic profile and to understand how GPER1 contributes to estrogen signaling. Here we give the compelling evidence for the GPER1-ERα signaling crosstalk. Our results underscore the fact that GPER1 signaling counteracts ERα-mediated estrogen actions in breast cancer cells.

8.2. RESULTS

8.2.1. GPER1 inhibits the E2-induced proliferation of MCF-7 cells

To check the effect of GPER1 activation on MCF-7 cells, we treated the cells with increasing concentrations of G1 in M1 and M2 media for 96 h. Our MTT assay results revealed that G1 stimulation reduced the viability of MCF-7 cells significantly at concentrations 1 µM and above in M1. Although compared to ethanol (EtOH) treated group there was a reduction in the viability at 1 µM G1 in M2, it was not statistically significant (Figure 8.1). For the observed difference in the G1 effects, we hypothesized that steroid deprivation might be resulting in reduced GPER1 expression. To test this, we assessed the mRNA and protein levels of GPER1 in MCF-7 cells cultured in M1 and M2. Surprisingly, GPER1 expression was significantly lesser in M2 as compared to M1 (Figure 8.2). Next, we checked the effect of G1 in the presence and absence of 10 nM E2. In the absence of E2, only a G1 concentration of 10 µM showed a significant reduction in cell viability compared to EtOH. The viability of cells at all tested concentrations of G1, in the presence of E2, was significantly lesser than that in E2 alone treatment (Figure 8.3).

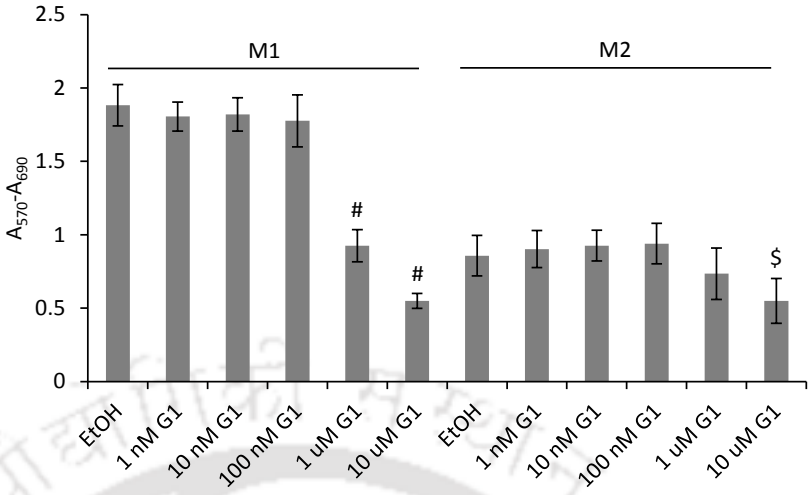

Figure 8.1. Effect of G1 stimulation on MCF-7 cells cultured in M1 and M2. MCF-7 cells were seeded into 96-well plate and grown for 48 h in M1. Cells were treated with indicated concentrations of G1 for 96 h in M1 or M2. The medium was replenished after every 48 h. After the treatment, the cell viability was measured by MTT assay as described in section 3.3 of Chapter 3. Bars represent mean ± SD of A_{570}-A_{690} values. n = 8, # indicates $p < 0.05$ versus EtOH group in M1-cultured cells, $ indicates $p < 0.05$ versus EtOH group in M2-cultured cells.

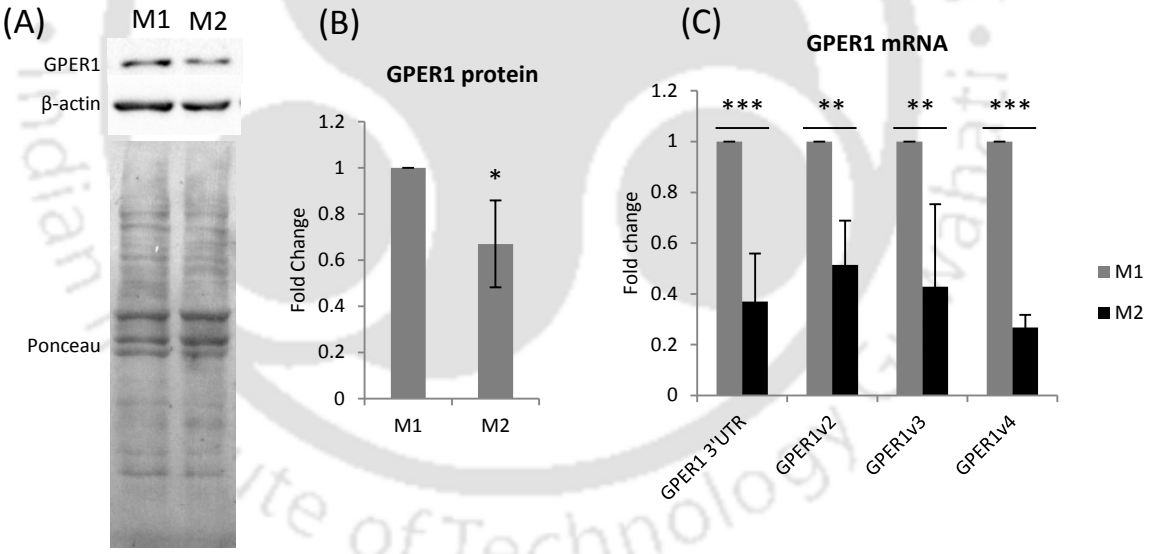

Figure 8.2. GPER1 expression in MCF-7 cells cultured in M1 or M2. MCF-7 cells were seeded in 35 mm dishes and grown for 48 h in M1. The medium was switched to M1 or M2 and cells were grown for 72 h, with medium replenishment after 48 h. Cells were lysed in either RIPA lysis buffer containing protease inhibitor cocktail or TRIzol. 30 µg of total protein was used in western blotting to assess the GPER1 and β-actin protein levels (A). The GPER1 bands were quantified and normalized against ponceau S (B). Total RNA was isolated and cDNA was synthesized from 2 µg of DNaseI treated total RNA. cDNA equivalent to 20 ng of total RNA was taken as the template in the qRT-PCR reactions. RPL35A was used as an internal control. The relative expression levels of the GPER1 mRNA variants were analyzed by $\Delta\Delta C_t$ method and expressed as fold change in M2 with respect to M1 (C). The bars in the graphs represent the mean fold-change ± SD, n = 5 for A, n = 6 for C, * $p < 0.05$, ** $p < 0.01$, *** $p < 0.001$.

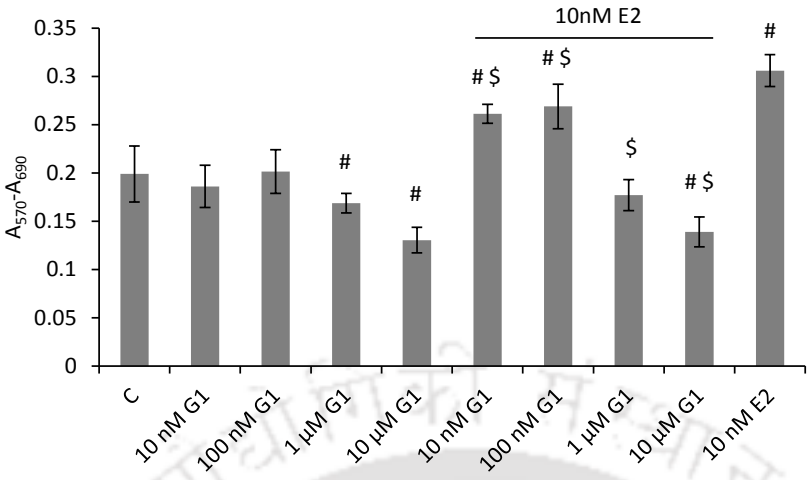

Figure 8.3. G1 stimulation inhibits estrogen-mediated cell growth in MCF-7 cells. MCF-7 cells were seeded into 96-well plate and grown for 48 h in M1. Cells were treated with indicated concentrations of G1 and E2 for 96 h in M2. The medium was replenished after every 48 h. After the treatment, the cell viability was measured by MTT assay as described in section 3.3 of Chapter 3. Bars represent mean ± SD of A_{570}-A_{690} values. n = 8, # indicates $p < 0.05$ versus EtOH, $ indicates $p < 0.05$ versus 10 nM E2.

8.2.2. GPER1 activation arrests MCF-7 cells at G2/M-phase and induces the apoptosis

The G1 treated cells were found to be morphologically different from controls. Unlike EtOH treated control group, G1 treated cells were spherical and were partially attached to the surface. This morphology resembled the cells in M-phase of the cell cycle (Figure 8.4). To check this possibility, we analyzed the cell cycle profile by flow cytometry and found that G1-simulation arrested the cells in G2/M-phase of the cell cycle (Figure 8.5). As a positive control for the mitotic arrest, cells were treated with 200 nM of colchicine. Further, we checked the levels of cleaved-PARP as an indicator of apoptosis. A drastic increase in the cleaved-PARP levels was observed in G1 treated cells as compared to EtOH group (Figure 8.6). Interestingly, assessment of GPER1 protein expression revealed its reduced expression in G1 stimulated cells as compared to EtOH treated cells, possibly indicating the degradation of the receptor after activation.

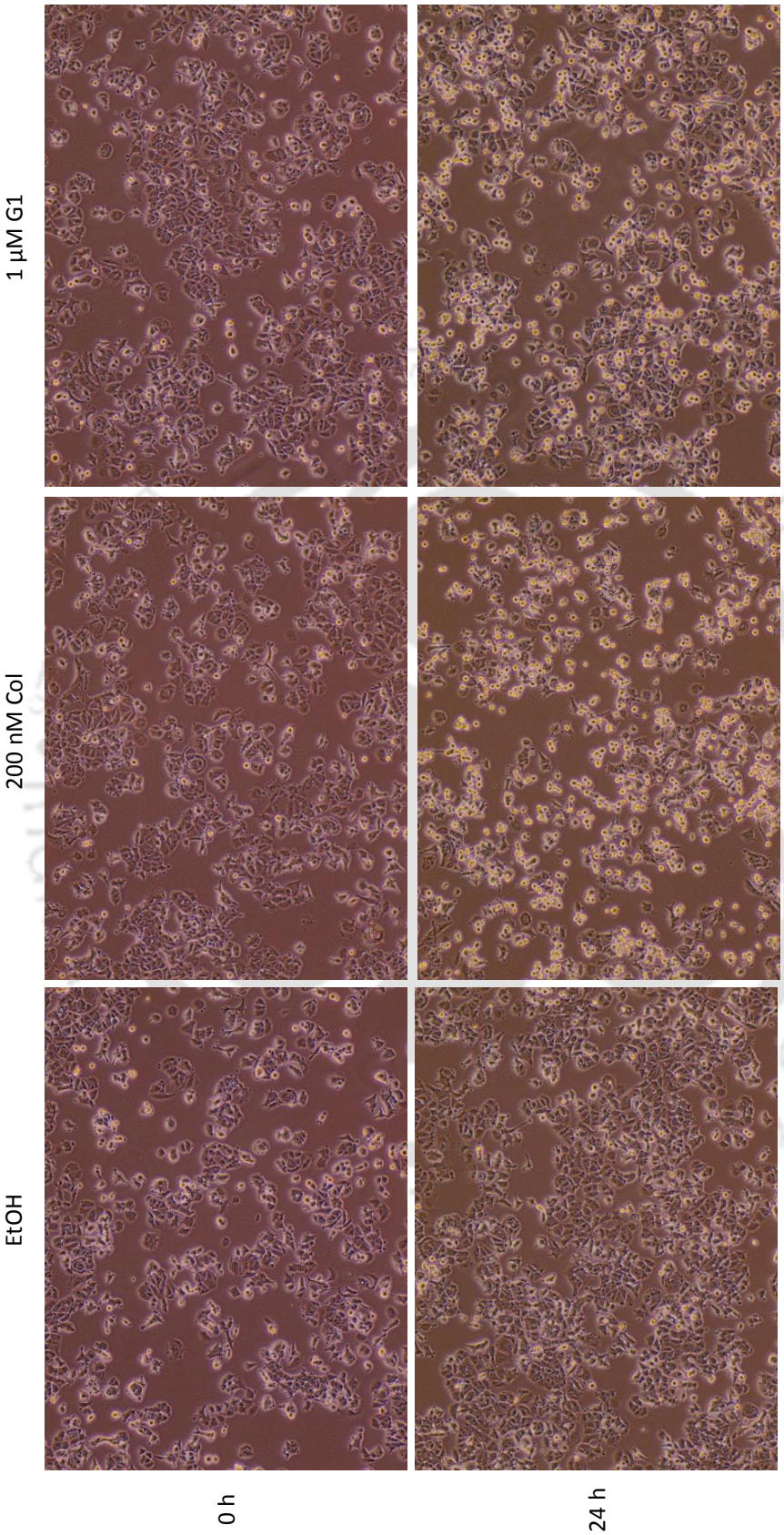

Figure 8.4. G1-induced morphological changes in MCF-7 cells. MCF-7 cells were seeded into 35 mm dishes and allowed to grow for 48 h. Cells were treated with 1 µM G1, 200 nM colchicine (Col) or EtOH for 48 h in M1. The images of the cells were captured at the beginning of the treatment (0 h), and after 24 hours (24 h). The images were taken in an EVOS XL core cell imaging system with 20X objective. Colchicine was used as positive control for mitotic arrest.

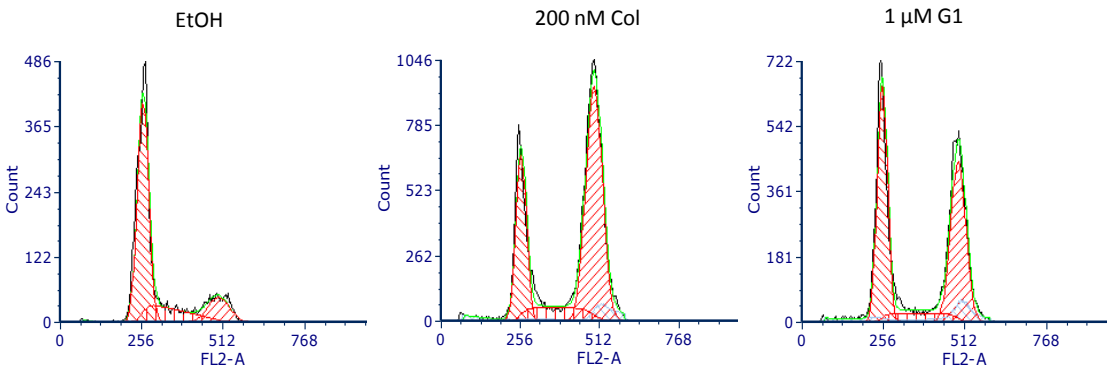

	G1	S	G2/M
EtOH	65.42	20.64	13.95
200 nM Col	26.35	11.74	61.91
1 µM G1	44.24	11.67	44.10

Figure 8.5. GPER1 activation arrests the cell cycle in G2/M-phase. MCF-7 cells were seeded into 35 mm dishes and allowed to grow for 48 h. Cells were treated with 1 µM G1, 200 nM colchicine (Col) or EtOH for 24 h in M1. After the treatment, cells were processed and analyzed using flow cytometer (as described in section 3.4 of Chapter 3). The PI fluorescence signal is plotted as a histogram. Colchicine was used as positive control for G2/M-arrested cell cycle profile. Percentage of cells in each phase of the cell cycle is given in the table. Numbers are average of two biological replicates.

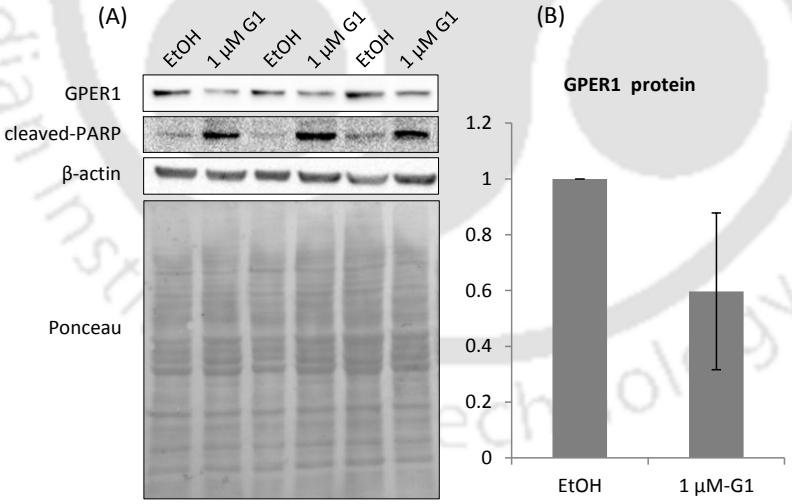

Figure 8.6. GPER1 activation induces apoptosis in MCF-7 cells. MCF-7 cells were seeded into 35 mm dishes and allowed to grow for 48 h. Cells were then treated with 1 µM G1 or equivalent volume of EtOH for 48 h in M1. Cells were lysed in RIPA lysis buffer containing protease inhibitor cocktail. 30 µg of total protein was used for western blotting to assess the protein levels GPER1, cleaved-PARP and β-actin. The chemiluminescence signal was captured and the images of all the three biological replicates are shown (A). The GPER1 bands were quantified and normalized against ponceau S (B). The fold change was not statistically significant.

8.2.3. GPER1 regulated genes in MCF-7 cells

MCF-7 cells were treated with EtOH, 100 nM or 1 µM G1 for 48 h in M1 medium and the transcriptional profiles were assessed by microarray. Genes with a minimum fold change of 1.5 and $p < 0.05$ were considered as significantly differentially regulated genes. Average values of the replicate probes were considered. In case of multiple probes representing same gene, probe with the highest fold-change was considered for further analysis. Microarray results revealed that with respect to EtOH treated group there were 2388 and 3612 genes differentially regulated in 100 nM and 1 µM G1 treated groups, respectively. Out of 2388 genes regulated by 100 nM G1 stimulation, 1132 were up-regulated, and 1256 were down-regulated. In case of 1 µM G1, out of 3612 genes, 1894 were up-regulated and 1718 were down-regulated. When the filtering criterion for significance was changed to false discovery rate (FDR, p.adj < 0.05), there were 986 differentially regulated genes with a minimum of 1.5 fold change in 1 µM G1 treated group. Surprisingly, none of the genes regulated by 100 nM G1 satisfied these stringent filtering criteria. List of top 100 up- and down-regulated genes in 1µM G1 group are given in supplementary table 8.1 and 8.2, respectively.

We analyzed the list of 986 genes, significantly regulated in 1 µM G1 group, for various gene signatures using "Investigate Gene Sets" tool from Molecular signature database (MSigDB). Here, genes from different curated gene sets are searched in the query gene list to identify overlapping genes. The probability of the observed overlap is assessed by a hypergeometric test. Analysis using the collection "hallmark gene sets"[183] revealed that 33 gene signatures are significantly (p.adj < 0.01) enriched in the list of 1 µM G1 regulated genes (Table 8.1). We acknowledge our use of the gene set enrichment analysis, GSEA software, and Molecular Signature Database (MSigDB)[184,185]

8.2.4. E2-target genes regulated by GPER1

In an attempt to identify estrogen-regulated extracellular matrix remodeling genes (ECMRGs), a microarray study was done by our group on the same MCF-7 cell lines. Where in, MCF-7 cells were treated with 10 nM E2 for 24 h and then the transcriptional response was profiled (GSE56245)[186,187]. There were 470 differentially regulated genes with a minimum of 1.5 fold change and p.adj value less than 0.05. These estrogen targets were

searched in 1 µM G1 regulated gene list (986 genes). Surprisingly, 74 estrogen targets were present in the list of G1 regulated genes. Further, these genes were found to be oppositely regulated by E2 and G1 treatments (Table 8.2).

8.3. DISCUSSION

The involvement of ERα in GPER1 signaling is reported independently by several groups. Both GPER1 and ERα are involved in the estrogen-mediated proliferation of mouse spermatogonial cells, GC-1[115]. Estrogen-induced migration in endometrial cancer cells was mediated by GPER1 via EGFR/PI3K/ERK/pFAK axis, in both ERα-positive (Ishikawa) and -negative (RL95-2) cells. Interestingly, in Ishikawa cells, this signaling axis was dependent on ERα expression[16]. The expression of ERα and GPER1 was essential for the estrogen-mediated c-fos induction and enhanced cell proliferation in ovarian cancer cells (BG-1 and 2008). Whereas in SkBr-3 cells, these estrogen-effects were brought about by GPER1 signaling alone[29]. Apart from this, recent reports reveal the involvement of yet another estrogen receptor, ERα-36 (a truncated version of ERα), in estrogen signaling[93,182,188]. The collaboration of ERα-36 with GPER1 in mediating estrogen signaling is also revealed[93,182]. Collectively, these evidence highlight crosstalk between genomic and non-genomic arms of estrogen signaling.

Despite the considerable achievements in the field of GPER1 signaling, its target transcriptome is not completely known. Towards this, Pandey et al., have identified GPER1-target genes in an ERα-negative SkBr-3 breast cancer cells[129]. Here, the early GPER1 targets were identified by profiling the transcriptome of SkBr-3 cells treated with E2 or Tam, for a short duration of 1 h. Induction of an array of transcription factors was the response to these stimuli and CTGF was identified as the most up-regulated gene. Further, it was revealed that CTGF is important in the E2-mediated induction of proliferation and migration of SkBr-3 cells. Another report studying the early GPER1 effects has highlighted the importance of ERs in GPER1 signaling[182]. In order to study the membrane initiated estrogen actions on gene expression, cell impermeable E2 (E2-BSA) was used to stimulate selectively the membrane bound GPER1.

Table 8.1. Hallmark gene sets enriched in G1-regulated genes.

Enriched gene set	K	k	k/K	FDR	Up	Down
E2F TARGETS	200	52	0.26	1.79E-42	3	49
G2M CHECKPOINT	200	51	0.255	1.77E-41	2	49
APOPTOSIS	161	24	0.1491	6.14E-14	21	3
MITOTIC SPINDLE	200	26	0.13	9.63E-14	8	18
MTORC1 SIGNALING	200	25	0.125	6.31E-13	14	11
ESTROGEN RESPONSE LATE	200	24	0.12	3.53E-12	6	18
HYPOXIA	200	24	0.12	3.53E-12	21	3
GLYCOLYSIS	200	21	0.105	1.11E-09	11	10
TNFA SIGNALING VIA NFKB	200	20	0.1	6.31E-09	20	0
UV RESPONSE UP	158	17	0.1076	3.14E-08	11	6
MYC TARGETS V1	200	19	0.095	3.14E-08	4	15
P53 PATHWAY	200	18	0.09	1.65E-07	17	1
DNA REPAIR	150	15	0.1	5.15E-07	3	12
UNFOLDED PROTEIN RESPONSE	113	13	0.115	6.34E-07	9	4
ESTROGEN RESPONSE EARLY	200	17	0.085	7.14E-07	4	13
XENOBIOTIC METABOLISM	200	16	0.08	3.40E-06	12	4
REACTIVE OXIGEN SPECIES PATHWAY	49	7	0.1429	8.94E-05	7	0
IL6 JAK STAT3 SIGNALING	87	9	0.1034	9.13E-05	8	1
EPITHELIAL MESENCHYMAL TRANSITION	200	13	0.065	2.26E-04	11	2
HEME METABOLISM	200	13	0.065	2.26E-04	9	4
MYOGENESIS	200	13	0.065	2.26E-04	9	4
INTERFERON GAMMA RESPONSE	200	12	0.06	8.27E-04	10	2
ANDROGEN RESPONSE	101	8	0.0792	1.23E-03	4	4
MYC TARGETS V2	58	6	0.1034	1.42E-03	1	5
ADIPOGENESIS	200	11	0.055	2.38E-03	6	5
COMPLEMENT	200	11	0.055	2.38E-03	10	1
INFLAMMATORY RESPONSE	200	11	0.055	2.38E-03	11	0
CHOLESTEROL HOMEOSTASIS	74	6	0.0811	4.35E-03	4	2
PI3K AKT MTOR SIGNALING	105	7	0.0667	5.74E-03	3	4
KRAS SIGNALING UP	200	10	0.05	6.55E-03	9	1
OXIDATIVE PHOSPHORYLATION	200	10	0.05	6.55E-03	6	4
HEDGEHOG SIGNALING	36	4	0.1111	6.55E-03	3	1
UV RESPONSE DN	144	8	0.0556	8.08E-03	4	4
WNT BETA CATENIN SIGNALING	42	4	0.0952	1.07E-02	1	3
ALLOGRAFT REJECTION	200	9	0.045	1.65E-02	8	1
IL2 STAT5 SIGNALING	200	9	0.045	1.65E-02	6	3
KRAS SIGNALING DN	200	9	0.045	1.65E-02	5	4
SPERMATOGENESIS	135	7	0.0519	1.67E-02	3	4
COAGULATION	138	7	0.0507	1.82E-02	5	2
TGF BETA SIGNALING	54	4	0.0741	2.17E-02	2	2
FATTY ACID METABOLISM	158	7	0.0443	3.34E-02	4	3

K: Genes in gene set, k:Genes in overlap, Up: up-regulated genes, Down: Down-regulated genes

Table 8.2. List of estrogen target genes regulated by G1.

Gene name	1 µM G1	10 nM E2	Gene name	1 µM G1	10 nM E2
MCM7	-1.8746	1.323855	C16orf59	-0.96292	1.051572
MCM5	-1.7188	1.145453	GPR19	-0.96132	1.433849
RAB31	-1.63452	1.905258	SGK3	-0.94226	1.849646
PKMYT1	-1.60994	1.519001	YBX2	-0.92385	0.893736
E2F1	-1.58432	1.378863	HEY2	-0.90384	1.484436
FANCD2	-1.5242	1.03245	CENPM	-0.89148	1.2707
RAD54L	-1.4519	1.623429	RERG	-0.87029	1.52135
BLM	-1.4475	1.275215	GINS3	-0.8596	1.061362
CENPN	-1.41469	0.861292	CENPO	-0.83405	0.896062
DTL	-1.41293	1.305097	RNASEH2A	-0.83116	0.908016
C15orf42	-1.41202	1.424104	KIF24	-0.81409	1.234306
TMEM164	-1.33719	1.971389	WDR62	-0.80002	1.343161
RAD51	-1.33026	1.167491	RAPGEFL1	-0.76458	1.728085
MYBL1	-1.31651	3.611214	TMEM26	-0.74714	1.255916
RECQL4	-1.2697	1.087215	FAM83D	-0.71563	1.082147
RAMP3	-1.23431	1.843027	TCF19	-0.71009	0.843353
CHAF1A	-1.2322	0.872528	CDC42EP2	-0.70648	1.057084
SFXN2	-1.22856	1.912252	OLFM1	-0.65451	1.142686
EXO1	-1.22037	1.376295	HCK	-0.61946	1.489888
GINS2	-1.19455	1.096147	CHST8	-0.60397	1.312156
MCM10	-1.19312	1.231196	PSCA	0.623905	-2.28751
IGSF1	-1.18636	2.507447	LIMA1	0.70917	-1.37293
FANCG	-1.17839	0.960443	BTG2	0.73317	-1.21656
GINS4	-1.1771	1.301797	NEDD9	0.745357	-1.69976
PGR	-1.16558	2.720212	FOS	0.871009	1.784813
AR	-1.15978	-0.82647	CEACAM6	0.871369	-0.85188
GPR68	-1.1576	1.755841	FABP5	0.872394	1.17617
TOP2A	-1.10416	1.190165	MALL	0.873517	-0.92637
ESPL1	-1.08965	1.173271	MGP	0.883861	2.428145
FANCA	-1.0862	1.194359	SIGLEC15	0.930828	0.893937
CDCA5	-1.08431	1.111656	PLA2G10	0.942869	-1.54875
FBXO5	-1.0594	1.085633	DHRS3	1.005663	-1.93001
PHF19	-1.02172	0.90658	CLEC2D	1.07028	-1.4183
SYTL4	-1.01717	1.110274	ANG	1.314214	-1.15925
POLQ	-1.00936	1.213923	S100A7	1.388545	1.857613
KIF2C	-1.00047	1.214723	IGFBP3	1.408892	-2.50984
CHAF1B	-1.0003	1.089293	TFPI	1.516058	-1.04488

The consequences of GPER1 activation were assessed in a panel of breast cancer cell lines (MCF-7, T47D, MDA-MB-231 and SkBr-3) which express different combinations of estrogen receptors. Using fulvestrant as a blocker of ERs, it is demonstrated that these classical estrogen receptors and their variants are involved in mediating the membrane-initiated GPER1 actions. While a majority of the E2-BSA regulated genes required both GPER1 and, ERα and its variants, a small set of genes were specifically regulated by GPER1. These GPER1-specific targets were enriched with FOXA2/FOXA3 transcription factor networks.

In the present study, we have attempted to identify the transcriptional response to the long-term GPER1 activation in MCF-7 cells. Considering the crosstalk between genomic and non-genomic arms of estrogen signaling, we have selected MCF-7 cells as our model system. These cells express both ERα and GPER1 (Figure 7.1). In our study, the selective activation of GPER1 was achieved by a non-steroidal synthetic ligand, G1. Because of its selective affinity towards GPER1 over ERα or ERβ[105], G1 is extensively being used to study the GPER1-specific effects.

G1 stimulation reduced the viability of MCF-7 cells culture in M1 and M2. Interestingly, the extent of G1-mediated reduction in viability was more in M1-culture cells as compared to M2-cultured cells. In accordance with this, we observed the reduced expression of GPER1 in M2-cultured cells, as compared to cells cultured in M1. Further, the presence of E2 enhanced the sensitivity of the cells to G1-stimulation. In light of our results from Chapter 6, this was expected as E2-stimulation induces the GPER1 expression. Collectively, these results suggest that GPER1 expression levels influence the efficacy of the G1-stimulation, in MCF-7 cells. Morphological changes associated with G1-stimulation suggested the mitotic arrest of cell cycle. Further investigations on these lines using flow cytometer revealed that cells are arrested in G2/M-phase of the cell cycle (Figure 8.5) and are destined to apoptosis (Figure 8.6). Taken together, these results indicate that selective activation of GPER1 in MCF-7 cells inhibits the proliferation by G2/M-phase arrest and induces apoptosis.

Taking the clue from our MTT assay results and also from the published reports we selected to work with two G1 concentrations, 100 nM and 1 μM. Since no gene in the 100

nM treatment group satisfied our filtering criterion of FDR (p.adj < 0.05), we performed our analysis with differentially regulated genes in 1 µM treatment group. Analysis of our microarray results revealed that, G1 stimulation perturbed the cell cycle checkpoints and apoptosis related genes. In light of our cell-based assay results, these were expected. Further, other enriched gene signatures include Hypoxia, TNF-α signaling via NFκB, IL6/JAK/STAT3 pathway, interferon gamma, PI3K/AKT/mTOR, Wnt/β-catenin, and TGF-β signaling. Interestingly, GPER1 signaling is reported to crosstalk with some of these signaling pathways[109,132,189–191]. Recent reports are increasingly highlighting the connection between GPER1 and IL6[109,181,191,192], in various contexts and IL6 is one of the top GPER1 up-regulated genes in our array.

Surprisingly, gene signatures related to estrogen response were also enriched in the list of G1 regulated genes. Further investigations in this line revealed that E2 and G1 oppositely regulate these genes. In the recent past, Ding et al., demonstrated the involvement of GPER1 in estrogen-induced apoptosis of vascular smooth muscle cells (VSMC)[69]. In VSMC transduced with GPER1, estrogen stimulation induced the phosphorylation of ERK1/2 and inhibited PKA activity. In contrast, estrogen stimulation inhibited ERK1/2 phosphorylation and induced PKA activity in the absence of GPER1. This effect was further enhanced with transduction of ERα. Although in a paracrine mode, GPER1 activation in the uterine epithelial cells abrogated the ERα-mediated estrogen actions in the stroma[67]. A recent attempt to identify the GPER1-mediated phosphoproteomic profile in MCF-7 cells revealed that GPER1 signaling counteracts ERα activity[66]. Taken together, these independent studies demonstrated the scenarios in which GPER1 signaling counteracts the ERα-mediated estrogen actions. At the same time, suggest that the final outcome of estrogen stimulation is a fine balance between the two counteracting signaling arms. Towards this, our comparative analysis of G1 and E2 regulated genes gives yet another proof. We propose that the strength of GPER1 signaling in case of 100 nM G1 treatment is not sufficient to completely overtake the ERα actions. Our MTT assay results and inputs from the findings of Chapter 6 also support this proposition. Nonetheless, these hypotheses are to be tested with the appropriate experimental setup.

Amidst these developments, few recent reports suspected the G1-mediated cellular changes as off-target effects, particularly at higher concentrations of G1. G1 induces apoptosis of ovarian cancer cells by blocking tubulin polymerization, in a GPER1-independent manner[193,194]. G1 was shown to bind to the colchicine-binding site of tubulin and inhibits the cell proliferation[195]. However, the experimental evidence reported by others convincingly prove that G1 effects are mediated by GPER1[24,66,67,112,115].

Chapter IX

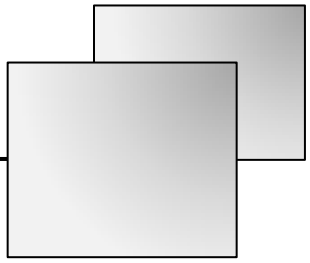

Conclusion

9.1. CONCLUSION

GPER1 is a novel G-protein coupled receptor, implicated in non-genomic actions of estrogen. Downstream effects of GPER1 signaling include the production of second messengers (cAMP, PI3, and calcium) and activation of enzyme cascades, which ultimately culminate in the regulation of gene expression. Since its discovery as an estrogen receptor, several independent groups have contributed towards understanding the role of GPER1 in physiological and pathological conditions. The influence of GPER1 signaling in reproductive, cardiovascular, skeletal, renal, nervous and immune systems is increasingly appreciated. Altered GPER1 expression and signaling have been observed in breast, ovarian, endometrium, thyroid, and lung malignancies. Its ability to crosstalk with various growth-factor signaling pathways highlights the potential of GPER1 signaling in tumor growth and progression. GPER1 effects are cell type and tissue-specific. This specificity is conferred by the combination of downstream players at the target site. GPER1 can be activated by a plethora of phytoestrogens, xenoestrogens, and most importantly, clinically approved drugs such as fulvestrant and tamoxifen. Presently, GPER1 is a center point of attraction in the field of estrogen biology. We believe that the present thesis work is a significant contribution to this emerging field.

The role of estrogen in breast cancer is well established. Involvement of nuclear estrogen receptor in mediating estrogen actions is indispensable. In the past decade, GPER1-mediated estrogen actions in breast cancer are extensively studied. In vitro studies have revealed the importance of GPER1 in breast cancer progression, development and drug resistance. However, its clinical utility in breast cancer is not completely understood. The present thesis work focuses on understanding the role of GPER1 expression and regulation in breast cancer. We assessed the expression of the GPER1 protein in breast tumors from patients of the North-East Indian population. To the best of our knowledge, this is the first attempt to study GPER1 expression in breast tumors from patients within the Indian population. The genetic diversity represented by the north-eastern part of the country is very well appreciated and growing incidence rate of breast cancer in this region is also reported. Considering the need for clinical inputs, to ascertain the clinicopathological significance of GPER1 in breast cancer, we initiated this study. Additionally, we assessed the GPER1

expression and its correlation with clinicopathological parameters using publically available data from TCGA. Our IHC and TCGA analyses result collectively support the notion that GPER1 is a potential tumor suppressor in breast cancer and its expression positively correlates with ERα. In light of confusion in the existing reports, our contribution is significant in ascertaining the role of GPER1 as a tumor suppressor in breast cancer. Further, we report here that the mutual association between the estrogen receptors is different in tumors as compared to normal breast tissues.

Clinical studies, including ours, have suggested the positive correlation between GPER1 and ERα expression in breast cancer. However, the underlying functional link was not known. In light of its role in tamoxifen resistance and metastasis, it becomes important to understand the molecular basis for the correlation. With the *in vitro* experimental setup we have demonstrated that ERα regulates the GPER1 expression. Supporting this, *in silico* analyses provided the strong evidence which led to the identification of a potential ERE in the GPER1 locus. Collectively, our results revealed the mechanism of estrogen-mediated regulation of GPER1 in breast cancer. Future investigations in the labs are focused on validating these observations and further characterizing the GPER1 expression regulation in normal and tumor contexts.

Another interesting outcome of this investigation was profiling of GPER1 mRNA transcript variants. We have successfully demonstrated the expression of three transcript variants of GPER1 in breast cancer cell lines. To the best of our knowledge, the expression profile of these variants in breast cancer was not reported earlier. However, we have not encountered any situation in which these transcript variants are differentially regulated. Despite the expression of GPER1 in diverse cell types (epithelial and neuronal cells) and its multiple cellular localization these variants remain unnoticed. Unraveling the biological role of these variants will be of importance in understanding GPER1 signaling. Towards this, the existing RNA-Seq data could be a good source of information.

Reduced expression of GPER1 is observed in breast tumors compared to normal breast tissue. Moreover, its expression decreases during the process of tumorigenesis. Along with these, the positive impact of GPER1 expression on patient survival collectively highlighted its tumor suppressor potential. However, the molecular underpinnings for the

reduced expression were not known. Our investigations in this regard demonstrated the importance of DNA methylation in regulation of GPER1 expression. We characterized the methylation status of two CpG islands in the GPER1 locus and highlighted the role of upCpGi in GPER1 expression regulation. We have also clearly demonstrated that the involvement of dnCpGi in the regulation of GPER1 expression is dispensable. With the bolstering evidence from the *in silico* analyses, the importance of shore regions of upCpGi in GPER1 expression regulation was revealed. Coincidentally, independent groups demonstrated the importance of methylation status of the same region in connection with GPER1 expression regulation. However, the influence of histone modifications on GPER1 expression regulation cannot be ruled out and need to be investigated.

Despite the considerable advancements in the field of GPER1 signaling, its target transcriptome is not clearly explored. Here we have made an attempt to capture the transcriptional response to long-term GPER1 activation, in MCF-7 cells. Our results show that selective activation of GPER1 inhibits the proliferation of MCF-7 cells by G2/M phase arrest followed by apoptosis. Interestingly, the G1 regulated gene list was enriched with estrogen-target genes. Further, the mode of regulation of these genes, by G1, was opposite to that by E2. Our results supported the hypothesis that GPER1 and ERα-signaling counteract each other. In a scenario where both GPER1 and ERα are expressed, the final outcome of estrogen stimulation is a balance between the strengths of individual signaling arms.

Taken together, the present study provides novel insights into the role of GPER1 in breast cancer. Our contributions are significant in terms of revealing the mechanisms of GPER1 expression regulation in breast cancer. In light of its tumor suppressor potential, the possibilities of epigenetic reactivation of GPER1 expression can be explored for better breast cancer management. The clinical work presented in the thesis is just the beginning and the study continues to investigate further with larger cohort size as the new samples accumulate. We hope this initiative will contribute significantly to the GPER1 community and ultimately to patients. With the new oncology department being established at NEIGRIHMS we hope that the data and sample collection and accessibility will be much more streamlined in the near future. Microarray results underscore the crucial role of GPER1 signaling in regulating the genomic estrogen actions. Along with these findings, our

research has opened certain intriguing leads. The biological roles of GPER1 transcript variants need to be revealed. We believe that the expression profiling of GPER1 transcript variants and protein in clinical samples will be of great value. Such studies will help us appreciate the biological significance of these variants. At the same time, possibly, might give a newer dimension to explain the cell-context-specific localization of GPER1. The altered mutual association between the estrogen receptors in tumors is interesting and it is important to reveal the underlying biology. Considering the cell context specific nature of GPER1 signaling, this will help us to understand as to how the signaling is differentially perceived by normal and tumor cells. Molecular characterization of GPER1- ERα crosstalk will be of great value. This will highlight the need for considering the contribution of GPER1 signaling when designing the treatment strategies for breast cancer management. Presently, research in the lab is focusing on some of these leads and we hope to keep contributing to the GPER1 community towards furthering our understanding of biological significance of GPER1.

Bibliography

BIBLIOGRAPHY

1. Takada, Y., Kato, C., Kondo, S., Korenaga, R. & Ando, J. Cloning of cDNAs Encoding G Protein-Coupled Receptor Expressed in Human Endothelial Cells Exposed to Fluid Shear Stress. **741,** 737–741 (1997).

2. Feng, Y. & Gregor, P. Cloning of a novel member of the G protein-coupled receptor family related to peptide receptors. *Biochem. Biophys. Res. Commun.* **231,** 651–654 (1997).

3. Dowd, B. F. O. *et al.* Discovery of Three Novel G-Protein-Coupled Receptor Genes. **313,** 310–313 (1998).

4. Carmeci, C., Thompson, D. A., Ring, H. Z., Francke, U. & Weigel, R. J. Identification of a gene (GPR30) with homology to the G-protein-coupled receptor superfamily associated with estrogen receptor expression in breast cancer. *Genomics* **45,** 607–617 (1997).

5. Kvingedal, A. M. & Smeland, E. B. A novel putative G-protein-coupled receptor expressed in lung , heart and lymphoid tissue. *FEBS Lett.* **407,** 59–62 (1997).

6. Bonini, J. A., Anderson, S. M. & Steiner, D. F. Molecular Cloning and Tissue Expression of a Novel Orphan G Protein-Coupled Receptor from Rat Lung. **193,** 190–193 (1997).

7. Owman, C., Blay, P., Nilsson, C. & Lolait, S. J. Cloning of human cDNA encoding a novel heptahelix receptor expressed in Burkitt's lymphoma and widely distributed in brain and peripheral tissues. *Biochem. Biophys. Res. Commun.* **228,** 285–292 (1996).

8. Filardo, E. J., Quinn, J. a, Bland, K. I. & Frackelton, a R. Estrogen-induced activation of Erk-1 and Erk-2 requires the G protein-coupled receptor homolog, GPR30, and occurs via trans-activation of the epidermal growth factor receptor through release of HB-EGF. *Mol. Endocrinol.* **14,** 1649–1660 (2000).

9. Filardo, E. J. Epidermal growth factor receptor (EGFR) transactivation by estrogen via the G-protein-coupled receptor, GPR30: a novel signaling pathway with potential significance for breast cancer. *J. Steroid Biochem. Mol. Biol.* **80,** 231–238 (2002).

10. Revankar, C. M., Cimino, D. F., Sklar, L. A., Arterburn, J. B. & Prossnitz, E. R. A transmembrane intracellular estrogen receptor mediates rapid cell signaling. *Science (80-.).* **307,** 1625–1630 (2005).

11. Thomas, P., Pang, Y., Filardo, E. J. & Dong, J. Identity of an estrogen membrane receptor coupled to a G protein in human breast cancer cells. *Endocrinology* **146,** 624–632 (2005).

12. Prossnitz, E. R. & Arterburn, J. B. International Union of Basic and Clinical Pharmacology. XCVII. G Protein–Coupled Estrogen Receptor and Its Pharmacologic Modulators. *Pharmacol. Rev.* **67,** (2015).

13. Prossnitz, E. R. & Barton, M. Estrogen biology: New insights into GPER function and clinical opportunities. *Mol. Cell. Endocrinol.* **389,** 71–83 (2014).

14. Vivacqua, A. *et al.* 17beta-estradiol, genistein, and 4-hydroxytamoxifen induce the proliferation of thyroid cancer cells through the g protein-coupled receptor GPR30. *Mol. Pharmacol.* **70,** 1414–1423 (2006).

15. Ignatov, A., Ignatov, T., Roessner, A., Costa, S. D. & Kalinski, T. Role of GPR30 in the mechanisms of tamoxifen resistance in breast cancer MCF-7 cells. *Breast Cancer Res. Treat.* **123,** 87–96 (2010).

16. Tsai, C. L. *et al.* Estradiol and Tamoxifen Induce Cell Migration through GPR30 and Activation of Focal Adhesion Kinase (FAK) in Endometrial Cancers with Low or without Nuclear Estrogen Receptor α (ERα). *PLoS One* **8,** e72999 (2013).

17. Ignatov, A. *et al.* G-protein-coupled estrogen receptor GPR30 and tamoxifen resistance in breast

cancer. *Breast Cancer Res Treat* **133,** 457–466 (2011).

18. Kuo, W. H. *et al.* The interactions between GPR30 and the major biomarkers in infiltrating ductal carcinoma of the breast in an asian population. *Taiwan. J. Obstet. Gynecol.* **46,** 135–145 (2007).

19. Huang, G. S. *et al.* Co-expression of GPR30 and ERbeta and their association with disease progression in uterine carcinosarcoma. *Am. J. Obstet. Gynecol.* **203,** 242.e1-242.e5 (2010).

20. Smith, H. O. *et al.* GPR30 predicts poor survival for ovarian cancer. *Gynecol. Oncol.* **114,** 465–471 (2009).

21. Jala, V. R., Radde, B. N., Haribabu, B. & Klinge, C. M. Enhanced expression of G-protein coupled estrogen receptor (GPER/GPR30) in lung cancer. *BMC Cancer* **12,** 624 (2012).

22. Franco, R. *et al.* GPR30 is overexpressed in post-puberal testicular germ cell tumors. *Cancer Biol. Ther.* **11,** 609–613 (2011).

23. Filardo, E. J. *et al.* Distribution of GPR30, a seven membrane-spanning estrogen receptor, in primary breast cancer and its association with clinicopathologic determinants of tumor progression. *Clin. Cancer Res.* **12,** 6359–6366 (2006).

24. Ariazi, E. a *et al.* The G protein-coupled receptor GPR30 inhibits proliferation of estrogen receptor-positive breast cancer cells. *Cancer Res.* **70,** 1184–1194 (2010).

25. Mo, Z. *et al.* GPR30 as an initiator of tamoxifen resistance in hormone-dependent breast cancer. *Breast Cancer Res.* **15,** R114 (2013).

26. Poola, I., Abraham, J., Liu, A., Marshalleck, J. J. & Dewitty, R. L. The Cell Surface Estrogen Receptor, G Protein- Coupled Receptor 30 (GPR30), is Markedly Down Regulated During Breast Tumorigenesis. *Breast Cancer (Auckl).* **1,** 65–78 (2008).

27. Zhou, X. *et al.* Estrogen regulates Hippo signaling via GPER in breast cancer. *J. Clin. Invest.* **125,** 2123–2135 (2015).

28. Arias-Pulido, H. *et al.* GPR30 and estrogen receptor expression: New insights into hormone dependence of inflammatory breast cancer. *Breast Cancer Res. Treat.* **123,** 51–58 (2010).

29. Albanito, L. *et al.* G protein-coupled receptor 30 (GPR30) mediates gene expression changes and growth response to 17beta-estradiol and selective GPR30 ligand G-1 in ovarian cancer cells. *Cancer Res.* **67,** 1859–1866 (2007).

30. Clark, S., Pollard, K., Rainville, J. & Vasudevan, N. in *Methods in Molecular Biology* **1366,** 457–470 (2016).

31. Wang, C. *et al.* GPR30 contributes to estrogen-induced thymic atrophy. *Mol. Endocrinol.* **22,** 636–648 (2008).

32. Vivacqua, A. *et al.* G protein-coupled receptor 30 expression is up-regulated by EGF and TGF alpha in estrogen receptor alpha-positive cancer cells. *Mol. Endocrinol.* **23,** 1815–1826 (2009).

33. Ignatov, T. *et al.* GPER-1 expression decreases during breast cancer tumorigenesis. *Cancer Invest.* **31,** 309–315 (2013).

34. Weißenborn, C. *et al.* GPER functions as a tumor suppressor in MCF-7 and SK-BR-3 breast cancer cells. *J. Cancer Res. Clin. Oncol.* **140,** 663–671 (2014).

35. Weißenborn, C. *et al.* GPER functions as a tumor suppressor in triple-negative breast cancer cells. *J. Cancer Res. Clin. Oncol.* **140,** 713–723 (2014).

36. Venkatakrishnan, A. J. *et al.* Molecular signatures of G-protein-coupled receptors. *Nature* **494,** 185–194 (2013).

37. Thomas, P. & Dong, J. Binding and activation of the seven-transmembrane estrogen receptor GPR30 by environmental estrogens: a potential novel mechanism of endocrine disruption. *J. Steroid Biochem. Mol. Biol.* **102,** 175–179 (2006).

38. Lucki, N. C. & Sewer, M. B. Genistein stimulates MCF-7 breast cancer cell growth by inducing acid ceramidase (ASAH1) gene expression. *J. Biol. Chem.* **286,** 19399–19409 (2011).

39. Chevalier, N., Bouskine, A. & Fenichel, P. Bisphenol A promotes testicular seminoma cell proliferation through GPER/GPR30. *Int. J. Cancer* **130,** 241–242 (2012).

40. Khan, K. *et al.* Prunetin signals via G-protein-coupled receptor, GPR30(GPER1): Stimulation of adenylyl cyclase and cAMP-mediated activation of MAPK signaling induces Runx2 expression in osteoblasts to promote bone regeneration. *J. Nutr. Biochem.* **26,** 1491–1501 (2015).

41. Lucas, T. F. G., Royer, C., Siu, E. R., Lazari, M. F. M. & Porto, C. S. Expression and signaling of G protein-coupled estrogen receptor 1 (GPER) in rat sertoli cells. *Biol. Reprod.* **83,** 307–317 (2010).

42. Kajta, M. *et al.* Isomer-nonspecific action of dichlorodiphenyltrichloroethane on aryl hydrocarbon receptor and G-protein-coupled receptor 30 intracellular signaling in apoptotic neuronal cells. *Mol. Cell. Endocrinol.* **392,** 90–105 (2014).

43. Maggiolini, M. *et al.* The G protein-coupled receptor GPR30 Mediates c-fos up-regulation by 17beta-estradiol and phytoestrogens in breast cancer cells. *J. Biol. Chem.* **279,** 27008–27016 (2004).

44. Nilsson, S. *et al.* Mechanisms of estrogen action. *Physiol. Rev.* **81,** 1535–1565 (2001).

45. Brisken, C. & O'Malley, B. Hormone action in the mammary gland. *Cold Spring Harb. Perspect. Biol.* **2,** a003178 (2010).

46. Manavathi, B. *et al.* Derailed Estrogen Signaling and Breast Cancer: An Authentic Couple. *Endocr. Rev.* **34,** 1–32 (2013).

47. Russo, J. & Russo, I. H. The role of estrogen in the initiation of breast cancer. *J. Steroid Biochem. Mol. Biol.* **102,** 89–96 (2006).

48. Saha Roy, S. & Vadlamudi, R. K. Role of estrogen receptor signaling in breast cancer metastasis. *Int. J. Breast Cancer* **2012,** 654698 (2012).

49. García-Becerra, R., Santos, N., Díaz, L. & Camacho, J. Mechanisms of resistance to endocrine therapy in breast cancer: focus on signaling pathways, miRNAs and genetically based resistance. *Int. J. Mol. Sci.* **14,** 108–145 (2012).

50. Dimri, G., Band, H. & Band, V. Mammary epithelial cell transformation: insights from cell culture and mouse models. *Breast Cancer Res.* **7,** 171–179 (2005).

51. Perou, C. M. *et al.* Molecular portraits of human breast tumours. *Nature* **406,** 747–752 (2000).

52. Hu, Z. *et al.* The molecular portraits of breast tumors are conserved across microarray platforms. *BMC Genomics* **7,** 96 (2006).

53. NIEHS. www.ntp.niehs.nih.gov. Available at: www.ntp.niehs.nih.gov. (Accessed: 29th August 2015)

54. Torre, L. A. *et al.* Global cancer statistics, 2012. *CA. Cancer J. Clin.* **65,** 87–108 (2015).

55. Kamangar, F., Dores, G. M. & Anderson, W. F. Patterns of cancer incidence, mortality, and prevalence

across five continents: Defining priorities to reduce cancer disparities in different geographic regions of the world. *Journal of Clinical Oncology* **24,** 2137–2150 (2006).

56. DeSantis, C. E. *et al.* Breast cancer statistics, 2015: Convergence of incidence rates between black and white women. *CA. Cancer J. Clin.* **66,** 31–42 (2016).

57. Ferlay, J., Héry, C., Autier, P. & Sankaranarayanan, R. in *Breast Cancer Epidemiology* 1–19 (Springer New York, 2010). doi:10.1007/978-1-4419-0685-4_1

58. Center for Disease Control and Prevention. Breast Cancer Statistics. (2010). Available at: http://cancerindia.org.in/index.php/know-about-cancer/statistics#breast-cancer. (Accessed: 11th September 2017)

59. Agarwal, G. & Ramakant, P. Breast Cancer Care in India: The Current Scenario and the Challenges for the Future. *Breast Care (Basel).* **3,** 21–27 (2008).

60. Howell, S. J., Johnston, S. R. . & Howell, A. The use of selective estrogen receptor modulators and selective estrogen receptor down-regulators in breast cancer. *Best Pract. Res. Clin. Endocrinol. Metab.* **18,** 47–66 (2004).

61. Altundag, K. Aromatase Inhibitors in Breast Cancer: An Overview. *Oncologist* **11,** 553–562 (2006).

62. Van Leeuwen, F. E. *et al.* Risk of endometrial cancer after tamoxifen treatment of breast cancer. *Lancet (London, England)* **343,** 448–452 (1994).

63. Aronica, S. M., Kraus, W. L. E. E. & Katzenellenbogen, B. S. Estrogen action via the cAMP signaling pathway : Stimulation of adenylate cyclase and cAMP-regulated gene transcription. **91,** 8517–8521 (1994).

64. Szego, C. M. & Davis, J. S. Adenosine 3',5'-monophosphate in rat uterus: acute elevation by estrogen. *Proc. Natl. Acad. Sci. U. S. A.* **58,** 1711–1718 (1967).

65. Pietras, R. J. & Szego, C. M. Endometrial cell calcium and oestrogen action. *Nature* **253,** 357–359 (1975).

66. Smith, L. C., Ralston-Hooper, K. J., Ferguson, L. L. & Sabo-Attwood, T. The G protein-coupled estrogen receptor agonist G-1 inhibits nuclear estrogen receptor activity and stimulates novel phosphoproteomic signatures. *Toxicol. Sci.* **151,** 434–446 (2016).

67. Gao, F., Ma, X., Ostmann, A. B. & Das, S. K. GPR30 activation opposes estrogen-dependent uterine growth via inhibition of stromal ERK1/2 and estrogen receptor alpha (ERα) phosphorylation signals. *Endocrinology* **152,** 1434–1447 (2011).

68. Hart, D. *et al.* Activation of the G-protein coupled receptor 30 (GPR30) has different effects on anxiety in male and female mice. *Steroids* **81,** 49–56 (2014).

69. Ding, Q., Gros, R., Limbird, L. E., Chorazyczewski, J. & Feldman, R. D. Estradiol-mediated ERK phosphorylation and apoptosis in vascular smooth muscle cells requires GPR 30. *Am. J. Physiol. - Cell Physiol.* **297,** 1178–1187 (2009).

70. Otto, C. *et al.* GPR30 Does Not Mediate Estrogenic Responses in Reproductive Organs in Mice. **41,** 34–41 (2009).

71. Haas, E. *et al.* Regulatory Role of G Protein-Coupled Estrogen Receptor for Vascular Function and Obesity. *Circ. Res.* **104,** 288–291 (2009).

72. Martensson, U. E. A. *et al.* Deletion of the G protein-coupled receptor 30 impairs glucose tolerance, reduces bone growth, increases blood pressure, and eliminates estradiol-stimulated insulin release in

female mice. *Endocrinology* **150,** 687–698 (2009).

73. Levin, E. R. G protein-coupled receptor 30: Estrogen receptor or collaborator? *Endocrinology* **150,** 1563–1565 (2009).

74. Otto, C. *et al.* G protein-coupled receptor 30 localizes to the endoplasmic reticulum and is not activated by estradiol. *Endocrinology* **149,** 4846–4856 (2008).

75. Madak-Erdogan, Z. *et al.* Nuclear and Extranuclear Pathway Inputs in the Regulation of Global Gene Expression by Estrogen Receptors. *Mol. Endocrinol.* **22,** 2116–2127 (2008).

76. Filardo, E. J. & Thomas, P. Minireview: G protein-coupled estrogen receptor-1, GPER-1: Its mechanism of action and role in female reproductive cancer, renal and vascular physiology. *Endocrinology* **153,** 2953–2962 (2012).

77. Magalhaes, A. C., Dunn, H. & Ferguson, S. S. Regulation of GPCR activity, trafficking and localization by GPCR-interacting proteins. *British Journal of Pharmacology* **165,** 1717–1736 (2012).

78. Duvernay, M. T., Filipeanu, C. M. & Wu, G. The regulatory mechanisms of export trafficking of G protein-coupled receptors. *Cellular Signalling* **17,** 1457–1465 (2005).

79. Tholanikunnel, B. G. *et al.* Novel Mechanisms in the Regulation of G Protein-coupled Receptor Trafficking to the Plasma Membrane. *J. Biol. Chem.* **285,** 33816–33825 (2010).

80. Funakoshi, T., Yanai, A., Shinoda, K., Kawano, M. M. & Mizukami, Y. G protein-coupled receptor 30 is an estrogen receptor in the plasma membrane. *Biochem. Biophys. Res. Commun.* **346,** 904–910 (2006).

81. Chevalier, N. *et al.* Gpr30, the non-classical membrane g protein related estrogen receptor, is overexpressed in human seminoma and promotes seminoma cell proliferation. *PLoS One* **7,** e34672 (2012).

82. Filardo, E. *et al.* Activation of the novel estrogen receptor G protein-coupled receptor 30 (GPR30) at the plasma membrane. *Endocrinology* **148,** 3236–3245 (2007).

83. Cheng, S. B., Graeber, C. T., Quinn, J. a. & Filardo, E. J. Retrograde transport of the transmembrane estrogen receptor, G-protein-coupled-receptor-30 (GPR30/GPER) from the plasma membrane towards the nucleus. *Steroids* **76,** 892–896 (2011).

84. Samartzis, E. P. *et al.* The G protein-coupled estrogen receptor (GPER) is expressed in two different subcellular localizations reflecting distinct tumor properties in breast cancer. *PLoS One* **9,** e83296 (2014).

85. Rago, V., Romeo, F., Giordano, F., Maggiolini, M. & Carpino, A. Identification of the estrogen receptor GPER in neoplastic and non-neoplastic human testes. *Reprod. Biol. Endocrinol.* **9,** 135 (2011).

86. Smith, H. O. *et al.* GPR30 : a novel indicator of poor survival for endometrial carcinoma. *Am. J. Obstet. Gynecol.* **196,** 386.e1-386.e11 (2007).

87. Cheng, S.-B., Quinn, J. A., Graeber, C. T. & Filardo, E. J. Down-modulation of the G-protein-coupled estrogen receptor, GPER, from the cell surface occurs via a trans-Golgi-proteasome pathway. *J. Biol. Chem.* **286,** 22441–22455 (2011).

88. Sandén, C. *et al.* G protein-coupled estrogen receptor 1/G protein-coupled receptor 30 localizes in the plasma membrane and traffics intracellularly on cytokeratin intermediate filaments. *Mol. Pharmacol.* **79,** 400–410 (2011).

89. Ignatov, T. *et al.* Role of GPR30 in endometrial pathology after tamoxifen for breast cancer. *Am. J. Obstet. Gynecol.* **203,** 595.e9-595.e16 (2010).

90. Samartzis, N. *et al.* Expression of the G protein-coupled estrogen receptor (GPER) in endometriosis: a tissue microarray study. *Reprod. Biol. Endocrinol.* **10,** 30 (2012).

91. Madeo, A. & Maggiolini, M. Nuclear Alternate Estrogen Receptor GPR30 Mediates 17 -Estradiol-Induced Gene Expression and Migration in Breast Cancer-Associated Fibroblasts. *Cancer Res.* **70,** 6036–6046 (2010).

92. Pupo, M. *et al.* The nuclear localization signal is required for nuclear GPER translocation and function in breast Cancer-Associated Fibroblasts (CAFs). *Mol. Cell. Endocrinol.* **376,** 23–32 (2013).

93. Pelekanou, V. *et al.* Estrogen anti-inflammatory activity on human monocytes is mediated through cross-talk between estrogen receptor ER 36 and GPR30/GPER1. *J. Leukoc. Biol.* **99,** 333–347 (2016).

94. Tadevosyan, A., Vaniotis, G., Allen, B. G., Hebert, T. E. & Nattel, S. G protein-coupled receptor signalling in the cardiac nuclear membrane: evidence and possible roles in physiological and pathophysiological function. *J Physiol* **590,** 1313–1330 (2012).

95. Bhosle, V. K., Gobeil, F., Rivera, J. C., Ribeiro-da-Silva, A. & Chemtob, S. in *Methods in molecular biology (Clifton, N.J.)* **1234,** 81–97 (2015).

96. Ahola, T. M. *et al.* Progestin upregulates G-protein-coupled receptor 30 in breast cancer cells. *Eur. J. Biochem.* **269,** 2485–2490 (2002).

97. De Marco, P. *et al.* GPER1 is regulated by insulin in cancer cells and cancer-associated fibroblasts. *Endocr. Relat. Cancer* **21,** 739–753 (2014).

98. De Marco, P. *et al.* Insulin-like growth factor-I regulates GPER expression and function in cancer cells. *Oncogene* **32,** 678–688 (2013).

99. Recchia, A. G. *et al.* The G protein-coupled receptor 30 is up-regulated by hypoxia-inducible factor-1alpha (HIF-1alpha) in breast cancer cells and cardiomyocytes. *J. Biol. Chem.* **286,** 10773–10782 (2011).

100. Giessrigl, B. *et al.* Fulvestrant induces resistance by modulating GPER and CDK6 expression: implication of methyltransferases, deacetylases and the hSWI/SNF chromatin remodelling complex. *Br. J. Cancer* **109,** 2751–2762 (2013).

101. Ruan, S.-Q. *et al.* Heregulin-β1-induced GPR30 upregulation promotes the migration and invasion potential of SkBr3 breast cancer cells via ErbB2/ErbB3-MAPK/ERK pathway. *Biochem. Biophys. Res. Commun.* **420,** 385–390 (2012).

102. Kolkova, Z., Noskova, V., Ehinger, A., Hansson, S. & Casslén, B. G protein-coupled estrogen receptor 1 (GPER, GPR 30) in normal human endometrium and early pregnancy decidua. *Mol. Hum. Reprod.* **16,** 743–751 (2010).

103. Witsch, E., Sela, M. & Yarden, Y. Roles for growth factors in cancer progression. *Physiology (Bethesda).* **25,** 85–101 (2010).

104. Filardo, E. J., Quinn, J. A., Frackelton, A. R. & Bland, K. I. Estrogen action via the G protein-coupled receptor, GPR30: stimulation of adenylyl cyclase and cAMP-mediated attenuation of the epidermal growth factor receptor-to-MAPK signaling axis. *Mol. Endocrinol.* **16,** 70–84 (2002).

105. Bologa, C. G. *et al.* Virtual and biomolecular screening converge on a selective agonist for GPR30. *Nat. Chem. Biol.* **2,** 207–212 (2006).

106. Dennis, M. K. *et al.* In vivo effects of a GPR30 antagonist. **5,** 421–427 (2009).

107. Dennis, M. K. *et al.* Identification of a GPER/GPR30 antagonist with improved estrogen receptor counterselectivity. *J. Steroid Biochem. Mol. Biol.* **127,** 358–366 (2011).

108. Scaling, A. L., Prossnitz, E. R. & Hathaway, H. J. GPER Mediates Estrogen-Induced Signaling and Proliferation in Human Breast Epithelial Cells and Normal and Malignant Breast. *Horm. Cancer* **5,** 146–160 (2014).

109. He, Y. Y., Cai, B., Yang, Y. X., Liu, X. L. & Wan, X. P. Estrogenic G protein-coupled receptor 30 signaling is involved in regulation of endometrial carcinoma by promoting proliferation, invasion potential, and interleukin-6 secretion via the MEK/ERK mitogen-activated protein kinase pathway. *Cancer Sci.* **100,** 1051–1061 (2009).

110. Royer, C., Lucas, T. F. G., Lazari, M. F. M. & Porto, C. S. 17Beta-estradiol signaling and regulation of proliferation and apoptosis of rat Sertoli cells. *Biol. Reprod.* **86,** 108 (2012).

111. Chimento, A. *et al.* Oleuropein and hydroxytyrosol activate GPER/ GPR30-dependent pathways leading to apoptosis of ER-negative SKBR3 breast cancer cells. *Mol. Nutr. Food Res.* **58,** 478–489 (2014).

112. Chimento, A. *et al.* Selective GPER activation decreases proliferation and activates apoptosis in tumor Leydig cells. *Cell Death Dis.* **4,** e747 (2013).

113. Vivacqua, A. *et al.* GPER mediates the Egr-1 expression induced by 17β-estradiol and 4-hydroxitamoxifen in breast and endometrial cancer cells. *Breast Cancer Res. Treat.* **133,** 1025–1035 (2012).

114. Skrzypczak, M. *et al.* G protein-coupled estrogen receptor (GPER) expression in endometrial adenocarcinoma and effect of agonist G-1 on growth of endometrial adenocarcinoma cell lines. *Steroids* **78,** 1087–1091 (2013).

115. Sirianni, R. *et al.* The novel estrogen receptor, G protein-coupled receptor 30, mediates the proliferative effects induced by 17beta-estradiol on mouse spermatogonial GC-1 cell line. *Endocrinology* **149,** 5043–5051 (2008).

116. Manikkam, M., Tracey, R., Guerrero-Bosagna, C., Skinner, M. K. & Gounon, P. Plastics Derived Endocrine Disruptors (BPA, DEHP and DBP) Induce Epigenetic Transgenerational Inheritance of Obesity, Reproductive Disease and Sperm Epimutations. *PLoS One* **8,** e55387 (2013).

117. Prossnitz, E. R. & Barton, M. The G protein-coupled estrogen receptor GPER in health and disease. *Nat Rev Endocrinol.* **7,** 715–726 (2012).

118. Kanda, N. & Watanabe, S. 17beta-Estradiol Inhibits Oxidative Stress-Induced Apoptosis in Keratinocytes by Promoting Bcl-2 Expression. *J. Invest. Dermatol.* **121,** 1500–1509 (2003).

119. Kanda, N. & Watanabe, S. 17beta-Estradiol Enhances the Production of Nerve Growth Factor in THP-1-Derived Macrophages or Peripheral Blood Monocyte-Derived Macrophages. *J. Invest. Dermatol.* **121,** 771–780 (2003).

120. De Francesco, E. M. *et al.* HIF-1α/GPER signaling mediates the expression of VEGF induced by hypoxia in breast cancer associated fibroblasts (CAFs). *Breast Cancer Res.* **15,** R64 (2013).

121. Pupo, M., Pisano, A., Abonante, S., Maggiolini, M. & Musti, A. M. GPER activates Notch signaling in breast cancer cells and cancer-associated fibroblasts (CAFs). *Int. J. Biochem. Cell Biol.* **46,** 56–67 (2014).

122. Petrie, W. K. *et al.* G protein-coupled estrogen receptor-selective ligands modulate endometrial tumor

growth. *Obstet. Gynecol. Int.* **2013,** 472720 (2013).

123. Zhang, J. *et al.* Gankyrin plays an essential role in estrogen-driven and GPR30-mediated endometrial carcinoma cell proliferation via the PTEN/PI3K/AKT signaling pathway. *Cancer Lett.* **339,** 279–287 (2013).

124. Du, G.-Q., Zhou, L., Chen, X.-Y., Wan, X.-P. & He, Y.-Y. The G protein-coupled receptor GPR30 mediates the proliferative and invasive effects induced by hydroxytamoxifen in endometrial cancer cells. *Biochem. Biophys. Res. Commun.* **420,** 343–349 (2012).

125. Li, S., Huang, S. & Peng, S.-B. Overexpression of G protein-coupled receptors in cancer cells: Involvement in tumor progression. *Int. J. Oncol.* **27,** 1329–1339 (2005).

126. Ignatov, T. *et al.* GPER-1 acts as a tumor suppressor in ovarian cancer. *J. Ovarian Res.* **6,** 51 (2013).

127. Teng, J., Wang, Z.-Y. Y., Prossnitz, E. R. & Bjorling, D. E. The G protein-coupled receptor GPR30 inhibits human urothelial cell proliferation. *Endocrinology* **149,** 4024–4034 (2008).

128. Ahola, T. M., Manninen, T., Alkio, N. & Ylikomi, T. G protein-coupled receptor 30 is critical for a progestin-induced growth inhibition in MCF-7 breast cancer cells. *Endocrinology* **143,** 3376–3384 (2002).

129. Pandey, D. P. *et al.* Estrogenic GPR30 signalling induces proliferation and migration of breast cancer cells through CTGF. *EMBO J.* **28,** 523–532 (2009).

130. Filardo, E. J., Quinn, J. a. & Sabo, E. Association of the membrane estrogen receptor, GPR30, with breast tumor metastasis and transactivation of the epidermal growth factor receptor. *Steroids* **73,** 870–873 (2008).

131. Fischer, O. M., Hart, S., Gschwind, A. & Ullrich, A. EGFR signal transactivation in cancer cells. *Biochem. Soc. Trans.* **31,** 1203–1208 (2003).

132. Kleuser, B., Malek, D., Gust, R., Pertz, H. H. & Potteck, H. 17-beta-Estradiol Inhibits Transforming Growth Factor-beta Signaling and Function in Breast Cancer Cells via Activation of Extracellular Signal-Regulated Kinase through the G Protein-Coupled Receptor 30. *Mol. Pharmacol.* **74,** 1533–1543 (2008).

133. Chen, Y. *et al.* Estrogen and pure antiestrogen fulvestrant (ICI 182 780) augment cell-matrigel adhesion of MCF-7 breast cancer cells through a novel G protein coupled estrogen receptor (GPR30)-to-calpain signaling axis. *Toxicol. Appl. Pharmacol.* **275,** 176–181 (2014).

134. Manjegowda, M. C., Gupta, P. S. & Limaye, A. M. Validation data of a rabbit antiserum and affinity purified polyclonal antibody against the N-terminus of human GPR30. *Data Br.* **7,** 1015–1020 (2016).

135. Schneider, C. A., Rasband, W. S. & Eliceiri, K. W. NIH Image to ImageJ: 25 years of image analysis. *Nat. Methods* **9,** 671–675 (2012).

136. Livak, K. J. & Schmittgen, T. D. Analysis of relative gene expression data using real-time quantitative PCR and. *Methods* **25,** 402–408 (2001).

137. Lowry, O. H., Rosebrough, N. J., Farr, A. L. & Randall, R. J. Protein measurement with the Folin phenol reagent. *J biol Chem* **193,** 265–275 (1951).

138. Fitzgibbons, P. L. *et al.* Prognostic factors in breast cancer. College of American Pathologists Consensus Statement 1999. *Arch. Pathol. Lab. Med.* **124,** 966–78 (2000).

139. Smyth, G. K. Linear models and empirical bayes methods for assessing differential expression in microarray experiments. *Stat. Appl. Genet. Mol. Biol.* **3,** Article3 (2004).

140. Ritchie, M. E. *et al.* A comparison of background correction methods for two-colour microarrays. *Bioinformatics* **23,** 2700–2707 (2007).

141. Xiong, Z. & Laird, P. W. COBRA: A sensitive and quantitative DNA methylation assay. *Nucleic Acids Res.* **25,** 2532–2534 (1997).

142. Larkin, M. A. *et al.* Clustal W and Clustal X version 2.0. *Bioinformatics* **23,** 2947–2948 (2007).

143. Koboldt, D. C. *et al.* Comprehensive molecular portraits of human breast tumours. *Nature* **490,** 61–70 (2012).

144. Zhu, J. *et al.* The UCSC Cancer Genomics Browser. *Nat. Methods* **6,** 239–240 (2009).

145. Györffy, B. *et al.* An online survival analysis tool to rapidly assess the effect of 22,277 genes on breast cancer prognosis using microarray data of 1,809 patients. *Breast Cancer Research and Treatment* **123,** 725–731 (2010).

146. Sproul, D. *et al.* Transcriptionally repressed genes become aberrantly methylated and distinguish tumors of different lineages in breast cancer. *Proc. Natl. Acad. Sci. U. S. A.* **108,** 4364–4369 (2011).

147. Afgan, E. *et al.* The Galaxy platform for accessible, reproducible and collaborative biomedical analyses: 2016 update. *Nucleic Acids Res.* **44,** W3 (2016).

148. Andrews, S. FastQC A Quality Control tool for High Throughput Sequence Data. . *http://www.bioinformatics.babraham.ac.uk/projects/fastqc/* Available at: http://www.bioinformatics.babraham.ac.uk/projects/fastqc/. (Accessed: 10th March 2016)

149. Blankenberg, D. *et al.* Manipulation of FASTQ data with Galaxy. *Bioinformatics* **26,** 1783–1785 (2010).

150. Langmead, B., Trapnell, C., Pop, M. & Salzberg, S. L. Ultrafast and memory-efficient alignment of short DNA sequences to the human genome. *Genome Biol.* **10,** R25 (2009).

151. Li, H. *et al.* The Sequence Alignment/Map format and SAMtools. *Bioinformatics* **25,** 2078–2079 (2009).

152. Zhang, Y. *et al.* Model-based analysis of ChIP-Seq (MACS). *Genome Biol.* **9,** R137 (2008).

153. Kent, W. J. *et al.* The human genome browser at UCSC. *Genome Res.* **12,** 996–1006 (2002).

154. Weber, R., Bertoni, A. P. S., Bessestil, L. W., Brum, I. S. & Furlanetto, T. W. Decreased Expression of GPER1 Gene and Protein in Goiter. *Int. J. Endocrinol.* **2015,** 869431 (2015).

155. Kolkova, Z. *et al.* The G protein-coupled estrogen receptor 1 (GPER/GPR30) does not predict survival in patients with ovarian cancer. *J. Ovarian Res.* **5,** 9 (2012).

156. Yu, X. *et al.* Activation of G protein-coupled estrogen receptor induces endothelium-independent relaxation of coronary artery smooth muscle Activation of G protein-coupled estrogen receptor induces endothelium- independent relaxation of coronary artery smooth muscle. *Am. J. Physiol. - Endocrinol. Metab.* **301,** E882–E888 (2011).

157. Rath, A., Glibowicka, M., Nadeau, V. G., Chen, G. & Deber, C. M. Detergent binding explains anomalous SDS-PAGE migration of membrane proteins. *Proc. Natl. Acad. Sci.* **106,** 1760–1765 (2009).

158. Zazzu, V. The human G Protein-Coupled Receptor GPR30: interaction partners and expression analysis in endothelial cells. (Charité University Medicine , Berlin, Germany, 2011).

159. Eishingdrelo, H. & Kongsamut, S. Minireview: Targeting GPCR Activated ERK Pathways for Drug Discovery. *Curr. Chem. genomics Transl. Med.* **7,** 9–15 (2013).

160. Bar-Shavit, R. *et al.* G Protein-Coupled Receptors in Cancer. *Int. J. Mol. Sci.* **17,** 1320 (2016).

161. Lappano, R. *et al.* Cross-talk between GPER and growth factor signaling. *J. Steroid Biochem. Mol. Biol.* **137,** 50–56 (2013).

162. Luo, H. *et al.* GPER-mediated proliferation and estradiol production in breast cancer-associated fibroblasts. *Endocr. Relat. Cancer* **21,** 355–369 (2014).

163. Steiman, J., Peralta, E. a, Louis, S. & Kamel, O. Biology of the estrogen receptor, GPR30, in triple negative breast cancer. *Am. J. Surg.* **206,** 698–703 (2013).

164. Tu, G., Hu, D., Yang, G. & Yu, T. The Correlation between GPR30 and Clinicopathologic Variables in Breast Carcinomas. *Technol. Cancer Res. Treat.* **8,** 231–234 (2009).

165. Luo, H. *et al.* G-protein Coupled Estrogen Receptor 1 Expression in Primary Breast Cancers and Its Correlation with Clinicopathological Variables. *J. Breast Cancer* **14,** 185–190 (2011).

166. Manjegowda, M. C., Gupta, P. S. & Limaye, A. M. Hyper-methylation of the upstream CpG island shore is a likely mechanism of GPER1 silencing in breast cancer cells. *Gene* **614,** 65–73 (2017).

167. Heldring, N. *et al.* Estrogen Receptors : How Do They Signal and What Are Their Targets. *Physiol. Rev.* **87,** 905–931 (2007).

168. Couse, J. F. & Korach, K. S. Estrogen Receptor Null Mice : What Have We Learned and Where Will They Lead Us ? " O. *Endocr. Rev.* **20,** 358–417 (1999).

169. Vaziri-Gohar, A., Zheng, Y. & Houston, K. D. IGF-1 Receptor Modulates FoxO1-Mediated Tamoxifen Response in Breast Cancer Cells. *Mol. Cancer Res.* **15,** 489–497 (2017).

170. Hutcheson, I. R. *et al.* Oestrogen receptor-mediated modulation of the EGFR/MAPK pathway in tamoxifen-resistant MCF-7 cells. *Breast Cancer Res. Treat.* **81,** 81–93 (2003).

171. Albanito, L. *et al.* Epidermal growth factor induces G protein-coupled receptor 30 expression in estrogen receptor-negative breast cancer cells. *Endocrinology* **149,** 3799–808 (2008).

172. Kent, W. J. BLAT - The BLAST-like alignment tool. *Genome Res.* **12,** 656–664 (2002).

173. Vyhlidal, C., Samudio, I., Kladde, M. P. & Safe, S. Transcriptional activation of transforming growth factor alpha by estradiol: Requirement for both a GC-rich site and an estrogen response element half-site. in *Journal of Molecular Endocrinology* **24,** 329–338 (BioScientifica, 2000).

174. Gruber, C. J., Gruber, D. M., Gruber, I. M. L., Wieser, F. & Huber, J. C. Anatomy of the estrogen response element. *Trends in Endocrinology and Metabolism* **15,** 73–78 (2004).

175. Azariadis, K. *et al.* Androgen Triggers the Pro-Migratory CXCL12/CXCR4 Axis in AR-Positive Breast Cancer Cell Lines: Underlying Mechanism and Possible Implications for the Use of Aromatase Inhibitors in Breast Cancer. *Cellular Physiology and Biochemistry* **44,** 66–84 (2017).

176. Ngwenya, S. & Safe, S. Cell context-dependent differences in the induction of E2F-1 gene expression by 17 beta-estradiol in MCF-7 and ZR-75 cells. *Endocrinology* **144,** 1675–1685 (2003).

177. Baylin, S. B. & Ohm, J. E. Epigenetic gene silencing in cancer – a mechanism for early oncogenic pathway addiction? *Nat. Rev. Cancer* **6,** 107–116 (2006).

178. Rao, X. *et al.* CpG island shore methylation regulates caveolin-1 expression in breast cancer.

Oncogene **32,** 4519–4528 (2013).

179. Jiang, Q.-F. *et al.* 17β-estradiol promotes the invasion and migration of nuclear estrogen receptor-negative breast cancer cells through cross-talk between GPER1 and CXCR1. *J. Steroid Biochem. Mol. Biol.* **138,** 314–324 (2013).

180. He, Y.-. Y. *et al.* Estrogenic transmembrane receptor of GPR30 mediates invasion and carcinogenesis by endometrial cancer cell line RL95-2. *J Cancer Res Clin Oncol.* **138,** 775–783 (2012).

181. Ren, J. *et al.* GPER in CAFs regulates hypoxia-driven breast cancer invasion in a CTGF-dependent manner. *Oncol. Rep.* **33,** 1929–1937 (2015).

182. Notas, G., Kampa, M., Pelekanou, V. & Castanas, E. Interplay of estrogen receptors and GPR30 for the regulation of early membrane initiated transcriptional effects: A pharmacological approach. *Steroids* **77,** 943–50 (2012).

183. Liberzon, A. *et al.* The Molecular Signatures Database Hallmark Gene Set Collection. *Cell Syst.* **1,** 417–425 (2015).

184. Subramanian, A., Tamayo, P., Mootha, V. K., Mukherjee, S. & Ebert, B. L. Gene set enrichment analysis : A knowledge-based approach for interpreting genome-wide. (2005).

185. Liberzon, A. *et al.* Molecular signatures database (MSigDB) 3.0. *Bioinformatics* **27,** 1739–1740 (2011).

186. Dixcy Jaba Sheeba, J. M. *et al.* Estrogen-regulated extracellular matrix remodeling genes in MCF-7 breast cancer cells. *Gene Reports* **3,** 14–21 (2016).

187. Manjegowda, M. C., Deb, G., Kumar, N. & Limaye, A. M. Expression profiling of genes modulated by estrogen, EGCG or both in MCF-7 breast cancer cells. *Genomics Data* **5,** 210–212 (2015).

188. Wang, Z. Y. & Yin, L. Estrogen receptor alpha-36 (ER-α36): A new player in human breast cancer. *Molecular and Cellular Endocrinology* **418,** 193–206 (2015).

189. Santolla, M. F. *et al.* Niacin activates the G protein estrogen receptor (GPER)-mediated signalling. *Cell. Signal.* **26,** 1466–1475 (2014).

190. Rudelius, M. *et al.* The G protein-coupled estrogen receptor 1 (GPER-1) contributes to the proliferation and survival of mantle cell lymphoma cells. *Haematologica* **100,** e458–e461 (2015).

191. Okamoto, M. & Mizukami, Y. GPER negatively regulates TNFalpha-induced IL-6 production in human breast cancer cells via NF-kappaB pathway. *Endocr J* **63,** 485–493 (2016).

192. Li, S., Wang, B., Tang, Q., Liu, J. & Yang, X. Bisphenol A triggers proliferation and migration of laryngeal squamous cell carcinoma via GPER mediated upregulation of IL-6. *Cell Biochem. Funct.* **35,** 209–216 (2017).

193. Wang, C. *et al.* The G-protein-coupled estrogen receptor agonist G-1 suppresses proliferation of ovarian cancer cells by blocking tubulin polymerization. *Cell Death Dis.* **4,** e869 (2013).

194. Wang, C., Lv, X., Jiang, C. & Davis, J. S. The putative G-protein coupled estrogen receptor agonist G-1 suppresses proliferation of ovarian and breast cancer cells in a GPER-independent manner. *Am. J. Transl. Res.* **4,** 390–402 (2012).

195. Lv, X. *et al.* G-1 inhibits breast cancer cell growth via targeting colchicine-binding site of tubulin to interfere with microtubule assembly. *Mol. Cancer Ther.* **16,** 1080–1091 (2017).

Appendix

Supplementary table 3.1: List of primers used for routine RT-PCR and real-time qRT-PCR.

Primer name	Sequence	Amplicon (bp)	Annealing temperature (°C)	Remarks
q-RPL35A-f	CGGCCTCCAAGCTCTCTAAG	131	60	Used in qRT-PCR
q-RPL35A-r	CAGGTCCAGGGGCTTGTACT			
q-GPER1-3'UTR-f	CATTCCAGACAGCACCGAGC	104	60	Used in qRT-PCR
q-GPER1-3'UTR-r	TGTGTGCAGCTCCCGAGTCA			
q-GPER1v2-f	ATCTGGACGGCAGGTACC	149	60	Used in qRT-PCR
q-GPER1v2-r	GAAGAACAGATGCTCCTCACAC			
q-GPER1v3-f€	TGGACGGCAGCCCTGCTC	154	60	Used in qRT-PCR
q-GPER1v4-f€	GCGGGTCTCTTCCTCTCTC	166	60	Used in qRT-PCR
q-GPER1v34-r	GCTGCTCACTCTCTGGGTAC			Used in qRT-PCR
hGPER1v23-f¥	CACCAACATCTGGACGGCAG	v2 = 208 v3 = 332	54	Used in routine RT-PCR
hGPER1v4-f¥	AGACTCACTGGCTCAGAGGG	403	54	Used in routine RT-PCR
hGPER1-RT-r	AGGAGGAGCACCTGTGGT			
GPER1-ORF-f	CCGGAATTCATGGATGTGACTTCCCAAGCC	1141	58	Used in routine RT-PCR
GPER1-ORF-r	TGCTCTAGACACGGCACTGCTGAACCTC			
ERα-f	AGCAGGTGCCCTACTACCTG	501	60	Used in routine RT-PCR
ERα-r	GCCAAAGGTTGGCAGCTCTC			
RPL35A-f	GGGTACAGCATCACTCGGA	220	53	Used in routine RT-PCR
RPL35A-r	ACGCCCGAGATGAAACAG			

f and r indicate sense and antisense primers respectively, v2 and v3 in the amplicon column refer to those that correspond to GPER1v2 and GPER1v3 respectively

€ used with anti-sense primer q-GPER1v34-r.

¥ used with anti-sense primer hGPER1-RT-r.

Supplementary table 3.2. List of primers used for modified COBRA assays and bisulfite sequencing.

Primer name	Sequence (5'----------->3')	Amplicon (bp)	Ta (°C)	Genomic location[@]		Amplicon Name	Digestion fragments[$]	
				Start	End		BstUI	TaqI
upCpGi-fT	ATTTAGAAGTAGGAGTGAGATT	465	53	1086886	1087350	upCpGi	115, 272, 78	163, 82, 122, 98
upCpGi-rT	ATCCCAAACATTCAAACCAA							
dnCpGi-faT	TGATTTTGGTGGTGAATATTAGT	314	56	1091964	1092277	dnCpGi-a	28, 286	46, 48, 129, 91
dnCpGi-raT	CATCCAAATAAAACCACAACTC							
dnCpGi-fbT	GAGTTGTGGTTTTATTTGGATG	300	55	1092256	1092555	dnCpGi-b	98, 162, 40	75, 48, 177
dnCpGi-rbT	TTCTCCAACAACCAACAAAC							
dnCpGi-fcT	GTTTGTTGGTTGTTGGAGAA	314	56	1092536	1092849	dnCpGi-c	No sites	284, 30
dnCpGi-rcT	ACACTACTAAACCTCACATCC							
dnCpGi-fdT	GGATGTGAGGTTTAGTAGTGT	410	55	1092829	1093238	dnCpGi-d	158, 252	371, 39
dnCpGi-rdT	TTCACCCACAATAACCTCTC							
dnCpGi-feT	GAGAGGTTATTGTGGGTGAA	355	56	1093219	1093573	dnCpGi-e	116, 239	161, 194
dnCpGi-reT	ACAAACAATAACTAAACCACCC							
upCpGi-fW	GAAGTAGGAGTGAGATTCGCTG	460	62	1086891	1087350	upCpGi-W	115, 272, 78	No sites
upCpGi-rW	GTCCCAAGCATTCAGACCAG							
dnCpGi-faW	TGATCCTGGTGGTGAACATCAGC	314	62	1091964	1092277	dnCpGi-aW	28, 286	223, 91
dnCpGi-raW	CATCCAGATGAGGCCACAGCTC							
dnCpGi-fbW	GAGCTGTGGCCTCATCTGGATG	300	65	1092256	1092555	dnCpGi-bW	98, 162, 40	123, 177
dnCpGi-rbW	TTCTCCGGCAGCCAGCAGAC							
dnCpGi-fcW	GTCTGCTGGCTGCCGGAGAA	314	65	1092536	1092849	dnCpGi-cW	No sites	No sites
dnCpGi-rcW	GCACTGCTGAACCTCACATCC							
dnCpGi-fdW	GGATGTGAGGTTCAGCAGTGC	410	62	1092829	1093238	dnCpGi-dW	158, 252	371, 39
dnCpGi-rdW	TTCACCCACAGTGGCCTCTC							
dnCpGi-feW	GAGAGGCCACTGTGGGTGAA	355	65	1093219	1093573	dnCpGi-eW	116, 239	No sites
dnCpGi-reW	ACAAGCAGTGACTGAACCACCC							

Ta indicates annealing temperature. f and r indicate forward and reverse primers respectively. Primer names ending with T and W amplify bisulfite converted and non-converted genomic DNA respectively. Amplicon names ending with W are generated using non-converted genomic DNA. TaqI digestion fragments generated due to the restriction sites created by bisulfite treatment are underlined. [@] coordinates of the expected amplicon on human chromosome 7 (NCBI, GRCh38.p7 Primary Assembly). [$] expected products of digestion with the indicated enzymes. Fragment sizes are indicated in bp, with respect to forward primer binding region.

Supplementary table 3.3. RNA concentration and purity of samples, estimated using Nanodrop spectrophotometer.

Sample Name	A_{260}/A_{280}	A_{260}/A_{230}	RNA (ng/µL)	Total yield (ng)	QC Purity	QC Yield	QC Integrity
EtOH_1	1.97	1.68	252.6	4546.8	Optimal	Optimal	Optimal
EtOH_2	1.9	2.33	952	19040	Optimal	Optimal	Optimal
EtOH_3	1.92	0.59	95.85	1725.3	Optimal	Optimal	Optimal
100nM G1_1	2.01	0.91	91.3	1643.4	Optimal	Optimal	Optimal
100nM G1_2	2.01	0.95	125.8	2264.4	Optimal	Optimal	Optimal
100nM G1_3	1.94	1.59	197.4	3553.2	Optimal	Optimal	Optimal
1µM G1_1	1.92	0.85	75.6	1360.8	Optimal	Optimal	Optimal
1µM G1_2	2.02	0.87	62.6	1126.8	Optimal	Optimal	Optimal
1µM G1_3	1.86	0.7	72	1296	Optimal	Optimal	Optimal

In the sixth column, Optimal: Optimal purity (OD 260/280 > 1.7 and <2.2; OD 260/230 > 0.5 and < 2.5); Sub-Optimal: Sub-Optimal purity (OD 260/280 < 1.7 and OD 260/230 < 0.5 and > 2.5). In the seventh column, Optimal: optimal concentration (> 30 ng/microlitre and < 2500 ng/microlitre); Sub-Optimal: Sub-optimal concentration (< 30 ng/microlitre).

Supplementary table 3.4. Quality assessment of labeled cRNA, using Nanodrop spectrophotometer.

Sample Name	Dye	pmol/µL	ng/µL	A_{260}/A_{280}	Specific activity
EtOH_1	Cy3	1.1	103.5	2.37	10.63
EtOH_2	Cy3	1.6	147.1	2.33	10.88
EtOH_3	Cy3	1.40	114.7	2.30	12.21
100nM G1_1	Cy3	1.8	168.4	2.32	10.69
100nM G1_2	Cy3	1.8	167	2.36	10.78
100nM G1_3	Cy3	1.6	154.5	2.33	10.36
1µM G1_1	Cy3	4.9	425.2	2.35	11.52
1µM G1_2	Cy3	1.7	170.5	2.33	9.97
1µM G1_3	Cy3	1.6	172.6	2.35	9.27

Specific Activity greater than 8.0 is good. Specific Activity 5.0 to 8.0 is Optimal. Specific Activity less than 5.0 is not suitable for Hybridization.

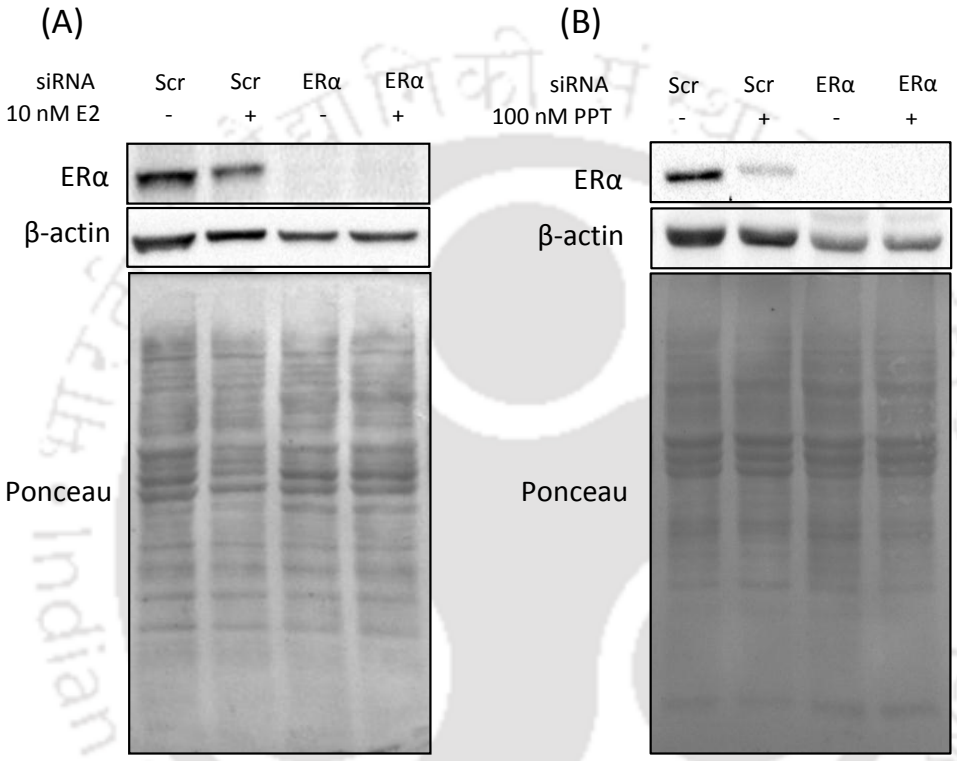

Supplementary figure 6.1. Efficiency of ERα knockdown in MCF-7 cells. MCF-7 cells were seeded into 35 mm dishes and grown for 48 h in M1. Cells were incubated with scrambled siRNA (Scr) or ERα-specific siRNA (ERα) for 24 h in M1. The medium was replaced by M2 and incubated for 24 h. Cells were treated with 10 nM E2 (A) or 100 nM PPT (B) for 48 h. Total protein was isolated from TRIzol fractions. 30 µg of total protein was used in western blotting to assess the ERα and β-actin protein levels.

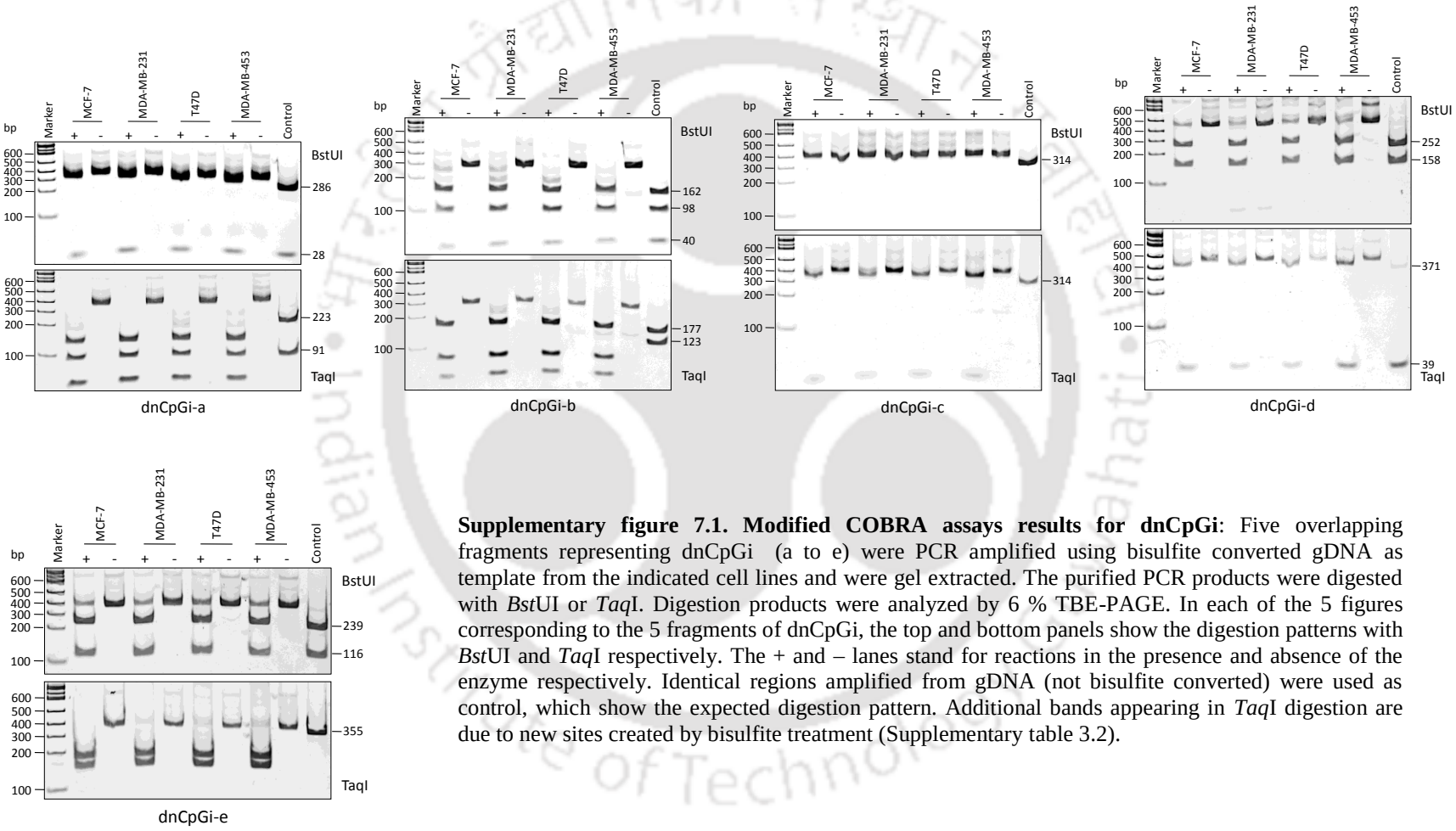

Supplementary figure 7.1. Modified COBRA assays results for dnCpGi: Five overlapping fragments representing dnCpGi (a to e) were PCR amplified using bisulfite converted gDNA as template from the indicated cell lines and were gel extracted. The purified PCR products were digested with *Bst*UI or *Taq*I. Digestion products were analyzed by 6 % TBE-PAGE. In each of the 5 figures corresponding to the 5 fragments of dnCpGi, the top and bottom panels show the digestion patterns with *Bst*UI and *Taq*I respectively. The + and – lanes stand for reactions in the presence and absence of the enzyme respectively. Identical regions amplified from gDNA (not bisulfite converted) were used as control, which show the expected digestion pattern. Additional bands appearing in *Taq*I digestion are due to new sites created by bisulfite treatment (Supplementary table 3.2).

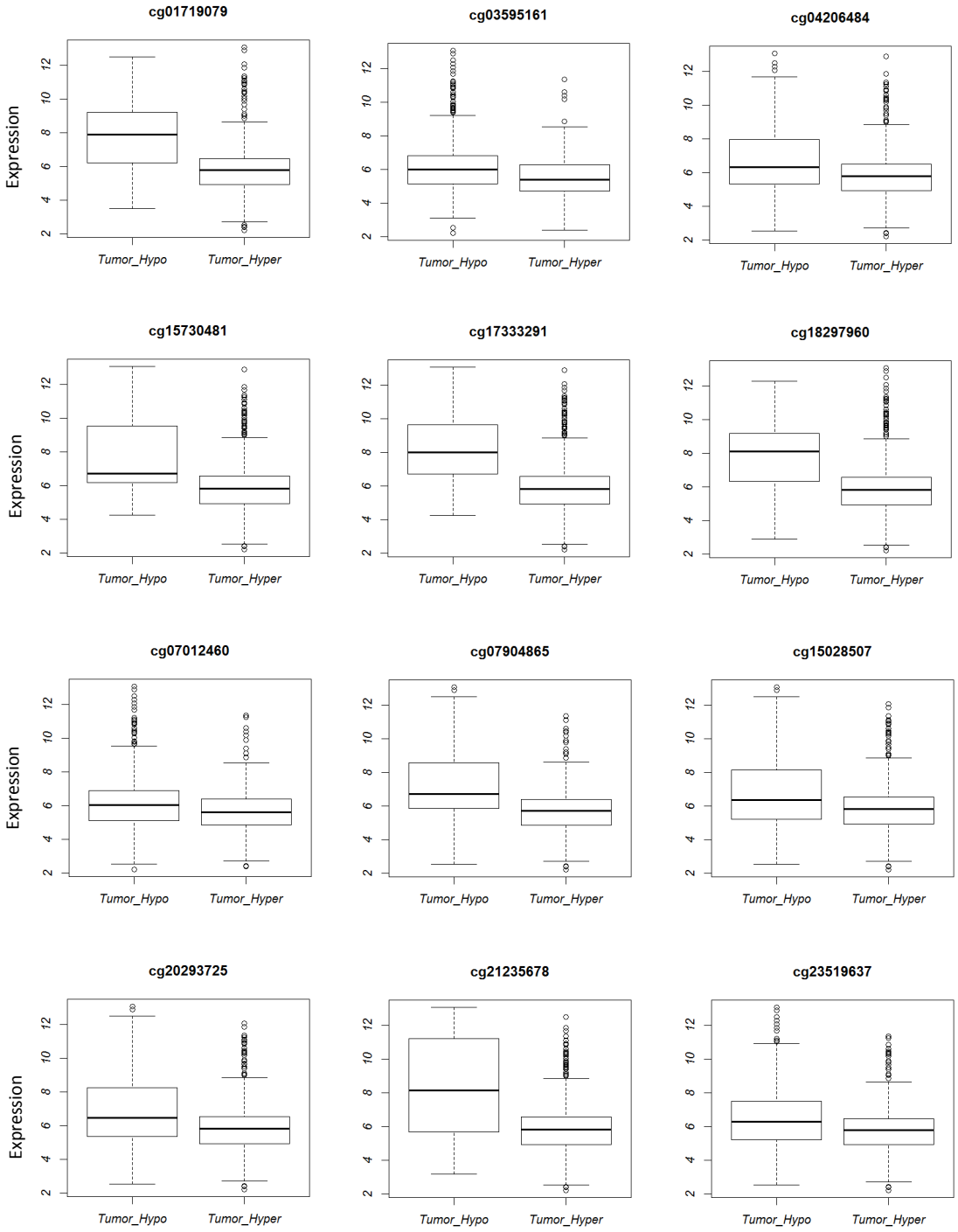

Supplementary figure 7.2. Box plots showing the distribution of GPER1 expression in breast tumors. Breast tumors were categorized into two groups, namely hypo-methylated or hyper-methylated based on a cutoff beta score of 0.3 for each of the probes indicated above the boxplots. The significance of the difference in the mean GPER1 expression was tested by a Welch two-sample *t*-test and analysis results are given in supplementary table 7.1.

Supplementary table 7.1. Results of probe-wise EMC analysis.

ProbeID	Spearman rho (ρ) (EMC analysis)	*p* value (EMC analysis)	*p* value (Welch two-sample *t*-test)
cg04206484	-0.2123	1.8343E-09	3.70696E-05
cg23519637	-0.2133	1.5519E-09	1.54545E-06
cg20293725	-0.2237	2.2576E-10	3.21586E-05
cg15028507	-0.2236	2.3035E-10	4.06598E-05
cg15730481	-0.3012	6.0975E-18	0.000207181
cg17333291	-0.3338	6.5073E-22	0.000977285
cg07904865	-0.3197	3.9405E-20	1.07739E-13
cg07012460	-0.2141	1.3438E-09	1.61034E-07
cg03595161	-0.2442	3.922E-12	4.46538E-10
cg21235678	-0.2413	7.0984E-12	0.000775902
cg01719079	-0.3488	6.7251E-24	1.65301E-10
cg18297960	-0.2612	1.0118E-13	0.000276958

P values in the fourth column are from Welch two-sample *t*-test used to compare the difference in the mean GPER1 mRNA expression between hypo and hyper methylated groups (supplementary figure 7.2).

Supplementary table 8.1. List of top 100 up-regulated genes in 1 µM G1 treated group.

Gene name	Description	Log_2FC
LOC400456	ref|Homo sapiens uncharacterized LOC400456 (LOC400456), non-coding RNA [NR_034095]	2.279794
XLOC_000630	linc|BROAD Institute lincRNA (XLOC_000630), lincRNA [TCONS_00002266]	3.073415
NP1252193	tc|GB|AACC02000041.1|EAL24421.1 similar to Huntingtin interacting protein K [Homo sapiens] [NP1252193]	2.866762
ANXA1	ref|Homo sapiens annexin A1 (ANXA1), mRNA [NM_000700]	2.738768
TNFSF13B	ref|Homo sapiens tumor necrosis factor (ligand) superfamily, member 13b (TNFSF13B), transcript variant 1, mRNA [NM_006573]	2.663678
CSNK1G1	ens|casein kinase 1, gamma 1 [Source:HGNC Symbol;Acc:2454] [ENST00000447727]	2.484036
CYP1A1	ref|Homo sapiens cytochrome P450, family 1, subfamily A, polypeptide 1 (CYP1A1), mRNA [NM_000499]	2.454695
LOC100131355	gb|Homo sapiens cDNA FLJ42223 fis, clone THYMU2039989. [AK124217]	2.33465
XLOC_l2_007456	linc|BROAD Institute lincRNA (XLOC_l2_007456), lincRNA [TCONS_l2_00013854]	2.322314
XLOC_011038	linc|BROAD Institute lincRNA (XLOC_011038), lincRNA [TCONS_00022755]	2.221639
S100A9	ref|Homo sapiens S100 calcium binding protein A9 (S100A9), mRNA [NM_002965]	2.117608
AKR1C3	ref|Homo sapiens aldo-keto reductase family 1, member C3 (3-alpha hydroxysteroid dehydrogenase, type II) (AKR1C3), mRNA [NM_003739]	1.998844
IL6	ref|Homo sapiens interleukin 6 (interferon, beta 2) (IL6), mRNA [NM_000600]	1.962483
DDIT3	ref|Homo sapiens DNA-damage-inducible transcript 3 (DDIT3), transcript variant 5, mRNA [NM_004083]	1.959085
RNU6ATAC	ref|Homo sapiens RNA, U6atac small nuclear (U12-dependent splicing) (RNU6ATAC), small nuclear RNA [NR_023344]	1.944533
DEFB4A	ref|Homo sapiens defensin, beta 4A (DEFB4A), mRNA [NM_004942]	1.934602
XLOC_000702	linc|BROAD Institute lincRNA (XLOC_000702), lincRNA [TCONS_00002290]	1.931551
UBD	ref|Homo sapiens ubiquitin D (UBD), mRNA [NM_006398]	1.869394

GADD45A	ref|Homo sapiens growth arrest and DNA-damage-inducible, alpha (GADD45A), transcript variant 1, mRNA [NM_001924]	1.863831
ENST00000435913	Unknown	1.848549
ATF3	ref|Homo sapiens activating transcription factor 3 (ATF3), transcript variant 4, mRNA [NM_001040619]	1.839896
ACTG2	ref|Homo sapiens actin, gamma 2, smooth muscle, enteric (ACTG2), transcript variant 1, mRNA [NM_001615]	1.822731
ANGPTL4	ref|Homo sapiens angiopoietin-like 4 (ANGPTL4), transcript variant 1, mRNA [NM_139314]	1.817274
UGT1A8	ref|Homo sapiens UDP glucuronosyltransferase 1 family, polypeptide A8 (UGT1A8), mRNA [NM_019076]	1.806673
LOC728978	ref|Homo sapiens uncharacterized LOC728978 (LOC728978), non-coding RNA [NR_038453]	1.79849
LOC100289026	ref|PREDICTED: Homo sapiens hypothetical LOC100289026 (LOC100289026), miscRNA [XR_110942]	1.784306
PSG8	ref|Homo sapiens pregnancy specific beta-1-glycoprotein 8 (PSG8), transcript variant 1, mRNA [NM_182707]	1.774121
S100A2	ref|Homo sapiens S100 calcium binding protein A2 (S100A2), mRNA [NM_005978]	1.762174
ANKRD20A8P	ref|Homo sapiens ankyrin repeat domain 20 family, member A8, pseudogene (ANKRD20A8P), non-coding RNA [NR_003366]	1.75613
XLOC_004836	linc|BROAD Institute lincRNA (XLOC_004836), lincRNA [TCONS_00010348]	1.717752
FBXO32	ref|Homo sapiens F-box protein 32 (FBXO32), transcript variant 1, mRNA [NM_058229]	1.67057
LCN2	ref|Homo sapiens lipocalin 2 (LCN2), mRNA [NM_005564]	1.661973
FAM118A	ref|Homo sapiens family with sequence similarity 118, member A (FAM118A), transcript variant 1, mRNA [NM_001104595]	1.638488
A_24_P110082	Unknown	1.630176
KYNU	ens|kynureninase [Source:HGNC Symbol;Acc:6469] [ENST00000410015]	1.607176
IFRD1	ref|Homo sapiens interferon-related developmental regulator 1 (IFRD1), transcript variant 2, mRNA [NM_001007245]	1.590701
GLRX	ref|Homo sapiens glutaredoxin (thioltransferase) (GLRX), transcript variant 1, mRNA [NM_002064]	1.588617
FGG	ref|Homo sapiens fibrinogen gamma chain (FGG), transcript variant gamma-A, mRNA [NM_000509]	1.577987

XLOC_006178	gb|EST9644 human nasopharynx Homo sapiens cDNA, mRNA sequence [CD693121]	1.565836
XLOC_l2_002351	gb|602622620F1 NCI_CGAP_Skn4 Homo sapiens cDNA clone IMAGE:4747804 5', mRNA sequence [BG676222]	1.561133
GPR87	ref|Homo sapiens G protein-coupled receptor 87 (GPR87), mRNA [NM_023915]	1.560496
ENST00000471222	gb|RST23433 Athersys RAGE Library Homo sapiens cDNA, mRNA sequence [BG204039]	1.553063
LOC100507025	ref|PREDICTED: Homo sapiens hypothetical LOC100507025 (LOC100507025), miscRNA [XR_108687]	1.552635
ENST00000420598	Unknown	1.544015
TNFRSF10C	ref|Homo sapiens tumor necrosis factor receptor superfamily, member 10c, decoy without an intracellular domain (TNFRSF10C), mRNA [NM_003841]	1.535455
C9orf169	ref|Homo sapiens chromosome 9 open reading frame 169 (C9orf169), mRNA [NM_199001]	1.534381
CT45A1	ref|Homo sapiens cancer/testis antigen family 45, member A1 (CT45A1), mRNA [NM_001017417]	1.52463
CLK1	ref|Homo sapiens CDC-like kinase 1 (CLK1), transcript variant 2, mRNA [NM_001162407]	1.52334
TFPI	ref|Homo sapiens tissue factor pathway inhibitor (lipoprotein-associated coagulation inhibitor) (TFPI), transcript variant 2, mRNA [NM_001032281]	1.516058
FAS	ref|Homo sapiens Fas (TNF receptor superfamily, member 6) (FAS), transcript variant 1, mRNA [NM_000043]	1.515454
C15orf48	ref|Homo sapiens chromosome 15 open reading frame 48 (C15orf48), transcript variant 2, mRNA [NM_032413]	1.5108
ADM	ref|Homo sapiens adrenomedullin (ADM), mRNA [NM_001124]	1.506813
TRIM58	ref|Homo sapiens tripartite motif containing 58 (TRIM58), mRNA [NM_015431]	1.493321
XLOC_010319	linc|BROAD Institute lincRNA (XLOC_010319), lincRNA [TCONS_00021734]	1.490947
ENST00000456460	Unknown	1.48115
LOC283403	ref|Homo sapiens uncharacterized LOC283403 (LOC283403), mRNA [NM_001242696]	1.480306
TMEM45B	ref|Homo sapiens transmembrane protein 45B (TMEM45B), mRNA [NM_138788]	1.474498

LOC254896	gb|Homo sapiens hypothetical protein MGC31957, mRNA (cDNA clone MGC:31957 IMAGE:3959651), complete cds. [BC021569]	1.455509
THC2682885	tc|Q6BEA3_RAT (Q6BEA3) WDNM1 homolog, partial (33%) [THC2682885]	1.455073
KIAA1875	ref|Homo sapiens KIAA1875 (KIAA1875), non-coding RNA [NR_024207]	1.453381
A_33_P3287105	Unknown	1.436997
FGB	ref|Homo sapiens fibrinogen beta chain (FGB), transcript variant 1, mRNA [NM_005141]	1.435398
XLOC_l2_010386	gb|RST23433 Athersys RAGE Library Homo sapiens cDNA, mRNA sequence [BG204039]	1.420075
ENST00000445977	ens|coatomer protein complex, subunit gamma 2 [Source:HGNC Symbol;Acc:2237] [ENST00000445977]	1.411405
TMEM45A	ref|Homo sapiens transmembrane protein 45A (TMEM45A), mRNA [NM_018004]	1.410208
IGFBP3	ref|Homo sapiens insulin-like growth factor binding protein 3 (IGFBP3), transcript variant 1, mRNA [NM_001013398]	1.408892
EDN2	ref|Homo sapiens endothelin 2 (EDN2), mRNA [NM_001956]	1.402608
PSG9	ref|Homo sapiens pregnancy specific beta-1-glycoprotein 9 (PSG9), mRNA [NM_002784]	1.39831
S100A7	ref|Homo sapiens S100 calcium binding protein A7 (S100A7), mRNA [NM_002963]	1.388545
XLOC_l2_001853	linc|BROAD Institute lincRNA (XLOC_l2_001853), lincRNA [TCONS_l2_00003387]	1.388005
A_33_P3247077	Unknown	1.383459
LOC100507307	ref|PREDICTED: Homo sapiens hypothetical LOC100507307 (LOC100507307), miscRNA [XR_109952]	1.372449
UCA1	ref|Homo sapiens urothelial cancer associated 1 (non-protein coding) (UCA1), non-coding RNA [NR_015379]	1.367978
LOC645638	ref|Homo sapiens WDNM1-like pseudogene (LOC645638), non-coding RNA [NR_030732]	1.364631
ANXA3	ref|Homo sapiens annexin A3 (ANXA3), mRNA [NM_005139]	1.362262
C9orf117	ref|Homo sapiens chromosome 9 open reading frame 117 (C9orf117), mRNA [NM_001012502]	1.33905
AK097143	gb|Homo sapiens cDNA FLJ39824 fis, clone SPLEN2011981. [AK097143]	1.33519

LCE1E	ref|Homo sapiens late cornified envelope 1E (LCE1E), mRNA [NM_178353]	1.332741
DEFB1	ref|Homo sapiens defensin, beta 1 (DEFB1), mRNA [NM_005218]	1.332346
LOC283335	ref|Homo sapiens uncharacterized LOC283335 (LOC283335), non-coding RNA [NR_033854]	1.32965
MKL2	ens|MKL/myocardin-like 2 [Source:HGNC Symbol;Acc:29819] [ENST00000389126]	1.326652
COX6B2	ref|Homo sapiens cytochrome c oxidase subunit VIb polypeptide 2 (testis) (COX6B2), mRNA [NM_144613]	1.324914
GNG10	ref|Homo sapiens guanine nucleotide binding protein (G protein), gamma 10 (GNG10), transcript variant 1, mRNA [NM_001017998]	1.32361
PSG1	ref|Homo sapiens pregnancy specific beta-1-glycoprotein 1 (PSG1), transcript variant 1, mRNA [NM_006905]	1.317351
XLOC_001485	linc|BROAD Institute lincRNA (XLOC_001485), lincRNA [TCONS_00003696]	1.315547
ANG	ref|Homo sapiens angiogenin, ribonuclease, RNase A family, 5 (ANG), transcript variant 1, mRNA [NM_001145]	1.314214
CDKN1A	ref|Homo sapiens cyclin-dependent kinase inhibitor 1A (p21, Cip1) (CDKN1A), transcript variant 2, mRNA [NM_078467]	1.307691
SAT1	ref|Homo sapiens spermidine/spermine N1-acetyltransferase 1 (SAT1), transcript variant 1, mRNA [NM_002970]	1.306747
ACBD7	ref|Homo sapiens acyl-CoA binding domain containing 7 (ACBD7), mRNA [NM_001039844]	1.304063
XLOC_007458	Unknown	1.297947
FABP6	ref|Homo sapiens fatty acid binding protein 6, ileal (FABP6), transcript variant 1, mRNA [NM_001040442]	1.296422
GSN	ref|Homo sapiens gelsolin (GSN), transcript variant 4, mRNA [NM_001127663]	1.29286
SPRR1A	ref|Homo sapiens small proline-rich protein 1A (SPRR1A), transcript variant 2, mRNA [NM_005987]	1.289482
A_33_P3392213	Unknown	1.28873
CGA	ref|Homo sapiens glycoprotein hormones, alpha polypeptide (CGA), transcript variant 2, mRNA [NM_000735]	1.286944
A_33_P3263512	Unknown	1.279905
A_33_P3258846	Unknown	1.275945
NUPR1	ref|Homo sapiens nuclear protein, transcriptional regulator, 1 (NUPR1), transcript variant 1, mRNA [NM_001042483]	1.274853

NEURL3	ref|Homo sapiens neuralized homolog 3 (Drosophila) pseudogene (NEURL3), non-coding RNA [NR_026875]	1.274048
C1orf63	ref|Homo sapiens chromosome 1 open reading frame 63 (C1orf63), mRNA [NM_020317]	1.268353

Supplementary table 8.2. List of top 100 down-regulated genes in 1µM G1 group.

Gene name	Description	Log_2FC
HIST1H4C	ref|Homo sapiens histone cluster 1, H4c (HIST1H4C), mRNA [NM_003542]	-2.50023
HIST1H4L	ref|Homo sapiens histone cluster 1, H4l (HIST1H4L), mRNA [NM_003546]	-2.31314
MCM2	ref|Homo sapiens minichromosome maintenance complex component 2 (MCM2), mRNA [NM_004526]	-2.06837
CBX5	ref|Homo sapiens chromobox homolog 5 (CBX5), transcript variant 1, mRNA [NM_001127322]	-2.02478
MCM3	ref|Homo sapiens minichromosome maintenance complex component 3 (MCM3), mRNA [NM_002388]	-1.88604
MCM7	ref|Homo sapiens minichromosome maintenance complex component 7 (MCM7), transcript variant 2, mRNA [NM_182776]	-1.8746
HIST2H3A	ref|Homo sapiens histone cluster 2, H3a (HIST2H3A), mRNA [NM_001005464]	-1.85361
MCM5	ref|Homo sapiens minichromosome maintenance complex component 5 (MCM5), mRNA [NM_006739]	-1.7188
E2F2	ref|Homo sapiens E2F transcription factor 2 (E2F2), mRNA [NM_004091]	-1.65675
POLA2	ref|Homo sapiens polymerase (DNA directed), alpha 2 (70kD subunit) (POLA2), mRNA [NM_002689]	-1.65158
E2F7	ref|Homo sapiens E2F transcription factor 7 (E2F7), mRNA [NM_203394]	-1.64634
RAB31	ref|Homo sapiens RAB31, member RAS oncogene family (RAB31), mRNA [NM_006868]	-1.63452
TIMELESS	ref|Homo sapiens timeless homolog (Drosophila) (TIMELESS), mRNA [NM_003920]	-1.6306
PKMYT1	ref|Homo sapiens protein kinase, membrane associated tyrosine/threonine 1 (PKMYT1), transcript variant 2, mRNA [NM_182687]	-1.60994
BRCA1	ref|Homo sapiens breast cancer 1, early onset (BRCA1), transcript variant 2, mRNA [NM_007300]	-1.60547
E2F1	ref|Homo sapiens E2F transcription factor 1 (E2F1), mRNA [NM_005225]	-1.58432
PARP1	ref|Homo sapiens poly (ADP-ribose) polymerase 1 (PARP1), mRNA [NM_001618]	-1.56845

PABPC4L	ref|Homo sapiens poly(A) binding protein, cytoplasmic 4-like (PABPC4L), mRNA [NM_001114734]	-1.56792
LOC729296	ref|PREDICTED: Homo sapiens hypothetical LOC729296 (LOC729296), miscRNA [XR_109632]	-1.55934
RMI2	ref|Homo sapiens RMI2, RecQ mediated genome instability 2, homolog (S. cerevisiae) (RMI2), mRNA [NM_152308]	-1.55231
FANCD2	ref|Homo sapiens Fanconi anemia, complementation group D2 (FANCD2), transcript variant 2, mRNA [NM_001018115]	-1.5242
UBE2C	ref|Homo sapiens ubiquitin-conjugating enzyme E2C (UBE2C), transcript variant 6, mRNA [NM_181803]	-1.49031
ASF1B	ref|Homo sapiens ASF1 anti-silencing function 1 homolog B (S. cerevisiae) (ASF1B), mRNA [NM_018154]	-1.48782
A_33_P3346533	Unknown	-1.47933
GFRA1	ref|Homo sapiens GDNF family receptor alpha 1 (GFRA1), transcript variant 1, mRNA [NM_005264]	-1.4678
TK1	ref|Homo sapiens thymidine kinase 1, soluble (TK1), mRNA [NM_003258]	-1.46084
CIT	ref|Homo sapiens citron (rho-interacting, serine/threonine kinase 21) (CIT), transcript variant 2, mRNA [NM_007174]	-1.45667
RAD54L	ref|Homo sapiens RAD54-like (S. cerevisiae) (RAD54L), transcript variant 1, mRNA [NM_003579]	-1.4519
BLM	ref|Homo sapiens Bloom syndrome, RecQ helicase-like (BLM), mRNA [NM_000057]	-1.4475
POGZ	ref|Homo sapiens pogo transposable element with ZNF domain (POGZ), transcript variant 1, mRNA [NM_015100]	-1.44602
NKAIN1	ref|Homo sapiens Na+/K+ transporting ATPase interacting 1 (NKAIN1), mRNA [NM_024522]	-1.43897
SMC1A	ref|Homo sapiens structural maintenance of chromosomes 1A (SMC1A), mRNA [NM_006306]	-1.43715
BARD1	ref|Homo sapiens BRCA1 associated RING domain 1 (BARD1), mRNA [NM_000465]	-1.4191
CENPN	ref|Homo sapiens centromere protein N (CENPN), transcript variant 2, mRNA [NM_001100624]	-1.41469
DTL	ref|Homo sapiens denticleless homolog (Drosophila) (DTL), mRNA [NM_016448]	-1.41293
C15orf42	ref|Homo sapiens chromosome 15 open reading frame 42 (C15orf42), mRNA [NM_152259]	-1.41202

CBX1	ref|Homo sapiens chromobox homolog 1 (CBX1), transcript variant 1, mRNA [NM_006807]	-1.39403
EPHA4	ref|Homo sapiens EPH receptor A4 (EPHA4), mRNA [NM_004438]	-1.37777
METTL7A	ref|Homo sapiens methyltransferase like 7A (METTL7A), mRNA [NM_014033]	-1.3535
PRC1	ref|Homo sapiens protein regulator of cytokinesis 1 (PRC1), transcript variant 1, mRNA [NM_003981]	-1.34922
MTHFD1	ref|Homo sapiens methylenetetrahydrofolate dehydrogenase (NADP+ dependent) 1, methenyltetrahydrofolate cyclohydrolase, formyltetrahydrofolate synthetase (MTHFD1), mRNA [NM_005956]	-1.34821
UHRF1	ref|Homo sapiens ubiquitin-like with PHD and ring finger domains 1 (UHRF1), transcript variant 2, mRNA [NM_013282]	-1.34782
RIBC2	ref|Homo sapiens RIB43A domain with coiled-coils 2 (RIBC2), mRNA [NM_015653]	-1.34463
TMEM164	ref|Homo sapiens transmembrane protein 164 (TMEM164), transcript variant 2, mRNA [NM_032227]	-1.33719
SF3B3	ref|Homo sapiens splicing factor 3b, subunit 3, 130kDa (SF3B3), mRNA [NM_012426]	-1.33596
RAD51	ref|Homo sapiens RAD51 homolog (S. cerevisiae) (RAD51), transcript variant 1, mRNA [NM_002875]	-1.33026
FEN1	ref|Homo sapiens flap structure-specific endonuclease 1 (FEN1), mRNA [NM_004111]	-1.32994
SETDB1	ref|Homo sapiens SET domain, bifurcated 1 (SETDB1), transcript variant 2, mRNA [NM_012432]	-1.32831
CDT1	ref|Homo sapiens chromatin licensing and DNA replication factor 1 (CDT1), mRNA [NM_030928]	-1.31855
MYBL1	ref|Homo sapiens v-myb myeloblastosis viral oncogene homolog (avian)-like 1 (MYBL1), transcript variant 1, mRNA [NM_001080416]	-1.31651
CDCA7	ref|Homo sapiens cell division cycle associated 7 (CDCA7), transcript variant 1, mRNA [NM_031942]	-1.27549
PRPF8	ref|Homo sapiens PRP8 pre-mRNA processing factor 8 homolog (S. cerevisiae) (PRPF8), mRNA [NM_006445]	-1.27438
RBM23	ref|Homo sapiens RNA binding motif protein 23 (RBM23), transcript variant 1, mRNA [NM_001077351]	-1.26983
RECQL4	ref|Homo sapiens RecQ protein-like 4 (RECQL4), mRNA [NM_004260]	-1.2697
CDC45	ref|Homo sapiens cell division cycle 45 homolog (S. cerevisiae) (CDC45), transcript variant 2, mRNA [NM_003504]	-1.26404

SPC24	gb|Homo sapiens cDNA FLJ90806 fis, clone Y79AA1000750. [AK075287]	-1.25368
CDC25C	ref|Homo sapiens cell division cycle 25 homolog C (S. pombe) (CDC25C), transcript variant 1, mRNA [NM_001790]	-1.24572
MTMR4	ref|Homo sapiens myotubularin related protein 4 (MTMR4), mRNA [NM_004687]	-1.24479
ZNF275	ref|Homo sapiens zinc finger protein 275 (ZNF275), mRNA [NM_001080485]	-1.24124
DSCAM	ref|Homo sapiens Down syndrome cell adhesion molecule (DSCAM), transcript variant 1, mRNA [NM_001389]	-1.23856
RAMP3	ref|Homo sapiens receptor (G protein-coupled) activity modifying protein 3 (RAMP3), mRNA [NM_005856]	-1.23431
SLC24A3	ref|Homo sapiens solute carrier family 24 (sodium/potassium/calcium exchanger), member 3 (SLC24A3), mRNA [NM_020689]	-1.23313
PPP1R10	ref|Homo sapiens protein phosphatase 1, regulatory subunit 10 (PPP1R10), mRNA [NM_002714]	-1.23232
CHAF1A	ref|Homo sapiens chromatin assembly factor 1, subunit A (p150) (CHAF1A), mRNA [NM_005483]	-1.2322
CHD8	ref|Homo sapiens chromodomain helicase DNA binding protein 8 (CHD8), transcript variant 2, mRNA [NM_020920]	-1.22913
SFXN2	ref|Homo sapiens sideroflexin 2 (SFXN2), mRNA [NM_178858]	-1.22856
CLN6	ref|Homo sapiens ceroid-lipofuscinosis, neuronal 6, late infantile, variant (CLN6), mRNA [NM_017882]	-1.22296
NCOA3	ref|Homo sapiens nuclear receptor coactivator 3 (NCOA3), transcript variant 1, mRNA [NM_181659]	-1.22072
EXO1	ref|Homo sapiens exonuclease 1 (EXO1), transcript variant 3, mRNA [NM_003686]	-1.22037
DSN1	ref|Homo sapiens DSN1, MIND kinetochore complex component, homolog (S. cerevisiae) (DSN1), transcript variant 3, mRNA [NM_024918]	-1.21578
AIF1L	ref|Homo sapiens allograft inflammatory factor 1-like (AIF1L), transcript variant 3, mRNA [NM_001185095]	-1.21451
USP4	ref|Homo sapiens ubiquitin specific peptidase 4 (proto-oncogene) (USP4), transcript variant 1, mRNA [NM_003363]	-1.2135
E2F8	ref|Homo sapiens E2F transcription factor 8 (E2F8), mRNA [NM_024680]	-1.20742
NFIB	ref|Homo sapiens nuclear factor I/B (NFIB), transcript variant 3, mRNA [NM_005596]	-1.20246

GINS2	ref|Homo sapiens GINS complex subunit 2 (Psf2 homolog) (GINS2), mRNA [NM_016095]	-1.19455
MCM10	ref|Homo sapiens minichromosome maintenance complex component 10 (MCM10), transcript variant 1, mRNA [NM_182751]	-1.19312
MPHOSPH8	ref|Homo sapiens M-phase phosphoprotein 8 (MPHOSPH8), mRNA [NM_017520]	-1.19288
FANCC	ref|Homo sapiens Fanconi anemia, complementation group C (FANCC), transcript variant 1, mRNA [NM_000136]	-1.18922
MCM6	ref|Homo sapiens minichromosome maintenance complex component 6 (MCM6), mRNA [NM_005915]	-1.187
IGSF1	ref|Homo sapiens immunoglobulin superfamily, member 1 (IGSF1), transcript variant 1, mRNA [NM_001555]	-1.18636
APPL1	ref|Homo sapiens adaptor protein, phosphotyrosine interaction, PH domain and leucine zipper containing 1 (APPL1), mRNA [NM_012096]	-1.18322
WBSCR16	ref|Homo sapiens Williams-Beuren syndrome chromosome region 16 (WBSCR16), mRNA [NM_030798]	-1.18155
FANCG	ref|Homo sapiens Fanconi anemia, complementation group G (FANCG), mRNA [NM_004629]	-1.17839
GINS4	ref|Homo sapiens GINS complex subunit 4 (Sld5 homolog) (GINS4), mRNA [NM_032336]	-1.1771
ATF5	ref|Homo sapiens activating transcription factor 5 (ATF5), transcript variant 1, mRNA [NM_012068]	-1.17636
NCSTN	ref|Homo sapiens nicastrin (NCSTN), mRNA [NM_015331]	-1.17383
TUBA1B	ref|Homo sapiens tubulin, alpha 1b (TUBA1B), mRNA [NM_006082]	-1.16659
PGR	ref|Homo sapiens progesterone receptor (PGR), transcript variant 2, mRNA [NM_000926]	-1.16558
NUCKS1	ref|Homo sapiens nuclear casein kinase and cyclin-dependent kinase substrate 1 (NUCKS1), mRNA [NM_022731]	-1.15991
AR	ref|Homo sapiens androgen receptor (AR), transcript variant 1, mRNA [NM_000044]	-1.15978
SRPK1	ref|Homo sapiens SRSF protein kinase 1 (SRPK1), transcript variant 1, mRNA [NM_003137]	-1.15846
GPR68	ref|Homo sapiens G protein-coupled receptor 68 (GPR68), transcript variant 2, mRNA [NM_003485]	-1.1576
PAFAH1B1	ref|Homo sapiens platelet-activating factor acetylhydrolase 1b, regulatory subunit 1 (45kDa) (PAFAH1B1), mRNA [NM_000430]	-1.15691

C14orf135	ens|chromosome 14 open reading frame 135 [Source:HGNC Symbol;Acc:20349] [ENST00000391611]	-1.15668
EML4	ref|Homo sapiens echinoderm microtubule associated protein like 4 (EML4), transcript variant 1, mRNA [NM_019063]	-1.15463
POLD3	ref|Homo sapiens polymerase (DNA-directed), delta 3, accessory subunit (POLD3), mRNA [NM_006591]	-1.14895
THBS1	ref|Homo sapiens thrombospondin 1 (THBS1), mRNA [NM_003246]	-1.1408
MYBL2	ref|Homo sapiens v-myb myeloblastosis viral oncogene homolog (avian)-like 2 (MYBL2), mRNA [NM_002466]	-1.13632
GOT2	ref|Homo sapiens glutamic-oxaloacetic transaminase 2, mitochondrial (aspartate aminotransferase 2) (GOT2), nuclear gene encoding mitochondrial protein, mRNA [NM_002080]	-1.13366
FANCE	ref|Homo sapiens Fanconi anemia, complementation group E (FANCE), mRNA [NM_021922]	-1.12499

LIST OF ABBREVIATION

µg	Microgram
µm	Micrometer
µM	Micromolar
µL	Microliter
5-aza	5-azacytidine
AF	Activation function
AKT	Serine-Threonine protein kinase
ANOVA	Analysis of variance
AP	Activator protein
BAM	Binary version of Sequence Alignment/Map
Bcl-2	B-cell lymphoma 2
BG-1	Bowman Gray-1
BLAT	BLAST-like alignment tool.
BPA	Bisphenol-A
BRCA	Breast Invasive Carcinoma
BSA	Bovine serum albumin
CAF	Cancer-associated fibroblasts
cAMP	Cyclic adenosine monophosphate
cDNA	Complementary DNA
CFA	Complete Freund's Adjuvant
ChIP-Seq	Chromatin immunoprecipitation sequencing
COBRA	Combined Bisulfite Restriction Analysis
Col	Colchicine
CREBP	cAMP-response element-binding protein
csFBS	Charcoal stripped FBS
CTGF	Connective tissue growth factor
DAB	3,3′-Diaminobenzidine
DDT	Dichlorodiphenyl-trichloro-ethane
DFS	Disease free survival
DMEM	Dulbecco's Modified Eagle's medium
DMR	Differentially methylated region
DMSO	Dimethyl sulfoxide
DNA	Deoxyribonucleic acid
DNase	Deoxyribonuclease
dnCpGi	Downstream CpG island
DNMT	DNA methyltransferase
DPBS	Dulbecco's phosphate-buffered saline
DPX	Distyrene plasticizer xylene
E2	17β-Estradiol
ECL	Dnhanced chemiluminescence
EDTA	Ethylenediaminetetraacetic acid
EGF	Epidermal growth factor
EGFR	Epidermal growth factor receptor

ELISA	Enzyme-linked immunosorbent assay
EMC	Expression-methylation correlation
ENCODE	Encyclopedia of DNA Elements
ER	Estrogen receptor
ERBB	Erythroblastic leukemia viral oncogene B
ERE	Estrogen response elements
ERK	Extracellular-signal-regulated kinase
ERsi	ERα siRNA transfected
EtOH	Ethanol
FBS	Fetal bovine serum
FISH	Fluorescent in situ hybridization
FOXA1	Forkhead box protein A1
gDNA	Genomic DNA
GPCR	G-protein coupled receptor
GPER1vx (x=2,3,4)	G-protein coupled estrogen receptor 1 transcript variant
GPR30	G protein-coupled receptor 30
HAIB	HudsonAlpha Institute for Biotechnology
HB-EGF	Heparin-binding EGF-like growth facto
HER2	Human epidermal growth factor receptor 2
HIF-1α	Hypoxia-inducible factor-1α
HRE	Hypoxia responsive element
HRG- β1	Heregulin-β1
HRP	Horseradish peroxidase
IFA	Incomplete Freund's Adjuvant
IGF-I	Insulin-like growth factor-I
IgG	Immunoglobulin G
IHC	Immunohistochemistry
IL6	Interleukin 6
IQR	The inter-quartile range
IUPHAR	International Union of Basic and Clinical Pharmacology
JAK	Janus kinase
kDa	Kilo Dalton
KLH	Keyhole Limpet Haemocyanin
KM Plotter	Kaplan-Meier plotter
LIMMA	Linear Models for Microarray
MACS	Model-based analysis of ChIP-Seq
MAPK	Mitogen-activated protein kinases
mL	Milliliter
MMP2	Matrix metalloproteinase 2
mRNA	Messenger ribonucleic acid
MSigDB	Molecular Signature Database
mTOR	Mechanistic target of rapamycin
MTT	Methylthiazolyldiphenyl-tetrazolium bromide
NCBI	National Center for Biotechnology Information

nER	Nuclear estrogen receptors
NFκB	Nuclear factor-κB
NGF	Nerve growth factor
NICPR	National Institute of Cancer Prevention and Research
NIEHS	National Institute of Environmental Health Sciences
OS	Overall survival
PARP	Poly (ADP-ribose) polymeras
PBS	Phosphate-buffered saline
PBST	PBS containing 0.05% Tween 20
PCR	Polymerase chain reaction
pFAK	Phospho focal adhesion kinase
PI	Propidium iodide
PI3K	Phosphatidylinositol 3-kinase
PIP3	Phosphatidylinositol 3,4,5-trisphosphate
PIS	Pre-immune sera
PKA	protein kinase A
pmol	Picomole
PPT	Propylpyrazoletriol
qRT-PCR	Quantitative reverse transcription polymerase chain reaction
RB3	Rabbit-B third bleed
RFS	Relapse free survival
RIPA	Radioimmuno precipitation assay
RNA	Ribonucleic acid
RNase	Ribonuclease
RPL35A	Ribosomal Protein L35A
RPMI-1640	Roswell Park Memorial Institute -1640 medium
RT-PCR	Reverse transcription polymerase chain reaction
RUNX2	Runt-related transcription factor-2
SAM	Sequence Alignment/Map
SD	Standard deviation
SDS-PAGE	Sodium dodecyl sulfate polyacrylamide gel electrophoresis
SERDs	Selective estrogen receptors down-regulators
SERMs	Selective estrogen receptor modulators
siRNA	Short interfering ribonucleic acid
SP1	Specificity protein 1
SRA	Sequence Read Archival
SRC	Sarcoma
STAT3	Signal transducer and activator of transcription 3
Sulfo-SMCC	Sulfosuccinimidyl 4-(N-maleimidomethyl) cyclohexane-1-carboxylate
TAM	4-hydroxytamoxifen
TBE-PAGE.	Tris Borate EDTA Polyacrylamide Gel Electrophoresis
TBST	Tris-buffered saline containing 0.05% Tween 20
TCGA	The Cancer Genome Atlas
TGF	Transforming growth factor

TMB	3,3',5,5'-Tetramethylbenzidine
TNM	Tumor, node, and metastases
TSS	Transcription start site
UCSC	University of California, Santa Cruz
upCpGi	Upstream CpG island
UTR	Untranslated region
VSMC	Vascular smooth muscle cells

LIST OF TABLES

LIST OF FIGURES

LIST OF PUBLICATIONS AND PRESENTATIONS

Publications from the thesis work

Mohan C Manjegowda, Paridhi Singhal Gupta and Anil M. Limaye. Hyper-methylation of the upstream CpG island shore is a likely mechanism of GPER1 silencing in breast cancer cells **Gene** (2017) 614: 65-73.

Mohan C Manjegowda, Paridhi Singhal Gupta and Anil Mukund Limaye. Validation data of a rabbit antiserum and affinity purified polyclonal antibody against the N-terminus of human GPR30. **Data in Brief**, (2016) 7: 1015-1020

Mohan C Manjegowda and Anil M. Limaye. "DNA methylation dependent suppression of GPER1 in colorectal cancer" **Medical Research Archive** (Accepted)

Publications from outside thesis work

Dixcy Jaba Sheeba J. M., **Mohan C Manjegowda,** Ajay Kumar, Sarbajeet Dutta, and Anil M Limaye. "The role of cystatin A in breast cancer and its functional link with ERα" **Journal of Genetics and Genomics** (2017) 44: 593-597.

DixcyJabaSheeba J. M., **Mohan C Manjegowda**, Marine Hussain, Gauri Deb, Neeraj Kumar and Anil M Limaye. Estrogen regulated extracellular matrix remodeling genes in MCF-7 breast cancer cells. **Gene Reports**, (2016) 3: 14-21

Mohan C Manjegowda, Gauri Deb, Neeraj Kumar, Anil M. Limaye. Expression profiling of genes modulated by estrogen, EGCG or both in MCF-7 breast cancer cells, **Genomics Data**, (2015) 5: 210-212.

Mohan C Manjegowda, Gauri Deb and Anil M Limaye. Epigallocatechein gallate induces the steady state mRNA levels of pS2 and PR genes in MCF-7 breast cancer cells. **Indian J Exp Biol. (**2014) 52: 312-316.

Manuscripts under preparation/communication

Mohan C. Manjegowda, Paridhi Singhal Gupta, Vandana Raphael, Deepak Modi and Anil Mukund Limaye. Estrogen regulates GPER1 expression in breast cancer via ERα. (Under preparation)

Mohan C. Manjegowda, Ajay Kumar, Uttariya Pal, Paridhi Singhal Gupta and Anil M. Limaye. GPER1 signalling in hormone responsive breast cancer: a potential therapeutic target. (Under preparation)

Poster presentations

Mohan C. Manjegowda, Paridhi Gupta and Anil Mukund Limaye. Hyper-methylation of the upstream CpG island shore is a likely mechanism of GPER1 silencingin breast cancer cells Poster presentation in "Gordon Research Conference: Cancer Genetics and Epigenetics", held in Barga, Italy (2017)

Ramya M, **Mohan C Manjegowda**, Sudipta Ghosh, Latha Rangan and Anil M. Limaye. Labdane diterpenes from *Alpinia Nigra* suppresses cancer cell proliferation by inducing apoptosis. Poster presentation at "Research Conclave", held in IIT Guwahati, India (2016).

Dixcy Jaba Sheeba JM, **Mohan C Manjegowda**, Ajay Kumar and Anil M. Limaye. Study of regulation of steady state mRNA levels of Cystatin A by estrogen in breast cancer cells. Poster presentation at "Research Conclave" held in IIT Guwahati, India (2016).

Mohan C Manjegowda, Paridhi Singhal and Anil M Limaye. Epigenetic component in expression of G-protein coupled Estrogen Receptor (GPER1) in Breast cancer. Poster presentation in "Recent Developments in Medical Biotechnology and Structure Based Drug Designing" held in IIT Guwahati, India (2015)

Dixcy Jaba Sheeba JM, **Mohan C Manjegowda**, Ajay Kumar and Anil M. Limaye. Regulation of Cystatin A by estrogen in breast cancer cells. Poster presentation at "International Conference of Cancer Research: New Horizons 2015", held in NCCS, Pune, India (2015).

Ajay Kumar, **Mohan C Manjegowda**, Dixcy Jaba Sheeba JM, Sachin Kumar and Anil M. Limaye. Regulation of HOXB2 by estrogen in breast cancer. Poster presentation at "Recent Development In Medical Biotechnology And Structure Based Drug Designing" held in IIT Guwahati, India (2015).

DixcyJabaSheeba J M, **Mohan C Manjegowda**, Marine Hussain, Gauri Deb, Neeraj Kumar, Anil M Limaye. Estrogen regulation of ECM remodeling and associated genes. Presented in "33rd Annual Convention of Indian Association for Cancer Research on Discovery, Innovation and Translation in Cancer Research", held in Kollam, Kerala (2014).

COPYRIGHTS AND PERMISSIONS

Chapter 5. Permission from the institute ethics committee to conduct IHC study on breast cancer tumors samples at NEIGRIHMS

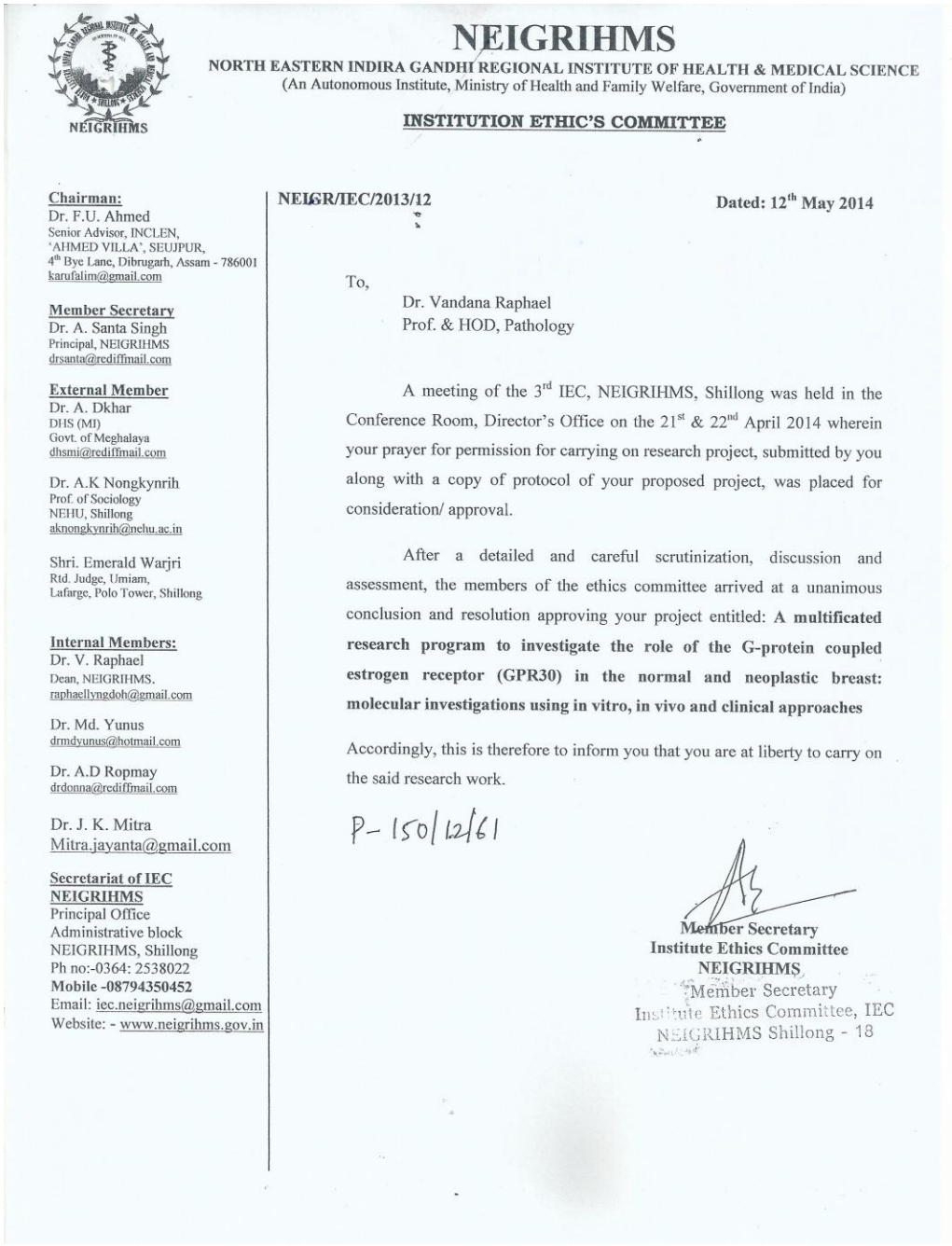

NEIGRIHMS

NORTH EASTERN INDIRA GANDHI REGIONAL INSTITUTE OF HEALTH & MEDICAL SCIENCE
(An Autonomous Institute, Ministry of Health and Family Welfare, Government of India)

INSTITUTION ETHIC'S COMMITTEE

Chairman:
Dr. F.U. Ahmed
Senior Advisor, INCLEN,
'AHMED VILLA', SEUJPUR,
4th Bye Lane, Dibrugarh, Assam - 786001
karufalim@gmail.com

Member Secretary
Dr. A. Santa Singh
Principal, NEIGRIHMS
drsanta@rediffmail.com

External Member
Dr. A. Dkhar
DHS (MI)
Govt. of Meghalaya
dhsmi@rediffmail.com

Dr. A.K Nongkynrih
Prof. of Sociology
NEHU, Shillong
aknongkynrih@nehu.ac.in

Shri. Emerald Warjri
Rtd. Judge, Umiam,
Lafarge, Polo Tower, Shillong

Internal Members:
Dr. V. Raphael
Dean, NEIGRIHMS.
raphaellyngdoh@gmail.com

Dr. Md. Yunus
drmdyunus@hotmail.com

Dr. A.D Ropmay
drdonna@rediffmail.com

Dr. J. K. Mitra
Mitra.jayanta@gmail.com

Secretariat of IEC
NEIGRIHMS
Principal Office
Administrative block
NEIGRIHMS, Shillong
Ph no:-0364: 2538022
Mobile -08794350452
Email: iec.neigrihms@gmail.com
Website: - www.neigrihms.gov.in

NEIGR/IEC/2013/12 **Dated: 12th May 2014**

To,
Dr. Vandana Raphael
Prof. & HOD, Pathology

A meeting of the 3rd IEC, NEIGRIHMS, Shillong was held in the Conference Room, Director's Office on the 21st & 22nd April 2014 wherein your prayer for permission for carrying on research project, submitted by you along with a copy of protocol of your proposed project, was placed for consideration/ approval.

After a detailed and careful scrutinization, discussion and assessment, the members of the ethics committee arrived at a unanimous conclusion and resolution approving your project entitled: **A multificated research program to investigate the role of the G-protein coupled estrogen receptor (GPR30) in the normal and neoplastic breast: molecular investigations using in vitro, in vivo and clinical approaches**

Accordingly, this is therefore to inform you that you are at liberty to carry on the said research work.

P-150/12/61

Member Secretary
Institute Ethics Committee
NEIGRIHMS
Member Secretary
Institute Ethics Committee, IEC
NEIGRIHMS Shillong - 18

Chapter 4 and 7. Author of the publication and no permission required.

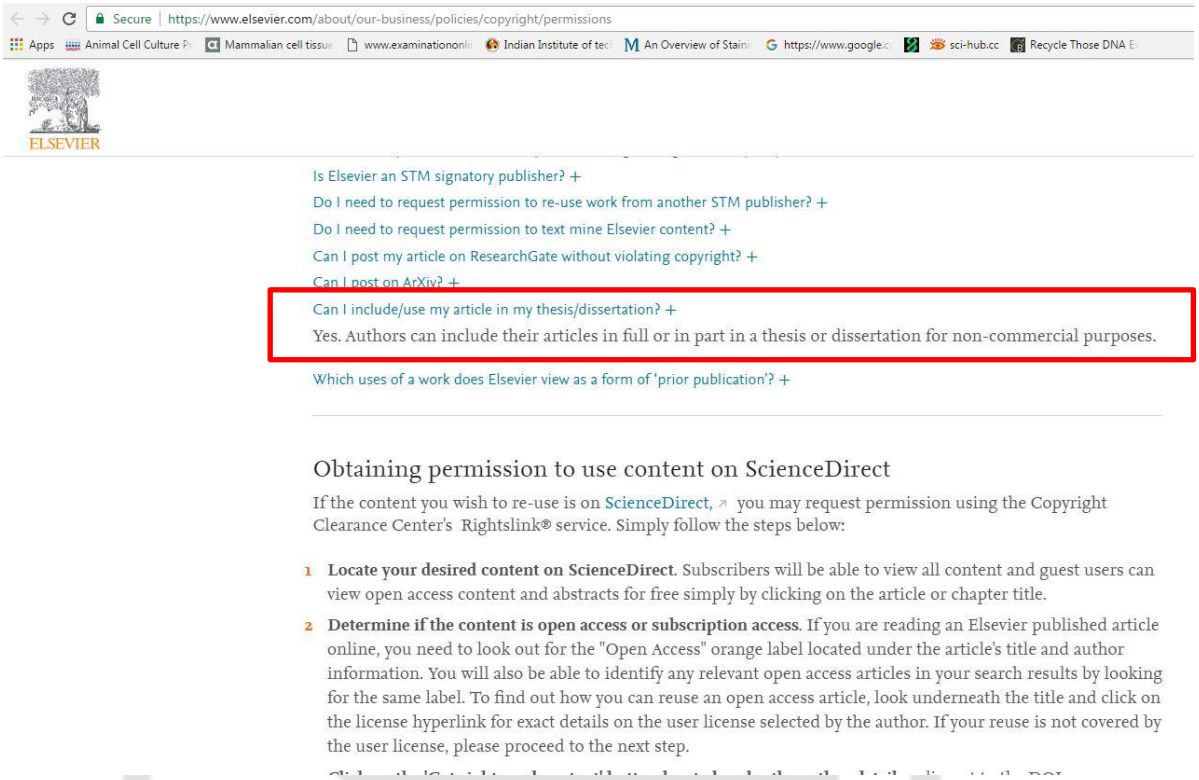

Secure | https://www.elsevier.com/about/our-business/policies/copyright/permissions

Apps Animal Cell Culture P Mammalian cell tissue www.examinationonli Indian Institute of tec An Overview of Stain https://www.google.c sci-hub.cc Recycle Those DNA E

ELSEVIER

Is Elsevier an STM signatory publisher? +

Do I need to request permission to re-use work from another STM publisher? +

Do I need to request permission to text mine Elsevier content? +

Can I post my article on ResearchGate without violating copyright? +

Can I post on ArXiv? +

Can I include/use my article in my thesis/dissertation? +

Yes. Authors can include their articles in full or in part in a thesis or dissertation for non-commercial purposes.

Which uses of a work does Elsevier view as a form of 'prior publication'? +

Obtaining permission to use content on ScienceDirect

If the content you wish to re-use is on ScienceDirect, you may request permission using the Copyright Clearance Center's Rightslink® service. Simply follow the steps below:

1 **Locate your desired content on ScienceDirect**. Subscribers will be able to view all content and guest users can view open access content and abstracts for free simply by clicking on the article or chapter title.

2 **Determine if the content is open access or subscription access**. If you are reading an Elsevier published article online, you need to look out for the "Open Access" orange label located under the article's title and author information. You will also be able to identify any relevant open access articles in your search results by looking for the same label. To find out how you can reuse an open access article, look underneath the title and click on the license hyperlink for exact details on the user license selected by the author. If your reuse is not covered by the user license, please proceed to the next step.